AD

REPORT R-1779

FERROELECTRICS: THEIR ELECTRICAL BEHAVIOR DURING, AND SUBSEQUENT TO, IONIZING RADIATIONS

by

I. LEFKOWITZ
K. KRAMER
P. KROEGER

AMCMS 5023.11.14200.01
DA Project IN22601A085

November 1965

UNITED STATES ARMY
FRANKFORD ARSENAL
PHILADELPHIA, PA.

DISCLAIMER NOTICE

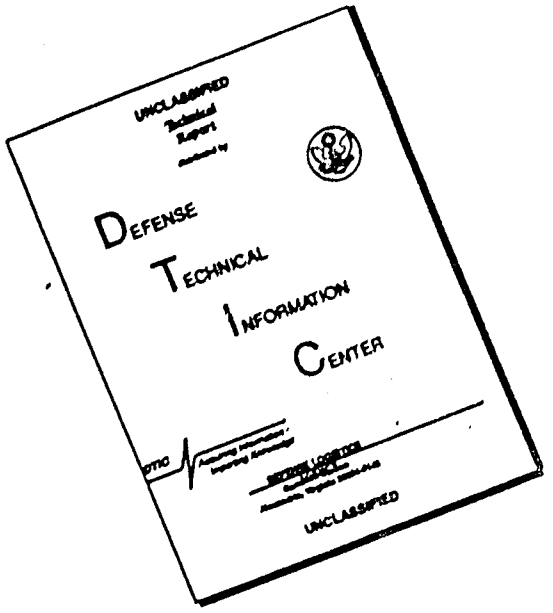

THIS DOCUMENT IS BEST QUALITY AVAILABLE. THE COPY FURNISHED TO DTIC CONTAINED A SIGNIFICANT NUMBER OF PAGES WHICH DO NOT REPRODUCE LEGIBLY.

REPORT R-1779

FERROELECTRICS:
THEIR ELECTRICAL BEHAVIOR DURING, AND SUBSEQUENT TO, IONIZING RADIATIONS

by

I. LEFKOWITZ
K. KRAMER
P. KROEGER

AMCMS Code 5023.11.14200.01
DA Project IN22601A085

Pitman-Dunn Research Laboratories
FRANKFORD ARSENAL
Philadelphia, Pa. 19137

November 1965

ABSTRACT

A study has been made on certain ferroelectric materials which are among those used extensively in military applications, both in a polarized condition in such items as impact fuzes and in an unpolarized condition as capacitors. The transient voltages across a load produced by charge generated on the surface of various types of ferroelectric specimens during irradiation have been measured. These outputs were found to vary widely in amplitude and polarity even from specimens ostensibly alike (i.e., from the same lot of a given manufacturer), and even from a single specimen pulsed repeatedly with gamma and neutron radiation. Pulses were found to vary from background levels to a high of 300 volts on a large specimen with a load of 10^7 ohms and radiation of 5.4×10^{14} fast (Pu) neutrons and associated gammas. The maximum voltage possible is unknown, as are the factors causing the variation. Both polarized and unpolarized specimens showed outputs well above background transients. Some specimens were identical to those used in impact fuze applications and were in simulated housings which reproduce the mechanical environment of the device. Some fuze circuits in present use are discussed with reference to their use of ferroelectric materials and a calculation of the energy transferred by a voltage pulse to a load is presented. An investigation of various specifications for Army devices shows that in many cases capacitor material is not specified at all and ~~ferroelectric~~ dielectric capacitors may be being used in applications where their presence as possible voltage generators in radiation environments could be dangerous or lead to unreliability. In view of this, the report recommends that a basic research program be instituted to determine the mechanism behind the phenomenon and that designers and safety engineers be appraised of the situation.

FOREWORD

The program described in this report was performed by Frankford Arsenal, U. S. Army Munitions Command, Philadelphia, Pa., for Picatinny Arsenal, Dover, N. J. The work was authorized under AMCMS Code 5023.11.14200.01, DA Project Number IN22601A085.

The authors gratefully acknowledge the following individuals for their helpful assistance: D. Rosenblatt, E. Thilo, R. Harborak and M. Shields at our own laboratory; J. Upham and F. Bennett of Forrestal Laboratories; G. Taylor and G. Chesnov of Picatinny Arsenal; and S. Marcus and P. Berman of the Harry Diamond Laboratories.

Acknowledgement is made to Nature Editorial and Publishing Offices, London, England, for permission to use material presented in Appendix B, Part 1. Acknowledgement is also made to The Institute of Electrical and Electronics Engineers Inc., New York, N. Y., for permission to use the material appearing in Appendix B, Part 3.

TABLE OF CONTENTS

TABLE OF CONTENTS (Cont'd)

LIST OF TABLES

LIST OF TABLES (Cont'd)

LIST OF ILLUSTRATIONS

INTRODUCTION

Ferroelectric materials find application in many items of military equipment. They may be used in an electronic circuit where they function as capacitors: (a) to prevent the conduction of electricity in a circuit; (b) to provide specific time-constants and delays; or (c) to provide a shunt for RF energy, etc. The open literature has reported that these ferroelectric materials can develop a voltage of variable magnitude when subjected to ionizing radiations of various kinds (both steady state and pulsed). A ferroelectric capacitor which functions spuriously in this manner (i.e. as a source of voltage) would seriously affect the functioning of many electronic circuits. Tubes could be made to conduct and current pass through a detonator, time-constants would change and a premature or delayed functioning occur, shunt capacitors would not be a shunt device, etc. The ferroelectric may be used in a fuze application where the piezoelectric property of the material is utilized to develop a voltage on impact. Any voltage which appeared prior to the impact could cause prematures.

The emf (voltage) observed when some ferroelectric materials and subjected to ionizing radiation is defined as "anomalous radiation sensitivity". This report covers recent work on anomalous radiation sensitivity in ferroelectric materials and collates material which has not been easily available to assist in the assessment of difficulties that may arise in the application of ferroelectric materials as capacitors and transducers (i.e., impact fuzes) when used in special environments (ionizing radiation).

The first section is a literature survey describing this anomalous effect. In the appendix are several of the pertinent papers included for the readers' convenience.

The results of new measurements made at the Diamond Ordnance Radiation Facility (DORF) are described and the data presented and analyzed. This work has hitherto been available only in the form of a letter report and provides confirmation of predictions made earlier.

A brief analysis is included in the next section for some typical fuze circuits and may be used to analyze vulnerability of military systems. Included in this section is a mathematical treatment in which two types of electrical waveforms are considered for energy transfer, so that the fuze applications engineer may estimate what maximum energy transfer could be expected for his particular circuit constants.

The last section is a short summary with the conclusions which may be drawn.

A BRIEF SUMMARY OF PERTINENT PAPERS AND REPORTS ON THE ANOMALOUS RADIATION SENSITIVITY IN FERROELECTRIC MATERIALS

This section has been written to give the reader a very brief introduction to the scientific literature discussing surface layers in ferroelectrics. It introduces the work which shows the interrelationship between the surface layers and the photo-voltaic effect and extends this to the anomalous radiation sensitivity under investigation. The last few pages describe studies undertaken on this anomalous radiation sensitivity. Some of the original papers are included in the appendix.

The first suggestion for the anomalous layer was made by Känzig (1955) on the basis of experiments with very small particles of barium titanate ($BaTiO_3$). The primary piece of direct evidence cited was that particles with an average diameter of 1000 Å still exhibited a tetragonal distortion of the order of 0.02% at 500° C, well above the Curie point. Electron diffraction experiments indicated the existence of a surface layer about 200 Å thick because a larger strain exists on the surface than in the bulk of the material, and the distortion of the surface layer was reported as practically independent of temperature. Other results, that of Merz (1956), also supported the conclusion that a surface layer existed, but this was based on the switching properties of the materials. Further work by Chynoweth (1956) showed that a space charge layer at the surface of $BaTiO_3$ could be detected directly by means of pyroelectric measurements. Further, he found a photo-voltaic effect and also found this effect behaves in the same way as the pyroelectric effect which had originally led him to conclude a surface space charge layer exists. One conclusion drawn was that there was a great similarity between the "anomalous" pyroelectric effect and the photovoltaic effect. The detailed correlating mechanism was not discussed however. Several experimentalists attempted direct measurement of this layer; all proved to be unsuccessful. However, the residual pyroelectric signals observed by Chynoweth at temperatures above the Curie point are

consistent with Kanzig's hypothesis of a polarized layer at the surface of $BaTiO_3$ crystals. Wieder and White (1959) attempted to determine some of the properties of a space charge layer. The effects were explained qualitatively in terms of a localized space charge layer, but detailed information as to the character of the layer could not be extracted from their results. Triebwasser (1960) showed the buildup of layers near the electrode surfaces by examining the birefringence induced by DC fields. The important result of this experiment was that a buildup of the space charge layer was found to be dependent upon the magnitude and duration of the applied field. Triebwasser suggested that the surface layer is that of a Schottky exhaustion barrier with donor concentrations of about $10^{19}/cm^3$ and a dielectric constant on the order of 200. Several other models have been suggested and examined theoretically and experimentally, but no one model has been wholly satisfactory. Harmon (1958) reported electrode luminescence during polarization from the layer and his model involves that of a material with an oxygen deficiency. Harmon's study showed that several perovskites gave the same results, including nonferroelectric calcium titanate.

As will be shown later, the existence of these layers may be intimately connected with the anomalous radiation sensitivity. Lefkowitz (1959) (Appendix B, Part 1) made a study of the radiation effects on ferroelectric materials, and showed clear evidence for the anomalous radiation sensitivity. He found some correspondence between intensity of radiation flux (both gammas and neutrons plus gammas) and the electrical energy produced. Instrumentation was developed which was highly reliable. Background effects were analyzed including those due to work function difference, and finally very good reproducibility of background currents was achieved while using glass in place of the ferroelectric material. The currents obtained from the ceramics generally exceeded those from the glass by as much as an order of magnitude. However, he found that there was a large degree of random scatter in his measured output even from ferroelectric materials made at the same time, polarized the same way, and placed in the same radiation flux. It was also found that the effect was not directly related to the primary pyroelectricity or the piezoelectricity.

In a later publication, Lefkowitz (1963) (Appendix B, Part 1) showed, through the interdependence of the piezoelectric effect and the anomalous radiation sensitivity, that a significant contribution to the piezo coefficient comes from the surface layer and that the radiation sensitivity may also be so related.

Kesselman (1963) (Appendix B, Part 2) reported preliminary data that Picatinny Arsenal obtained on nuclear effects using lead zirconate-lead titanate ($Pb(Ti, Zr)O_3$) materials. Using a Triga reactor, he reported that with a neutron pulse spike of 10^{16} neutrons/cm^2/sec and a total neutron dose of 10^{14} neutrons/cm^2/pulse the maximum detected voltage was 0.2 volts. Further, he cited work of the Sandia Corporation at the Godiva Pulse Reactor where less than one volt was observed under similar conditions. Subsequent to this, he reported that in a measurement using seven samples, three of $BaTiO_3$, and three of $Pb(Ti, Zr)O_3$, plus a dummy, he obtained one to ten volts from the dummy and the $BaTiO_3$, and about 40 volts from the $Pb(Ti, Zr)O_3$. This measurement was with 10^6 ohms in parallel with the sample, but the samples were operating into the pre-amplifier of an oscillograph whose self-impedance is of the order of 50,000 ohms. Therefore, the 40 volt pulse which was delivered across the 50K ohm load represents a sizeable voltage for the circuit constants.

Hester, Glower and Overton (1964) of the Sandia Corporation have suggested the use of ferroelectrics for a gamma-ray dosimeter. The following is an abstract of a paper published by them (Appendix B, Part 3):

> "A gamma-ray dosimeter employing a poled ferroelectric as the transducer element has been studied. Irradiation with gamma rays causes a release of charge by the ferroelectric element. The magnitude of the charge released has been determined experimentally to vary linearly with gamma-ray dose. The current in a shunting resistor with no external voltage applied varies linearly with gamma-ray dose rate. A constant of proportionality of 10^{-12} coul per rad (H_2O) per cm^2 of electroded ferroelectric surface has been measured for polycrystalline $Pb(Zr_{.65} Ti_{.35})O_3$ plus 1 w% Nb_2O_5 irradiated in the Sandia Pulsed Reactor. The contribution to the charge release from the neutron irradiation has been determined experimentally to be negligible. Irradiation in the 0.6 Mvp flash X-ray also produces a linear relationship between current and gamma-ray dose rate. A similar release of charge has been observed in poled ceramic barium titanate."

Our conversation with these authors led to the information that only ten samples were in fact investigated. Small variations in the observed outputs were ignored or attributed to inaccuracies in the dosimetry normally taken as a standard. It should be stressed that the released electric charge when ferroelectric materials are irradiated is the effect we have termed "anomalous

radiation sensititivity" and Hester, et al suggest using this effect in dosimetry. Contrary to the experience of Lefkowitz and possibly Kesselman, this group states that all the samples that they used showed the same radiation sensitivity.

RESULTS OF IRRADIATION EXPERIMENTS

The following investigations were carried out at the Diamond Ordnance Radiation Facility in Silver Springs, Maryland, using a General Atomic TRIGA Mark F "swimming pool" pulsed reactor. The investigation covers two periods of time, a year apart, and is reported in this manner.

Investigation During July-August, 1964

Samples were obtained from Picatinny Arsenal as well as from several different manufacturers. These samples are representative of (and in some cases identical to) materials in present use in components specified for military circuitry. In part these had been specified according to their electrical characteristics only. As a result the age and details of composition were unknown. The specimens were mainly polarized ceramic discs made of barium titanate ($BaTiO_3$) and of hot pressed solid solutions of lead titanate and lead zirconate (PZT) as well as two single crystals of barium titanate. The physical dimensions varied considerably and are tabulated in Table I. Nominal capacities are also given. Eighty samples, all with silver electrodes, were used and subjected to as many as 62 pulses each. A total of 95 pulses was obtained from the pulse reactor.

The specimens were placed on long glass slides 1/4" thick and held in place by brass strips, one touching each side of the specimen and attached to the glass by screws approximately 1" apart (Figure 1). A few assemblies were encapsulated in Silastic, a rubber-like material, to minimize pulse degredation due to "shorting" effects through the ionized atmosphere. There were positions for ten specimens on each glass slide although during each pulse some positions were left empty so that the output from the cabling and glass itself could be determined. Two glass slide assemblies were irradiated at a time.

Table 1. SPECIMEN STATISTICS (1964)

Designation	Total Number	Number Irradiated	Nominal (in.)			Typical		Nominal Curie Temp.	Composition	Designation	Source & Lot
			Diameter	Electrode Diameter	Thickness	Capacity (μuf)	Dielectric Const.				
1-3	4	4	1.0	1.0	0.1	2000	1100	325°[a]	PZT	4	Clevite I3
C-4	4[b]	4	1.0	1.0	0.1	2900	1640	365°[a]	PZT	5	Clevite C4
779	6	6	1.0	1.0	0.1	1900	1075	>300°[a]	PZT	C43B	Sprague 305779
780	6	6	1.0	1.0	0.1	2800	1580	>300°[a]	PZT	C43C	Sprague 305780
S	3	2	.01[c]	.01[c]	.006			125	$BaTiO_3$	Single Crystal	Lefkowitz
D	39	2	7/16; 3/64[d]	3/8; 3/22[d]	1/16	540	1650				
C	39[e]	8	.184	.184	.185	55	1680	380°	PZT	5A	Clevite (Benson)
K	61	32	1/2	1/2	3/32	700	1480				Kesselman
N	91	9	5/8	9/16	1/16	1500	1680	370°	PZT		Picatinny Arsenal
R	69	7	13/16	21/32	1/16	1600	1300	130°	$BaTiO_3$		Picatinny Arsenal

NOTES:

[a] Mfg's data

[b] Numbered 5-8

[c] Area given (irregular)

[d] Donut shaped

[e] Numbered 1-14A, 1-14B, 15-25; 1st 14 matched pairs

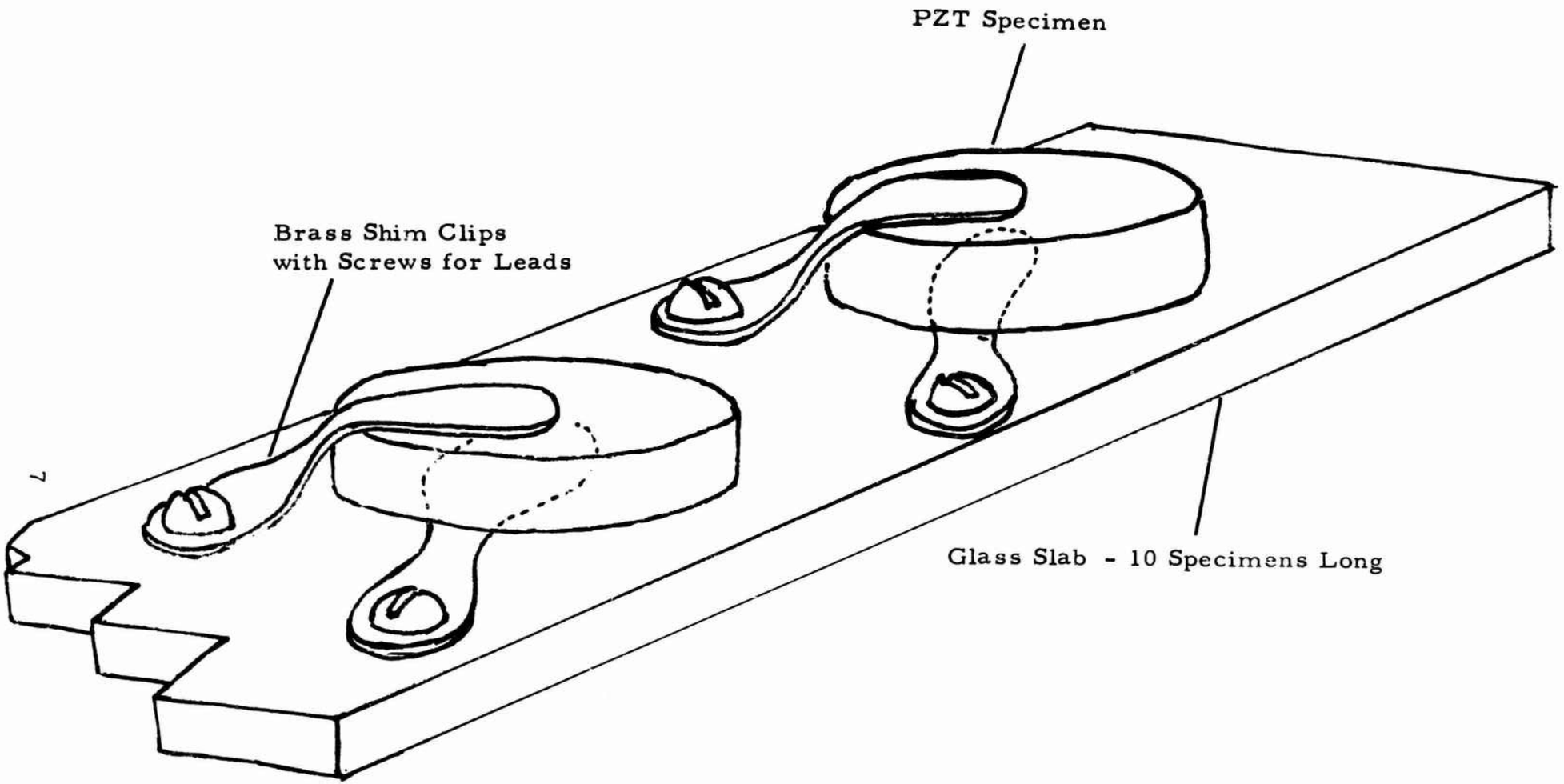

Figure 1. Specimen Assembly (1964)

These glass slides were centered inside weighted dummy fuel elements, which were placed in the outer or "F", ring of the core. One coaxial cable, type RG-62/U, led from each specimen (via the pair of screws) up through approximately 10' of water above the core to the monitoring equipment. The cables ran inside watertight polyethylene tubing.

The pulses were fed through preamplifiers with 50 K ohm input impedances per channel and then into two Honeywell Model 1108 "Visicorder" oscillographs. These were equipped with M8000 galvanometers with sensitivity of about 1-1/3 volts/in.

By putting carbon resistors in parallel with the preamplifiers, the input loads were varied at times between 1000 ohms and 50,000 ohms.

A few specimen outputs were monitored with Polaroid cameras on Type 555 and Type 535 Tektronix oscilloscopes with 10^6 and 10^7 ohm input impedances. These impedances were also varied by means of parallel resistors and the outputs measured from a given specimen were the same on oscilloscope or oscillograph in the overlapping range of load. Triggering was done both internally by the pulses themselves and externally by the output from a Čerenkov counter.

Radiation

The specimens were mounted in the outer ring of the core with both edge and face towards the center of the core. At this distance the source of neutrons cannot be considered a point source, of course, and so the radiation was not unidirectional, but neither was it isotropic. As the samples were rotated no variation in output as a function of orientation was observed. The nominal radiation flux at the mid-core-height position is given in Table II.

Integrated and peak dosages varied as much as 10% to 15% but there was no correlation between these variations and the voltage output variations observed.

Table II. PARTICLE FLUX IN "F" RING OF CORE

Type of Radiation	Peak Dose (sec/cm^2) (mid-core-height)	Integrated Dose (pulse/cm^2) (mid-core-height)	Integrated Dose (pulse/cm^2) (10 cm off center)
Gammas (R)	$4.5 - 6.0 \times 10^7$	$7.5 - 10 \times 10^5$	$7.5 - 10 \times 10^5$
Neutrons <0.4 ev (thermal)	2.0×10^{16}	3.5×10^{14}	2.0×10^{14}
Neutrons <10 ev (fast-Pu)	3.3×10^{16}	5.4×10^{14}	3.5×10^{14}

Results

The following effects were noted:

There were short term changes in the capacity due to the integrated radiation. These were small, about 10% or smaller, and seemed to anneal as time went on, returning to the original value after several hours or days.

Of the 80 samples examined, about 80% showed some radiation sensitivity, and of these between 5% and 10% gave sizeable outputs. One specimen (I-3-1) gave an output of about 300 volts (pulse No. 80) with a load of 107 ohms and 80 volts (pulses Nos. 82 and 88) with a 10^6 ohm load. The samples which showed themselves to be radiation sensitive continued to be so over many nuclear pulses. Even when these samples were removed and returned to a new sample position, they continued to show sensitivity. There were spontaneous changes both in the polarity of the output and in the amplitude of the output. But once a new equilibrium was reached the polarity of the sample remained stable over a fairly long period of time. The specimen outputs were mainly but not exclusively of the same polarity while the dummy outputs were rather evenly distributed in polarity. The distribution of maximum outputs for each specimen is given in Table III while the complete data can be found in Appendix A, Part 1.

Table III. DISTRIBUTION OF MAXIMUM OUTPUTS (1964)

Volts	0-1	1-2	2-4	4-10	10-20	20-100	100-300
50 K Ohm Load							
Dummies	23	8	1				
1" Discs			3	15			
Smaller Specimens	14	28	13	1			
10^6 Ohm Load							
Dummies	4		2	2			
1" Discs			1		3	8	
Smaller Specimens			1		5	4	
10^7 Ohm Load							
Dummies	1		1	1			
1" Discs						8	1
Smaller Specimens					6	4	2

Having found samples which reproducibly gave large outputs, a series of measurements was made varying the load on the sample (see Figure 2), and load curves were obtained. These curves permit some estimate to be made of the energy that can be delivered if the properties of the load device can be defined. Hester, et al., predict that maximum voltage should vary linearly with load, and this is found to be approximately true.

Investigation During July, 1965

Specimen Materials

The specimens used in the second experiment were exclusively ceramics made from hot-pressed mixtures of lead titanate and lead zirconate (PZT). These were specimens of the materials used commonly in components of fuze circuits. A total of 125 specimens and 15 quartz "dummy" samples were irradiated during 32 pulses. Each specimen received about 3 pulses. The outputs were monitored on oscilloscopes.

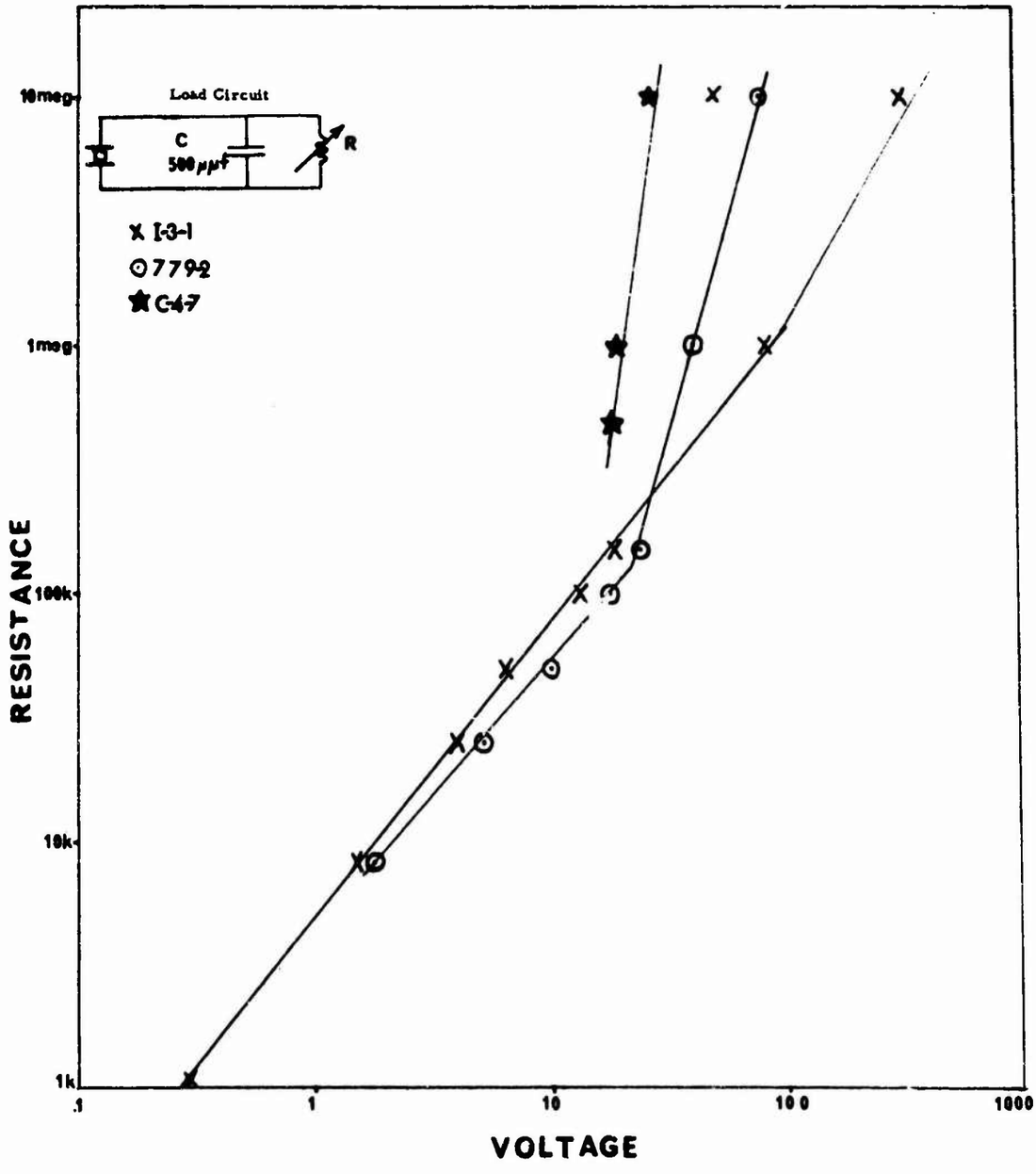

Figure 2. Peak Output Voltage vs. Resistive Load

The PZT specimens came from several sources and were treated in various ways. There were large discs 1" in diameter and 0.1" thick, and cylinders 0.185" high and 0.185" in diameter. Both were electroded with silver on the top and bottom. Two of the manufacturers supplied discs in both polarized and unpolarized states, but otherwise identical. The third manufacturer supplied only polarized discs. Half of the latter were mechanically loaded with spring clamps of about 10 lbs force. Half of the disc shaped dummies were similarly loaded.

The cylinders were all polarized. They were mounted in pairs in parallel in the following configurations: (1) "plus", i.e., both cylinders with positive faces connected to the cable and negative faces grounded; (2) "minus", i.e., both cylinders with negative faces connected to the cable and positive faces grounded; and (3) "neutral", i.e., one cylinder in each of the above orientations in an antiparallel configuration. The sample conditions are shown in Table IV.

Table IV. STATES AND CONFIGURATIONS OF SAMPLES

Type :	LARGE DISCS							
Mfg. :	Gulton		Clevite		Erie		Dummies	
Condition:	poled	unpoled	poled	poled & loaded	poled	unpoled	un-loaded	loaded
Quantity :	15	15	15	15	15	15	5	5

Type :	SMALL CYLINDER PAIRS					
Mfg. :	Gulton		Clevite		Unknown	Dummies
Condition:	plus	minus	plus	neutral	plus	----
Quantity :	8	7	11	4	5	5

The dummies were made from optical quality quartz and were the same sizes as the specimens. The material of unknown source probably came from Clevite and was at least a year older than the other material. The Clevite and Erie products are probably of the same composition while those specimens from Gulton probably contained more lead zirconate. Table V summarizes the properties of the materials as listed by the three manufacturers.

Table V. SPECIMEN STATISTICS (1965)

Mfg.	:	Clevite	Gulton	Erie
Type	:	PZT-5	HST-41	2003
Lot	:	55425	U6698	-
Curie point, T_c (°C)	:	365	260	>300
Dielectric constant, E	:	1700	1800	1600
d_{33} (x 10^{-12})	:	374	320	320

Nominal capacities and loss tangents as measured on a General Radio type 1620A transformer ratio arm bridge for the various types of specimens are given in Table VI.

Table VI. SPECIMEN CAPACITIES (1965)

Specimen Type	Nominal Capacity (pf)	Tan δ
Discs:		
Gulton, poled	2840	.014
Gulton, unpoled	2600	.019
Clevite, poled	2940	.013
Erie, poled	2690	.013
Erie, unpoled	2060	.015
	1820	.017
Quartz	1	.000
Cylinders (single):		
Gulton	51	.003
Clevite	54	.003
Unknown source	55	.003
Quartz	1	.0005

The discs were mounted in "sandwiches" (see Figure 3) which consisted of 1" discs of 1/4" thick quartz on the outside, then 1/32" thick aluminum with tabs for the leads and the PZT or quartz dummy in the center. The sandwich was held together with rubber bands in the case of the unloaded samples and with a spring steel clip for the loaded samples. This assembly was encapsulated in Silastic. The cables were crimped to the aluminum tabs, the center wire going to the positive face of the specimen and the shield to the other.

The cylinders were mounted one above the other in pairs in an aluminum housing with a BNC connector providing electrical access (see Figure 4). The central pin of the BNC was connected to a small aluminum plate which lay between the two cylinders. The ground connection was made through the case housing. A Teflon sleeve around the cylinders prevented shorting. A small coil spring provided a mechanical loading of 12.5 ± 2.0 lbs of force.

Monitoring Equipment

Each specimen was connected to a seven foot type RG-62/U coaxial cable, the discs via crimped leads and the cylinder pairs through the BNC connector on the housing. These cables connected to 25' cables of the same type which ran from the middle of the exposure room through the concrete shielding of the ceiling via a helical tube to the monitoring equipment. The long cables were re-used throughout the experiment. The connection was made with BNC's also, with care taken to avoid ground loops due to connectors touching. All connectors had Teflon insulation. The cables had a total capacity of 440 pf ± 10 pf (D = 0.00008).

Twenty specimens were irradiated at a time and the outputs monitored with Polaroid cameras on five type 535 Tektronix oscilloscopes, each with a four-trace type M beam splitter. Channel switching occurs at approximately a 250 Kc/sec rate, and therefore transients of as little as 0.5 msec duration can be well delineated, and even shorter transients may be detected. With the sweep rates of 5 msec/cm used, this corresponds to a width of under 1 mm. Input impedances in all cases were 1 megohm in parallel with 37 pf.

Since the magnitude and polarity of the sample pulses were unknown there was some difficulty in selecting the proper triggering mode initially. Both internal and external modes were used. However, throughout the latter part of the experiment all scopes were triggered in parallel,

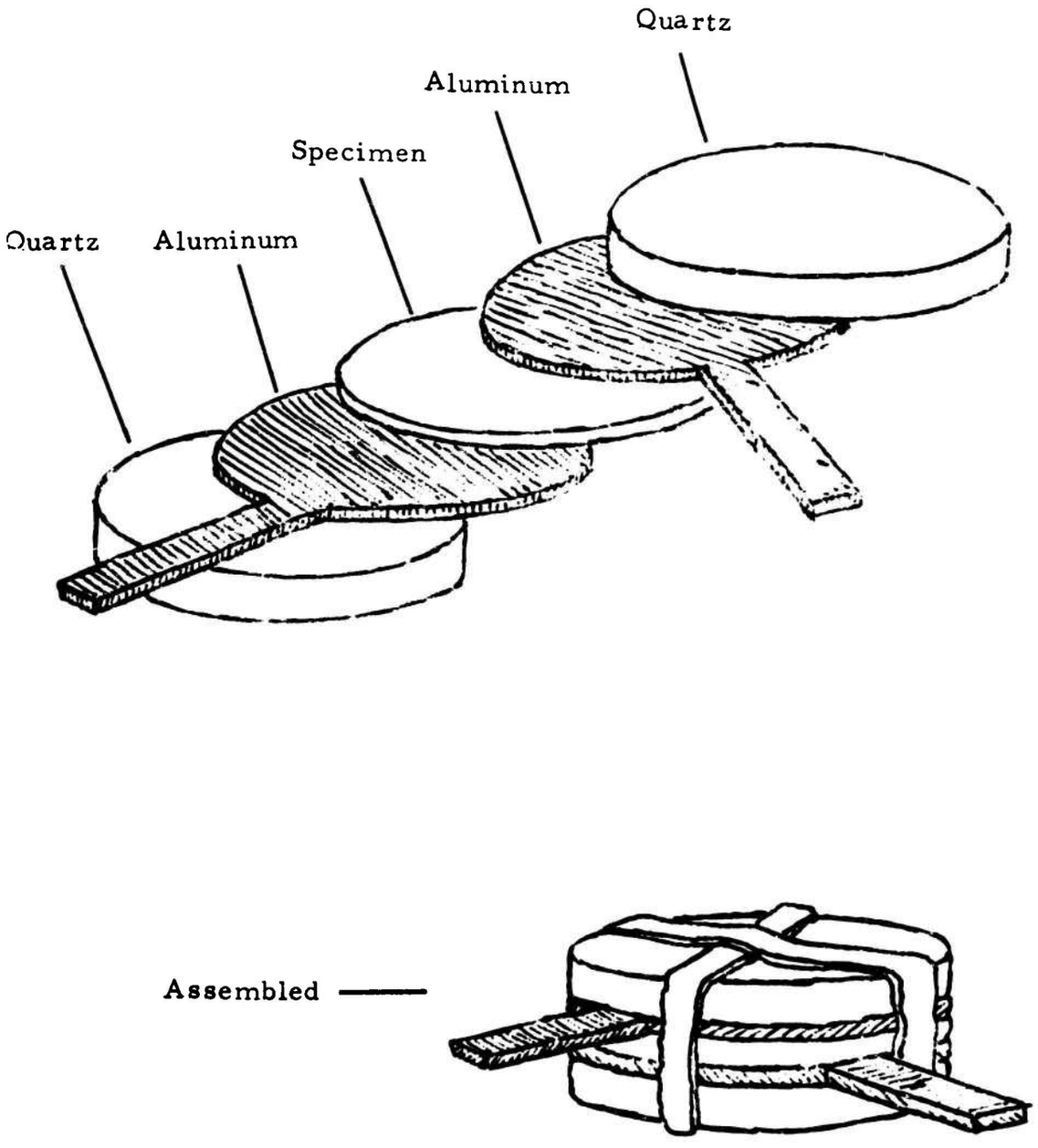

Figure 3. Specimen Assembly (1965)

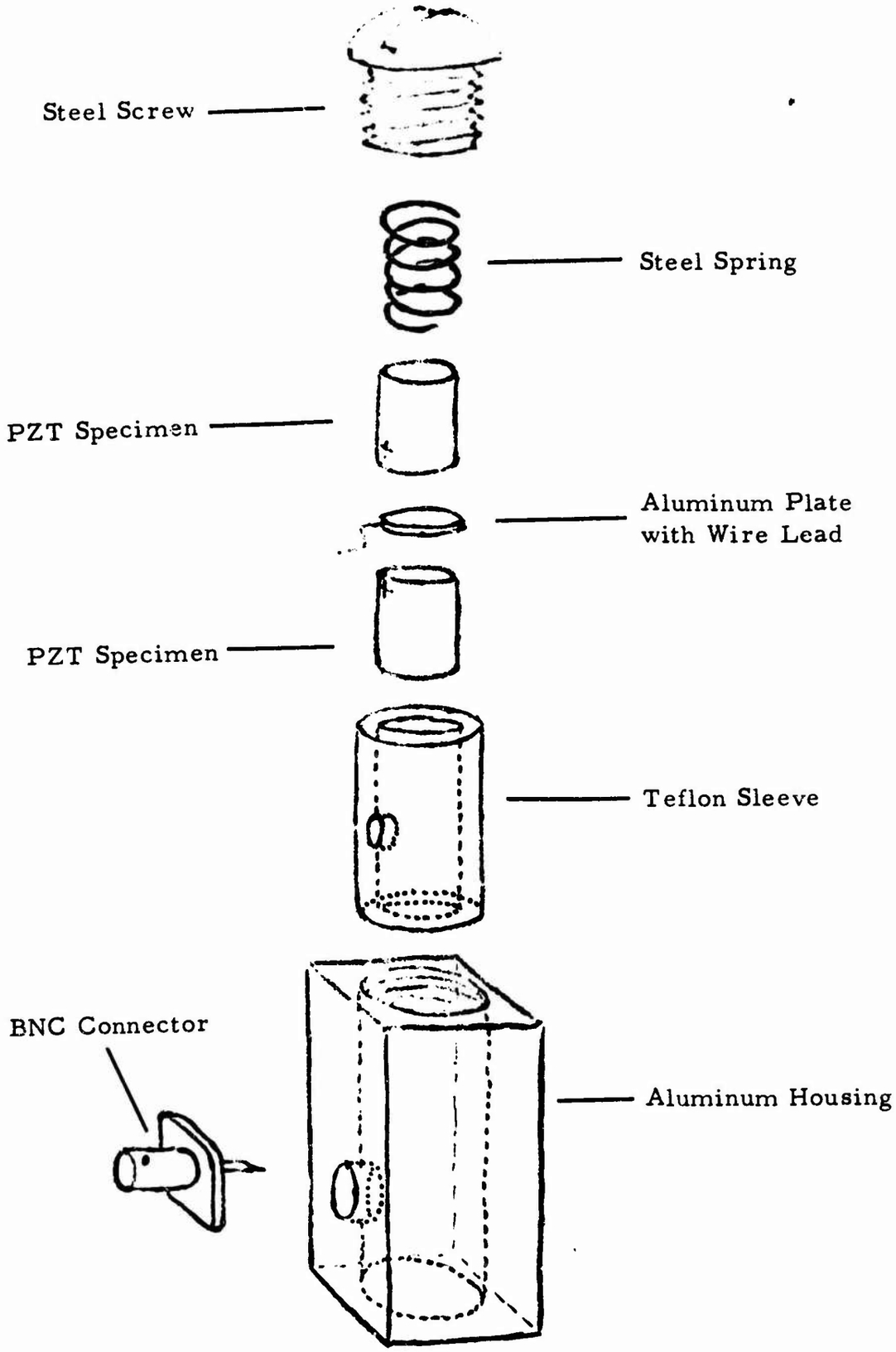

Figure 4. Specimen Assembly (1965)

externally, by an ionization chamber in the pool near the core. Trigger levels were set so that less than the first millisecond of the pulses was lost. A long tail distorted the pulse somewhat and made time comparisons difficult. A schematic of the specimen and monitoring equipment is given in Figure 5.

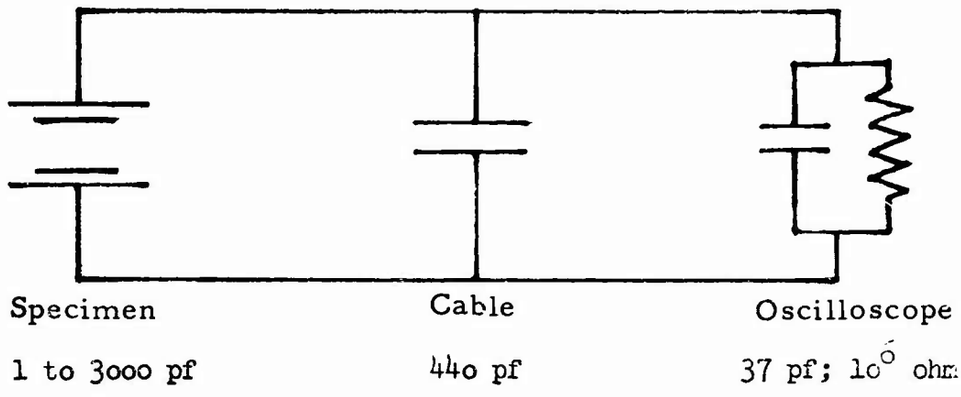

Figure 5. Monitoring Circuit

Radiation

The disc specimens were in most cases mounted with one face towards the radiation source. In some cases an attempt was made to orient the positive face forward. However, twisting of the cables usually turned the specimens enough to make the final orientation relatively random. Half of the cylinder pairs were mounted with their sides towards the core and half with their bottoms (the face away from the spring) towards the core.

In all cases the specimens rested on wooden boards against the wall of the exposure room nearest to the radiation source at the mid-height of the core. The core was in the dimple position, i.e., as close to the exposure room as possible. A few of the cylinder pairs were positioned as high as 20 cm above the core midpoint but this made no difference in their outputs.

No specific dosimetry was done in the exposure room during the irradiation but with the above configuration, the nominal radiation flux would be as given in Table VII.

Table VII. PARTICLE FLUX AT EXPOSURE ROOM WALL

Type of Radiation	Peak Dose (sec/cm^2) (mid-core-height)	Integrated Dose (pulse/cm^2) (mid-core-height)	Integrated Dose (pulse/cm^2) (10 cm off center)
Gammas (R)	3×10^7	5×10^5	5×10^5
Neutrons <0.4 ev (thermal)	9×10^{14}	1.5×10^{13}	1×10^{13}
Neutrons <10 ev (fast-Pu)	4×10^{15}	7×10^{13}	6×10^{13}

Integrated and peak dosages varied as much as 10% but there was no correlation between these variations and the voltage outputs observed.

Results and Discussion

The results of the irradiation are tabulated in detail in Appendix A, Part 2. The cylinder pairs were arranged in a housing designed to approximate an actual impact fuze. The output from the pairs was small – of the order of the background effects – and all except one or two gave negative pulses varying from -0.05 to -2.2 volts. The pulses from the quartz dummies varied about a value of -1.4 volts, and were all negative. There was little variation between the specimens from different sources. Possibly those specimens irradiated on their bottom faces gave slightly higher pulses than those irradiated on the sides. There were quite a few small odd shaped pulses whose origin is unknown.

Variations among the large discs were considerable. The largest pulse observed was 36 volts, with a fairly continuous distribution down to levels comparable to the dummy outputs. Disregarding the odd-shaped pulses, every pulse from every polarized specimen was positive. Among the unpolarized specimens 3/4 gave negative pulses, varying from +6 to -7 volts fairly continuously. The dummy specimens gave negative pulses (with one exception) varying from -0.4 to -3.0 volts. Although samplings are very small considering the variations observed, we can estimate that unpolarized specimens give pulses on the average 3 to 4 times the dummy output and polarized ones give pulses up to 20 times the dummy output or more, depending on manufacturer. Some typical pulses are shown in Figure 6.

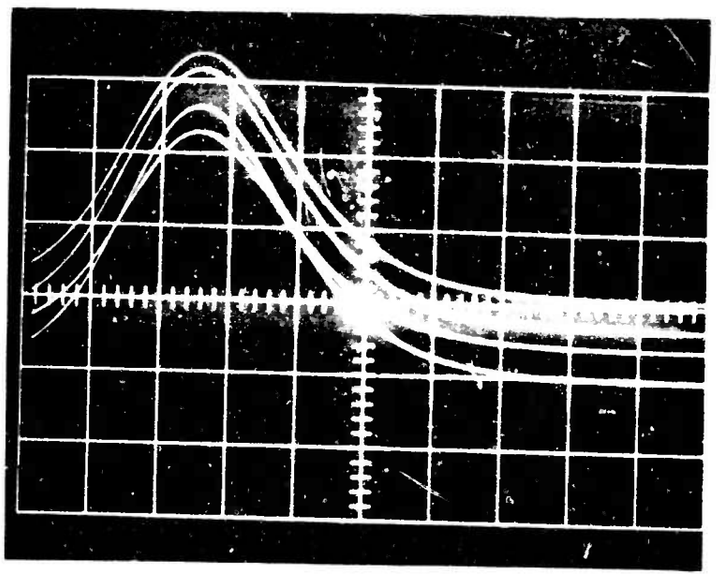

Pulse: 11
Trigger: internal
Sweep: 5 msec/cm
Sensitivity: 10 v/cm
Specimen: G-5,G-6,G-7,G-8

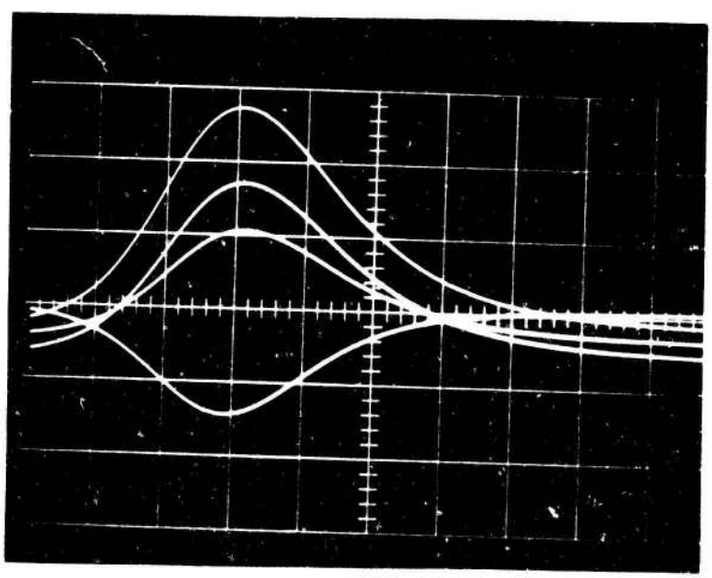

Pulse: 17
Trigger: external
Sweep: 5 msec/cm
Sensitivity: 2 v/cm
Specimen: G-3o, E-1o,
E-11, E-12

Figure 6. Typical Specimen Output Pulses

The most dramatic differences are observed between the supposedly similar poled specimens from the three manufacturers. However, this is probably due in part to differences in the immediate "history" of the specimens. There did not appear to be any significant differences between the unpoled specimens of Gulton and Erie. Also, no difference was observed between the loaded and unloaded specimens from Clevite.

The polarized specimens G-1 to G-15 were numbered at random and irradiated in two different groups, which show a definite difference in average output although all instrumentation was the same. There was a definite tendency for the output levels to increase from pulse to pulse and this effect would explain the differences between the average outputs from discs G-1 to G-9 and the lower averages from G-10 to G-15 which are from the same lot. The former group was irradiated 7 times before data was taken (while calibrating the oscilloscopes), and the increase in pulse magnitude occurred during this time. The quartz dummy specimens Q-9 and Q-10, which also were in the group that received the extra pulses of radiation, show a slight enhancement also; however, the unpoled specimens in the group, G-16 to G-24, do not.

The discs have a nominal capacity of 2500 pf and a load of 10^6 ohms. This gives a specimen time constant of 2.5 msec. Since the half width of the radiation pulse is 12.8 msec, we would expect the output from the disc to follow the radiation level variation. This was evidentally the case since the voltage pulses monitored invariably had half-widths of about 13 msec ± 1 msec, if well formed, with a peak position spread of not more than one or two milliseconds. The same is true for specimens of smaller capacity and specimens pulsed with smaller loads since the time constants are even shorter in these cases. Some dummy pulses preceeded the specimen pulses by as much as 3 msec. The trigger pulse, unfortunately, had a long time constant which gave it a 0.1 second tail and displaced the peak so that no comparisons are available.

Hester, et al., have irradiated some PZT specimens under similar circumstances and predict that the voltage maximum should be $V_{max} = ARk\dot{\gamma}$, where A is the cross-sectional area of the specimen, R the resistive load, $\dot{\gamma}$ the maximum radiation rate in RADS/sec, and k a constant equal to 0.96×10^{-12} coulombs/cm^2 RADS (H_2O). Since the peak dose rate at our specimen positions was about 3×10^7 we would expect pulses of about 150 volts from the 1" diameter discs with loads of 10^6 ohms. The pulses seen were about an order of magnitude less than this.

Some capacity measurements were made in situ. In general no changes or short term changes of up to 10% were noted directly after pulsing with a possible decrease in tan δ. However, the sensitivity of the bridge used at the reactor was not high and only a few measurements were taken.

ANALYSIS OF SOME TYPICAL FUZE CIRCUITS IN PRESENT USE

The following analysis treats only three specific fuze circuits (supplied by Picatinny Arsenal). Thousands of other circuits exist where the material is used as a capacitor. In the second part of this section there is a mathematical analysis of Circuit No. 1, in which energy transfer is considered in terms of wave shape and circuit constants.

Circuit Description

For Circuit No. 1, there are two principle components: a piezoid (usually made of a polarized ferroelectric ceramic) and a load. The circuit schematic is given in Figure 7. The load, of necessity, is a low energy, highly sensitive device with initiation threshold levels of the order of tens of volts and microcoulombs of charge. It is particularly prone to pre-ignition and several safety devices have been installed to minimize this (e.g., a leakage resistor in parallel with the piezoid permitting

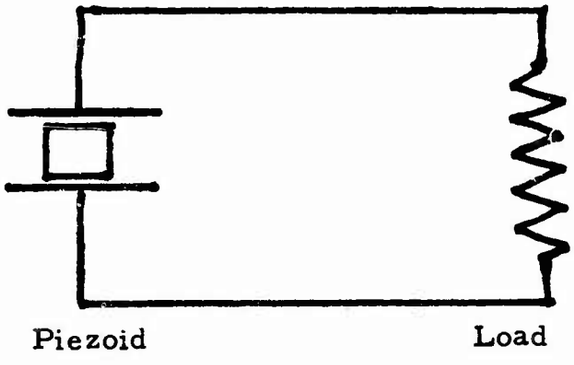

Figure 7. Circuit I

electrical charge to leak off since the latter may build up due to setback forces of accelerating the round to its flight velocity). It would be useful to investigate earlier designs to see if these safety features have been omitted. A mathematical treatment of this circuit has been done permitting the design engineer to evaluate the energy transfer from piezoid to load for two types of impulse wave forms.

The piezoid in the fuze design in Circuit II (see Figure 8) may be (and usually is) multiple, i.e., in series, parallel configuration. Here the system will not fire until a threshold voltage is exceeded (supplied by the piezoid) and the total energy stored in the charge storage capacitor C_C (externally charged) is permitted to empty into the load, activating the device. This circuit usually does not have the C_C charged until the system is in flight; but again, anomalies in the piezoid may cause difficulties. However, the amount of energy required to activate the load is high; therefore, the radiation sensitivity is not likely to produce a difficulty here.

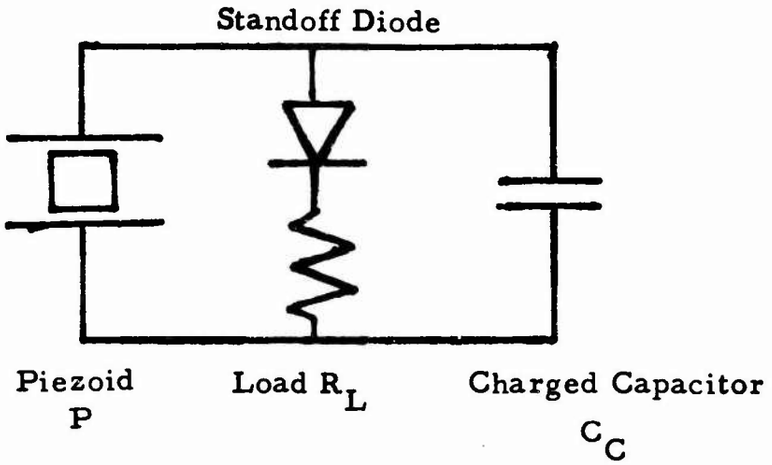

Figure 8. Circuit II

Circuit III (see Figure 9) is a type particularly prone to activation by the anomalous radiation sensitivity, but because the piezoid is usually expected to be a voltage source, considerable care is taken in the safety arrangements for isolating the piezoid from the load until activation is required.

We know that radiation sensitivities yield both positive and negative polarities. Therefore, one may envision two types of difficulties, one where the voltage on C_T would cancel that from the piezoid causing malfunction of the device as well as an addition of voltage which would cause anomalous pre-ignition, both minimizing the effectiveness of the device.

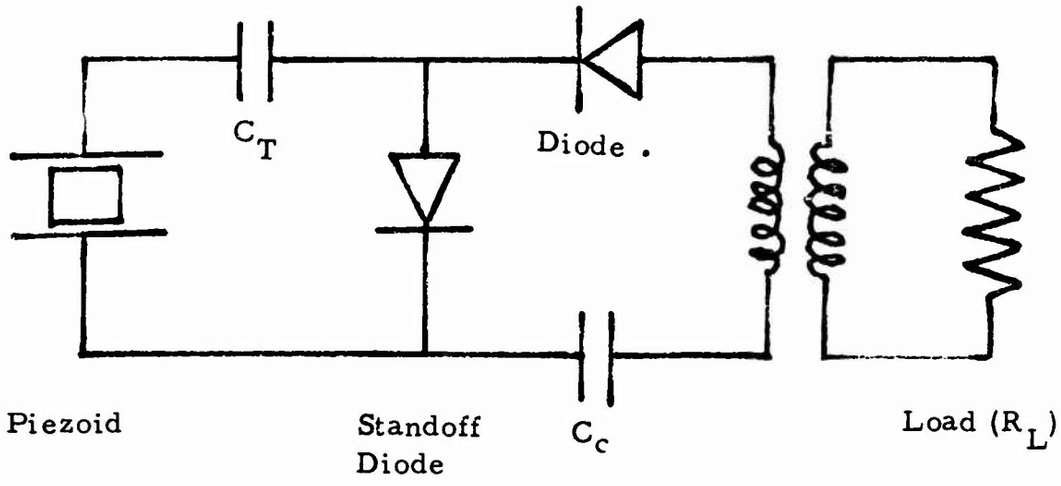

Figure 9. Circuit III

The circuits discussed are a small fraction of those using ceramic ferroelectrics. Further, the greatest danger lies in the systems where ceramic capacitors are used which are supposedly "inert" and may act as voltage sources. The circuits just discussed illustrate the problem.

Mathematical Analysis

The following treatment analyses Circuit I (Figure 10) in terms of energy transfer for two different types of waveforms. It invokes Thevinin's

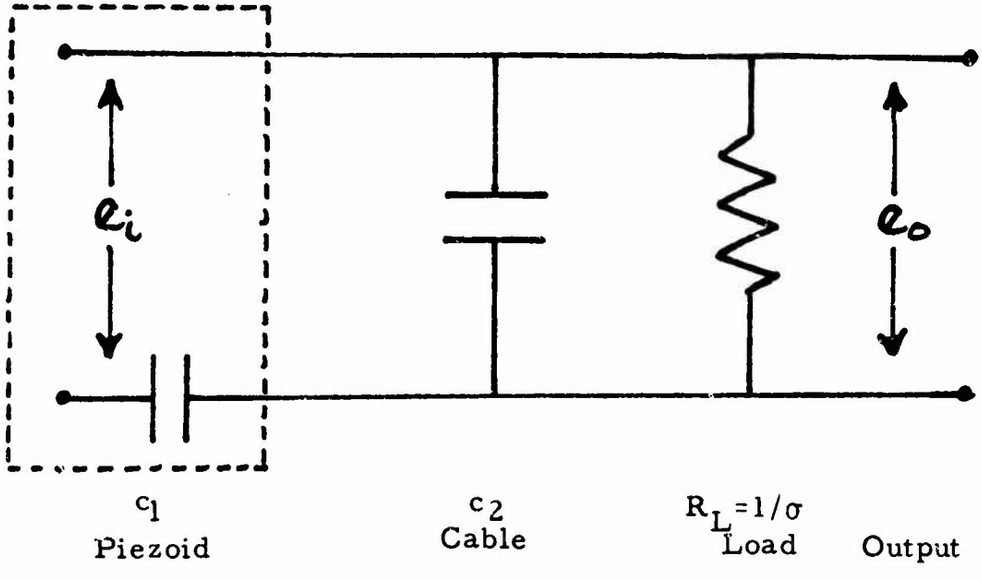

Theorem, utilizing Laplace transforms and obtaining a differential equation to evaluate energy transfer as a function of circuit parameters and wave shape. Part 1 treats a square waveform and Part 2 a triangular waveform.

$$\left[\sigma + s(c_1 + c_2)\right] L(e_o) - sc_1 L(e_i) = 0$$

$$L(e_o) = \frac{sc_1}{\sigma + s(c_1 + c_2)} L(e_i)$$

$$= \frac{c_1}{c_1 + c_2}\left[1 - \frac{\sigma}{\sigma + s(c_1 + c_2)}\right] L(e_i)$$

$$e_o = \frac{c_1}{c_1 + c_2}\left[e_i - \int_o^t \frac{\sigma}{c_1 + c_2} e^{-\frac{\sigma(t - \tau)}{c_1 + c_2}} e_i(\tau)d\tau\right]$$

$$\boxed{\sigma e_o + (c_1 + c_2)\dot{e}_o - c_1\dot{e}_i = 0}$$

Part 1

$$\sigma e_o^2 + (c_1 + c_2) e_o\dot{e}_o - c_1\dot{e}_i e_o = 0$$

$$\int \sigma e_o^2 dt + \frac{1}{2}(c_1 + c_2) e_o^2 \Big| - c_1 \int e_o\dot{e}_i dt = 0$$

$$E_{\Pi} = \int \sigma e_o^2 dt = \frac{1}{2} \frac{c_1^2}{c_1 + c_2} e_i^2 \Big| - \frac{1}{2}(c_1 + c_2) e_o^2 \Big|$$

$$- \frac{c_1^2}{c_1 + c_2} \int \dot{e}_i e^{-\frac{\sigma t}{c_1 + c_2}} \int \frac{\sigma}{c_1 + c_2} \dot{e}_i e^{\frac{\sigma \tau}{c_1 + c_2}} d\tau dt$$

$$= -\frac{1}{2}(c_1 + c_2) e_o^2 \Big| + \frac{c_1^2}{c_1 + c_2} \int_o^T \dot{e}_i e^{-\frac{\sigma t}{c_1 + c_2}} \int_o^t \dot{e}_i e^{\frac{\sigma \tau}{c_1 + c_2}} d\tau dt$$

$$\int_o^t \frac{\sigma}{c_1 + c_2} e_i e^{\frac{\sigma \tau}{c_1 + c_2}} d\tau = e^{\frac{\sigma t}{c_1 + c_2}} - 1 \qquad ; \; 0 < t < T$$

$$= e^{\frac{\sigma T}{c_1 + c_2}} - 1 \qquad ; \; T < t < \infty$$

$$\boxed{E_{\Pi} = V_p^2 \frac{c_1^2}{c_1 + c_2} \left(1 - e^{-\frac{\sigma T}{c_1 + c_2}}\right)} \quad ;$$

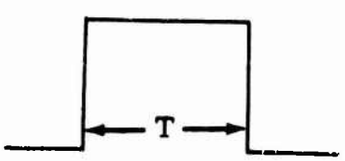

Part 2

Letting $k = 2V/T$

$$\int_0^t \dot{e}_i e^{\frac{\sigma\tau}{c_1 + c_2}} d\tau = k \frac{c_1 + c_2}{\sigma} \left(e^{\frac{\sigma t}{c_1 + c_2}} - 1 \right) \qquad ; \ 0 < t < \frac{T}{2}$$

$$= k \frac{c_1 + c_2}{\sigma} \left[e^{\frac{\sigma \frac{T}{2}}{c_1 + c_2}} - 1 - \left(e^{\frac{\sigma t}{c_1 + c_2}} - e^{\frac{\sigma \frac{T}{2}}{c_1 + c_2}} \right) \right] \ ; \ \frac{T}{2} < t < T$$

$$= k \frac{c_1 + c_2}{\sigma} \left(2e^{\frac{\sigma \frac{T}{2}}{c_1 + c_2}} - 1 - e^{\frac{\sigma t}{c_1 + c_2}} \right)$$

$$= k \frac{c_1 + c_2}{\sigma} \left(2e^{\frac{\sigma \frac{T}{2}}{c_1 + c_2}} - 1 - e^{\frac{\sigma T}{c_1 + c_2}} \right) \qquad ; \ T < t < \infty$$

$$E_{\Lambda} = \frac{c_1^2}{c_1 + c_2} \left\{ \int_0^{\frac{T}{2}} k^2 \frac{c_1 + c_2}{\sigma} \left(1 - e^{-\frac{\sigma t}{c_1 + c_2}} \right) dt \right.$$

$$\left. + \int_{\frac{T}{2}}^{T} k^2 \frac{c_1 + c_2}{\sigma} \left[\left(1 - 2e^{\frac{\sigma \frac{T}{2}}{c_1 + c_2}} \right) e^{-\frac{\sigma t}{c_1 + c_2}} + 1 \right] dt \right\}$$

$$= \left(\frac{2V}{T}\right)^2 \frac{c_1^2}{\sigma} \left\{ T + \frac{c_1 + c_2}{\sigma} \left[e^{-\frac{\sigma \frac{T}{2}}{c_1 + c_2}} - 1 \right] \right.$$

$$\left. - \frac{c_1 + c_2}{\sigma} \left(1 - 2e^{\frac{\sigma \frac{T}{2}}{c_1 + c_2}}\right) \left(e^{-\frac{\sigma T}{c_1 + c_2}} - e^{-\frac{\sigma \frac{T}{2}}{c_1 + c_2}}\right) \right\} 2$$

$$- 3e^{-\frac{\sigma \frac{T}{2}}{c_1 + c_2}} + e^{-\frac{\sigma T}{c_1 + c_2}}$$

$$E_{\Lambda} = \left(\frac{2V}{T}\right)^2 \frac{c_1^2}{\sigma} \left\{ T + \frac{c_1 + c_2}{\sigma} \left[-3 + 4e^{-\frac{\sigma \frac{T}{2}}{c_1 + c_2}} - e^{-\frac{\sigma T}{c_1 + c_2}} \right] \right\}$$

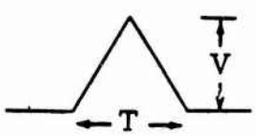

For a typical example, we take

$$c_1 >> c_2$$

and

$$T \approx \frac{c_1 + c_2}{\sigma} \approx \frac{c_1}{\sigma}$$

and we can simplify as follows:

$$E_{\wedge} = \left(\frac{2V}{T}\right)^2 \frac{c_1^2}{\sigma} \left\{ T + \frac{c_1 + c_2}{\sigma} \left[-3 + 4 \exp\left(-\frac{1}{2} \cdot \frac{\sigma T}{c_1 + c_2}\right) - \exp\left(-\frac{\sigma T}{c_1 + c_2}\right) \right] \right\}$$

$$= \frac{4V^2 c_1}{T} \left\{ T + T \left[-3 + 4 \exp\left(-\frac{1}{2}\right) - \exp\left(-1\right) \right] \right\}$$

$$= 4V^2 c_1 \left\{ 1 - 3 + \frac{4}{e^{1/2}} - \frac{1}{e} \right\}$$

$$= .23 V^2 c_1$$

$$E_{\sqcap} = V_p^2 \frac{c_1^2}{c_1 + c_2} \left[1 - \exp\left(\frac{-\sigma T}{c_1 + c_2}\right) \right]$$

$$= V_p^2 c_1 \left[1 - \frac{1}{e} \right]$$

$$= .63 V_p^2 c_1$$

Now, assume:

$$V = 500 \text{ volts (worst case)}$$

$$c_1 = 2450 \text{ pf}$$

$$c_2 = 50 \text{ pf}$$

$$\sigma = 10^{-6} \text{ mhos} \left[\text{or } R = 10^6 \text{ ohms}\right]$$

$$\tau = R(c_1 + c_2) = 2.5 \times 10^{-3} \text{ sec}$$

$$\therefore E_{\Lambda} = .23 V^2 c_1 = 140 \text{ ergs}$$

and

$$E_{\Pi} = .63 V_p^2 c_1 = 390 \text{ ergs}$$

which are the energies transferred for the two pulse shapes.

SUMMARY AND CONCLUSIONS

The results obtained from these experiments show conclusively that sizeable outputs of electrical energy can be expected when perovskite ferroelectrics are irradiated. Further, there exists a wide range of radiation sensitivities, even with specimens ostensibly alike. The maximum sensitivity and the amount of electrical energy that can be delivered when the ferroelectric materials are irradiated is not known.

The output observed is not due to the piezoelectric* or secondary pyroelectric effects because there is no mechanical loading associated

*Piezoelectricity is the emf produced across a material when it is mechanically loaded. It is normally not found in ferroelectric materials in their ceramic form, but can be induced by application of a large DC field while the ceramic is cooled thru the Curie temperature.

with the reactor pulse. The direct pyroelectric* effect may be ruled out on several grounds: (1) the wide variation of the pulses would not occur if they were due only to pyroelectric effects; (2) the pulse shapes are symmetrical and show no tail or reverse dip which would be seen with pyroelectric effect pulses since the specimens would cool more slowly than they heat and cooling would give a negative pulse; and (3) the output seen by the nonpolarized specimens could not be due to pyroelectric effect.

Since the mechanism is not understood, any series of tests must be planned to take into consideration variation of fabrication (e.g., particle size distribution of powder used for the ceramic) or testing (e.g., voltages used to measure breakdown in ceramic or polarization voltages) or possibly other factors. The wholly independent work of the group at Sandia (Hester et al.) suggest that this effect be used as a dosimeter. They claim that 100% of their samples gave reproducible outputs. This is in conflict with our work and possibly that of Kesselman, where wide variation in sensitivity was found. It should be emphasized that the Sandia group worked with only about ten samples, while the new work covers a total of about 200 samples.

A further difficulty can arise if designs are produced which do not recognize this radiation sensitivity as a possible source of electrical energy. A case in point is the development of a ferrite-ceramic RF attenuator (Report No. 2400-5754-3 by Genistron, Inc., Los Angeles, Calif., for the Naval Weapons Laboratory) in which there is a shunt capacity for attenuation of RF energy. A ferroelectric capacitor in just such an application could provide sufficient electrical energy to produce anomalies in operation which would be wholly unexpected.

Previous studies have given a very misleading picture of the ultimate safety of these devices because this radiation sensitivity had not been identified. It is clear that an understanding of this phenomenon may lead to its control.

The real danger lies in this phenomenon going unrecognized and undisclosed as a possible difficulty in circuits that use these materials. Capacitor applications have not been discussed here in detail because of the magnitude of the problem. Mr. Ralph Brown of this laboratory visited the U. S. Army Missile Command, Huntsville, Alabama, and to quote directly from the trip report:

---

*Pyroelectricity is the emf produced across a material due to a change with temperature of its positive and negative polarization charges.

"Since Lance, Shillelagh, and TOW are still in the Research and Development stage, no specifications on materials of capacitors would be available.

"Hercules, Hawk, Pershing, and Sergeant are in Procurement and Production. Hundreds of drawings and specifications of components of circuits would be available for review. But in general only the electrical characteristics of the capacitors would be described – no materials. The specifications would include only such requirements as tolerances, temperature restrictions, etc. In some cases manufacturers' numbers only would be indicated. The consensus was that the specific type of capacitor material used in a circuit could only be obtained from the contractor and/or manufacturer".

The point here is that the responsible command does not specify the capacitor material that is used.

Normally where a system utilized a device as a source of voltage or electrical energy, care is taken to isolate it from anomalies associated with the production of voltages at an inopportune time. In the case of capacitors, this danger is never considered since the design engineer never considers the possibility of a capacitor as a voltage generator.

RECOMMENDATIONS

It is recommended that the following action be taken immediately on this problem. The impetus for this must come from an authority high enough to cross many areas of responsibility.

There should be a concerted attempt to understand the mechanism of the phenomenon. This should include (1) an analysis of potential gradients in single crystals and ceramic materials; (2) studies of electrodes and electrode materials; (3) an analysis of differences in manufacturing techniques producing different radiation sensitivities; and (4) a theoretical study of the role of trapping centers and their dynamics in ferroelectric materials.

A warning should be given that ferroelectric materials used in ceramic capacitors may act as voltage sources in a pulsed radiation environment. (The new monolithic ferroelectric capacitors have many advantages and are being used in large quantities because of their small size, flat temperature coefficient and large effective dielectric constant.) If circuits are found to be particularly vulnerable to malfunctions due to the generation of an electric charge in their ferroelectric components, such components must be identified. The manufacturers fabrication technique must be established and a pulse reactor testing program devised for such ferroelectrics. Until a complete understanding is at hand it would be safer to replace these capacitors with glass or mica in critical circuits.

REFERENCES

1. Känzig, W., Phys. Rev. 93, 549 (1955).

2. Merz, W. J., J. Appl. Phys. 22, 938 (1956).

3. Chynoweth, A. G., Phys. Rev. 102, 705 (1956).

4. Wieder, H. H. and White, D. J., NOL Corona, Tech. Memo No. 42-28, May (1959); cited in Jona and Shirane: Ferroelectricity, Macmillan, 1962.

5. Triebwasser, S., Phys. Rev. 118, 100 (1960).

6. Harmon, G. G., Phys. Rev. 111, 27 (1958).

7. Lefkowitz, I., Frankford Arsenal Summary Report, Contr. No. DA-30-069-507-ORD-1866 (1960) (Gulton Industries, Inc.).

8. Lefkowitz, I., Nature, 198, #4881, p. 657-659 (1963).

9. Kesselman, R., Picatinny Arsenal Tech. Report No. 3045 (Jan 1963).

10. Hester, D. H., et al, I.E.E.E. Transactions on Nuclear Science (Nov 1964).

APPENDIX A

REDUCED DATA

Part 1: July-August 1964

The data accumulated at the Diamond Ordnance Radiation Facility during 95 pulses is presented in the following pages. Between 10 and 20 specimen positions were utilized for each pulse for a total of 1675 specimen-pulses. Of these 350 were from so-called "dummy" positions, i.e., control sample positions which monitor background potentials which may result from the irradiation of glass and cable assembly. The remaining 1325 were divided among 80 different specimens, each receiving between 8 and 62 radiation pulses.

Dielectric constant versus temperature determinations were run of samples S-1, S-2, and R-25 before the irradiation and these were presumably the only unpolarized specimens.

The specimen coding was given in Table 1. In the following display the voltage output across a load of 50K ohms in parallel with 47 mmf is entered for each pulse and each specimen. The following explanations will be useful:

Polarity was not noted on the first 8 pulses.

A dash indicates the specimen was in the core but no reading was taken.

A "*" - asterisk indicates a significant output change.

"INIT" indicates that the specimen output went to a simulated detonator.

A specimen label in brackets in the "dummy" outputs means that there was a specimen in the position but capacity measurements indicated that the specimen had slipped partially or totally out of position.

The data tabulation is followed by Table IX giving the peak power and integrated power of the reactor output for each pulse.

Notes to Tables VIII and IX.

a. Oscilloscope used with 10^6 ohm load on specimen.

b. Oscilloscope used with 10^7 ohm load on specimen.

c. Amplifier channel changed previous to pulse labeled.

d. Data difficult to read.

e. Endevco amplifier used to monitor specimen pulse.

f. Pulse off scale.

g. Amplifier gain changed previous to pulse labeled.

h. "Hash"; partially obscured pulse.

i. Dummy fuel element with specimen rotated previous to pulse labeled.

j. Short in monitoring line.

k. Specimen physically reversed.

ℓ. Load on specimen not 50K ohms if on oscillograph; not 10^6 or 10^7 ohms if on oscilloscope.

m. Oscillograph paper ran out.

n. Specimen leads reversed.

Table VIII-a. REDUCED DATA

Specimen	Pulse - July 14								Pulse - July 28				
	1	2	3	4	5	6	7	8	9	10	11	12	13
I-3-1	-[b]	-[b]	-[b]	-[b]	-[b]	-[b]	-[b]	-[b]	+>3[c]	+>3	+6.3[g]	+6.3	-
I-3-2	-	-	>3	>3	-	-	>3	>3	+>3[c]	+>3	+5.2[g]	+5.0[g]	-
I-3-3													
I-3-4													
C-4-5	-	>3	>3	>3	-	-	>3	>3	-[a]	-[a]	+20[a,d]	+20[a,d]	-
C-4-6									+2.8[c]	*+>3[c]	+>3	+5.7[g]	-
C-4-7													
C-4-8													
779-1									+>3	+>3	+4.0[g]	+3.8[g]	-
779-2	-	-	3.1	3.1	3.1	3.1	3.1	3.1	*+>3[c]	+9.9[g]	+10.0	+10.0	-
779-3													
779-4													
779-5													
779-6													
780-1	-	>3	>3	>3	>3	>3	>3	>3	+>3[c]	+7.0[g]	+6.8	+6.8	-
780-2									+2.0	-[j]	-[j]	-[j]	-
780-3	-	-	-	-	-	-	-	-	-	-	-	-	-
Ba-2													
Ba-3													
Ba-4													
Ba-25	1.7[d]	1.5	1.5	1.5	1.5	1.5	1.5	1.6	*+.7[c]	*-[j]	-[j]	+1.9	
Ba-31													
Ba-50	-	2.1	2.1	2.1	2.1	2.1	2.1	2.1	*+1.4[c]	+>1.5[c,f]	+1.9	+2.0	
Ba-64	-	.2	.2	.2	.2	.2	.2	.2	*+1.8[c]	*-.7[c]	-.7	*+>1[f]	
Ba-89													

Table VIII-a. (Cont'd)

Specimen	Pulse - July 29													
	14	15	16	17	18	19	20	21	22	23	24	25	26	27
I-3-1	*+7.2	+7.2	+7.2	+7.3	+7.3	+6.7[l]	+6.1[l]	+4.0[l]	+4.2[l]	+3.2[l]	+7.7[l]	+1.5[l]	+2.8[l]	*+8.0
I-3-2	+5.3	-[m]	+5.0	+5.0	+5.0	+5.1	+5.1	+2.5[l]	+2.6[l]	+2.4[l]	+5.2	+.15[l]	+.93[l]	+5.3
I-3-3														
I-3-4														
C-4-5	-[a]	-[a]	-[a]	+20[a,d]	-[a]	+20[a,d]	-[a]	-[a]	-[a]	+20[a,d]	+7.8	+7.7	+7.7	+7.7
C-4-6	*+7.4	+7.2	+7.1	+7.2	+7.1	+7.1[l]	+6.8[l]	+4.0[l]	+3.8[l]	+3.4[l]	+7.1	+1.4[l]	+.21[l]	+7.3
C-4-7														
C-4-8														
779-1	+3.9	+3.8	+3.8	+3.8	+3.8	+3.8	+3.8	+3.8	+3.8	+3.8	+3.8	+3.8	+3.8	+3.8
779-2	+10.2	-	+5.2[l]	+5.0[l]	+5.0[l]	+10.3	+7.9[l]	+1.8[l]	+1.7[l]	+1.8[l]	*+5.3	+5.3	+5.3	+5.3
779-3														
779-4														
779-5														
779-6														
780-1	+6.7	-[m]	+6.6	+6.6	+6.8	+6.0[l]	+5.4[l]	+3.8[l]	+3.8[l]	+2.5[l]	+6.8	+.2[l]	+1.4[l]	+6.7
780-2	*+>3	+6.5[g]	+6.5	+6.5	+6.5	+6.7	+6.7	+6.5	+6.5	+6.5	-[b]	-[b]	+60[b]	+55[b]
780-3	-	-	-[f]	-[f]	+4.8	+4.9	+4.9	+4.7	+4.8	+2.5[l]	+4.9	+.9[l]	+.1[l]	+5.0
780-4														
780-5														
780-6														
Ba-2														
Ba-3														
Ba-4														
Ba-25	+2.4	+2.3	+2.3	+2.2	+2.1	+2.1	+2.1	+2.1	+2.1	+2.1	+2.1	+2.1	+2.1	+2.1
Ba-31														
Ba-50	+2.1	+2.1	+2.1	+2.1	+2.1	+2.1	+2.1	+2.1	+2.1	+2.1	+2.1	+2.1	+2.1	+2.1
Ba-64	+1.5	+1.5	+1.5	+1.5	+1.5	+1.8	+1.6	*-.7	-.7	*+1.5	+1.6	+1.6	+1.6	+1.6
Ba-89														

Table VIII-a. (Cont'd)

Specimen	Pulse - July 30					Pulse - July 31								
	28	29	30	31	32	33	34	35	36	37	38	39	40	41
I-3-1	+8.5	+50[b]												
I-3-2	+5.1	+5.1												
I-3-3			-[b]	+3.5	+3.8	+3.5	+3.6	-[c,j]	+3.2	+3.4[n]	+3.4	+3.4	-[m]	+3.3
I-3-4			+5.0	+5.2	+5.0	+5.3	+5.3	+3.4[l]	+2.3[l]	+5.1	+5.2	-[j]	-[m]	-[j]
C-4-5	+7.4	*+8.3[c]												
C-4-6	+6.9	+7.2												
C-4-7			+2.9	*+6.4	+6.8	+6.8	+7.0	-[b]	+25[b]	+26[b]	-[a]	+20[a]	+19[a,l]	+18[a]
C-4-8			-[j]	-[j]	-[j]	-[j]	-[j]	-[j]	-[j]	-[j]	-[j]	-[j]	-[j]	-[j]
779-1	+3.7	+3.8												
779-2	+5.0	+5.2												
779-3														
779-4			+2.2	+2.0[g]	+2.0	+2.0	+2.0	+2.0	+2.0	+1.9	+1.9	+2.1	-[m]	+2.0
779-5			-	+1.3	+1.2[g]	+1.2	-[j]	*+3[n]	+3.5[g]	+3.6	+3.6[h]	+3.5	-[m]	+3.5
779-6			+4.8	*-[a]	+15[a]	-[a]	4[a,h]	+3.0	+2.8	+3.0	+3.0	+2.9	-[m]	+2.8
780-1	+6.5	*+7.5												
780-2	+60[b]	+6.6												
780-3	+4.9	+4.8												
780-4			+5.8	*+7.3	+7.3	+7.3	-[b]	+38[b]	-[b]	-[b]	-[a]	-[a]	+25[a]	-[a]
780-5														
780-6			+4.4	*+5.9	+6.0	+6.0	+6.1	+3.7[l]	+2.7[l]	+5.9	-[j]	-[j]	-[m]	-[e]
Ba-2														
Ba-3														
Ba-4														
Ba-25	+2.2	+2.2												
Ba-31			+2.0	+2.1[g]	+2.0	+2.0	+2.0	+2.0	+2.0	+2.0	+1.9	+1.9	-[m]	+1.9
Ba-50	+2.2	+2.1												
Ba-64	*-.7	-.7												
Ba-89			+.7	+.5[g]	+.5	+.4	+.5	+.5	+.4	+.5	+.5	+.4	-[m]	+.4

Table VIII-a. (Cont'd)

Specimen	Pulse - August 4							Pulse - August 5								
	42	43	44	45	46	47	48	49	50	51	52	53	54	55	56	57
I-3-1				*+2.8[c,k]	+2.3[g]	+2.5	+2.6	+2.5	+1.9[h]	+1.9[d]	+2.2[h]	+2.5	+2.4	*+>3.0[c,f]	-[m]	+5.1[g]
I-3-2																
I-3-3	+3.3	+3.3	+3.3													
I-3-4	*+>3[g]	+4.4[c]	+4.4													
C-4-5				+8.0[c]	+8.2	+8.2	+8.2	+7.9	+7.9	-[a]	-[a]	-[a]	-[a]	-[a]	+11[a]	-[a]
C-4-6				+7.4[c]	+7.5	+7.5	+7.5	+6.8	+7.3	+7.4	+7.4	+7.4	+8.0	+8.0	-[m]	+8.1
C-4-7	-[a]	-[a]	-[a]													
C-4-8	-[j]	-[j]	-[j]													
779-1																
779-2				*-2.5[c,k]	*-1.8	-1.8	-1.9	-1.7	-1.7	*+1.4	+1.5	+1.4	+1.5	+1.4	-[m]	+1.4[n]
779-3				+4.7[c]	+4.7	+4.7	+4.7	+4.4	+4.4	+4.5	+4.5	+4.5	*+5.3	+5.4	-[m]	+5.3
779-4	*+2.4	+2.5	+2.5													
779-5	+3.5	+3.5	+3.5													
779-6	+2.9	+2.9	+2.9													
780-1																
780-2																
780-3																
780-4	-[a]	-[a]	-[a]													
780-5				+3.4[c]	-[d]	*+4.6	+4.6	+4.4	+4.4	-[a]	-[a]	-[a]	-[a]	+25[a]	-[a]	-[a]
780-6	*+5.3	-[e]	-[e]													
Ba-2				+2.8	+2.3[g]	+2.3	+2.3	+2.3	+2.3	-[a]	+2.3	+2.3	+2.3	+2.3	+2.4	+2.4
Ba-3				+2.9	+>2[g]	+>3[c]	+3.1[g]	+2.8	+2.8	-[e]	-[e]	-[e]	-[e]	-[c,e]	-[c,e]	-[c,e]
Ba-4				+2.0	-[d,g]	+2.2	+2.2	+2.2	+2.2	+2.3	+2.3	+2.2	+2.2[c]	+2.1	+2.1	+2.1
Ba-25																
Ba-31	+2.0	+2.0	+2.0													
Ba-50																
Ba-64																
Ba-89	+.5	+.5	+.5													

Table VIII-a. (Cont'd)

Specimen	Pulse - August 6								Pulse - August 7						
	58	59	60	61	62	63	64	65	66	67	68	69	70	71	72
I-3-1	+5.2	*+4.8[i]	*+5.2	+5.6	+6.0	+6.5[i]	*+7.0	+6.5[i]							
I-3-2															
I-3-3															
I-3-4															
C-4-5	-[a]	-[a]	-[a]	+20[a]	+22[a]	+20[a]	-[b]	-[b]							
C-4-6	+7.7	*+8.3[i]	+7.7	+7.7[i]	+7.3	-[a,i]	-[a]	-[a,i]							
C-4-7															
C-4-8															
779-1															
779-2	+1.2	*-.8	-.8[c]	-.8	-.8	-.6	-.6	-.7							
779-3	+5.2	+5.3[i]	+5.2	*+4.8[i]	+4.7	+4.6[i]	+4.9	+4.5[i]							
779-4															
779-5															
779-6															
780-1															
780-2															
780-3															
780-4															
780-5	+27[a]	-[c,e]	-[e]	-[e]	-[e]	-[c,e]	-[e]	-[e]							
780-6															
Ba-2	+2.3	+2.3[i]	+2.4	+2.7[i]	+2.7	*+>3[i]	+4.8[g]	+4.8[i]							
Ba-3	*-.2	-.2[c]	-.3	-.2	-.2	-.3	-.2	-.3							
Ba-4	+2.1	+2.1[g]	+2.1	+2.1	+2.1	+2.0	+2.4	+2.1							
Ba-25															
Ba-31															
Ba-50															
Ba-64															
Ba-89															

Table VIII-a. (Cont'd)

Specimen	Pulse - August 10			Pulse - August 13							
	73	74	75	76	77	78	79	80	81	82	83
I-3-1				*-6.9[c]	->20[a]	-80[a]	-[b]	-300[b]	-280[b]	-80[a]	INIT
I-3-2											
I-3-3											
I-3-4											
C-4-5											
C-4-6											
C-4-7											
C-4-8											
779-1											
779-2				-[c]	-	-	-[a]	+40[b]	+75[b]	*+3.1	+3.0
779-3											
779-4											
779-5											
779-6											
780-1											
780-2											
780-3											
780-4											
780-5											
780-6											
Ba-2											
Ba-3				-	-	-	-.3	-.2[g]	-.2	-.2	-.3
Ba-4											
Ba-25											
Ba-31											
Ba-50											
Ba-64											
Ba-89											

Table VIII-a. (Cont'd)

Pulse - August 14

Specimen	84	85	86	87	88	89	90	91	92	93	94	95
I-3-1												
I-3-2	*+6.0[c]	+6.2	+6.2	+6.2	+25[b]	+>15[a]	+20[a]	+5[a,l]	+5.3	+5.3	+5.3	+5.2
I-3-3	*+6.4[c]	+6.5	-[e]	-[e]	-[e]	-[e]	-[e]	-[e,i]	-[e]	-[e]	-[e]	+5.0
I-3-4	*+5.3[c]	+5.3	+5.3	+5.3	+25[b]	+>15[a]	+20[a]	+5[a,l]	*+4.8	+4.8	+4.8	+4.8
C-4-5	+>12[a,c]	+21[a]	-[b]	-[b]	*+5.8	+>3[g]	+>3	+5.5[g,i]	+5.2[c,f]	+6.0[n]	+6.0	+6.0
C-4-6	*+5.1[c]	+5.5	+5.6	+5.5	+5.3	+5.7	+5.6	+5.6	*+7.1	-[a]	+18[a]	-
C-4-7												
C-4-8												
779-1	-	-	-	-	-	-	-	-	-	-	-	-
779-2												
779-3	*+2.3[c]	+2.5	+2.5	+2.5	+2.3	+2.3	+2.3	+2.3	+2.3	+2.3	+2.3	+2.4
779-4												
779-5												
779-6												
780-1	*+5.3[c]	+5.3	+5.4	+5.4	+5.3	+5.3	+5.3	+5.4	+5.2	+5.2	-[b]	+23[b]
780-2	*+5.6[c]	+5.8	+5.8	+5.8	+5.6	+5.7	+5.7	+5.7[i]	+15[b]	+20[b]	+5.1[c]	+5.1
780-3	*+6.4[c]	+6.5	+6.7	+6.6	+18[a]	-[b]	+25[b]	-[a,l]	+7[a,l]	+6.7	+6.8	+6.7
780-4	*+5.5[c]	+5.7	+5.8	+5.6	+5.5	+5.6	+5.7	+5.5[i]	+15[a]	+18[a]	*+6.8	*+5.5
780-5												
780-6												
Ba-2												
Ba-3												
Ba-4												
Ba-25												
Ba-31												
Ba-50												
Ba-64												
Ba-89												

Table VIII-b. REDUCED DATA

Pulse - July 29

Specimen	17	18	19	20	21	22	23	24	25	26	27
PZT 70	+2.8	+2.9	+3.0	+2.9	+2.9	+2.9	+3.0	+3.0	+3.0	+3.0	+3.0
71	+2.7	+2.7	+2.8	+2.7	+2.7	+2.7	+2.7	+2.7	+2.8	+2.7	+2.8
72	+1.6	+1.6	*+2.1	*+1.6	+1.6	*2.1	*+1.7	+1.6	+1.6	+1.6	+1.6
74	+1.8	+1.8	+1.7	+1.7	+1.7	+1.7	+1.7	+1.7	+1.7	+1.7	+1.7
77	-	-	-	-	-	-	-	-	-	-	-
78	+1.4	+1.4	+1.5	+1.5	+1.4	+1.4	+1.4	+1.5	+1.5	+1.4	+1.4
79											
80											
D-1											
D-2											
1-A											
2-A											
3-A											
4-A											
1-B											
2-B											
3-B											
4-B											
S-1											
S-2											

Table VIII-b. (Cont'd)

Specimen	Pulse - July 30					Pulse - July 31								
	28	29	30	31	32	33	34	35	36	37	38	39	40	41
PZT 70	+2.9	+2.9												
71	+2.8	+2.7												
72	+1.6	+1.5												
74	+1.7	+1.7												
77	-	-												
78	+1.5	+1.4												
79														
80														
D-1			+.3	+.3g	+.3	+.3	+.3	+.3	+.3	+.3	+.3	+.3	-m	+.3
D-2			-	-	-	-	-	-	-	-	-	-	-	-
1-A			+.8	+.7g	+.7	+.7	+.7	+.7	+.7	+.7	+.7	+.7	-m	+.7
2-A			-	-	-	-	-	-	-	-	-	-	-	-
3-A														
4-A														
1-B			+.5	+.7g	+.5	+.5	+.5	+.5	+.5	+.5	+.5	+.5	-m	+.5
2-B			-	-	-	-	-	-	-	-	-	-	-	-
3-B														
4-B														
S-1														
S-2														

Table VIII-b. (Cont'd)

Specimen	Pulse - August 4							Pulse - August 5								
	42	43	44	45	46	47	48	49	50	51	52	53	54	55	56	57
PZT 70																
71																
72																
74																
77																
78																
79				+2.7	+3.0[g]	+3.0	+3.0	+3.0	+3.0	+3.0	+3.0	+3.0	+3.0	*+2.6	+2.6	+2.6
80				+1.3	+1.5[g]	+1.5	+1.5	+1.5	+1.7	+1.7[c]	+1.7	+1.7	+1.7	+1.7	+1.7	+1.7
D-1	+.2	+.2	+.2													
D-2	-	-	-													
1-A	+.5	+.5	+.5													
2-A	-	-	-													
3-A				-1.4	-1.2[g]	-1.2	-1.2	-1.2	-1.2	-1.2	-1.2	-1.2	-1.2	-1.2	-1.2	-1.2
4-A				-.b	-.b	-.b	-.b	-.b	-.b	-.7	-.7	-.7	-.7[c]	-.6	-.6	-.6
1-B	+.6	+.6	+.6													
2-B	-	-	-													
3-B				-1.0	-1.2[g]	-1.2	-1.2	-1.2	-1.2	-1.2	-1.2	-1.2	-1.2	-1.2	-1.2	-1.2
4-B				-.a	-.a	-.a	-.a	-.a	-.a	-.7	-.2	-.5	-.5[c]	-.5	-.5	-.5
S-1				-.7	-.9[g]	-.9	-.9	-.9	-.8	-.8	-.8	-.8	-.8	-.9	-.9	-.9
S-2				-.2	-.2[g]	-.2	-.2	-.2	-.2	*+3.1[c]	+3.0	+3.1[c]	+3.0[f]	*+1.5[c]	-.m	+1.5

Table VIII-b. (Cont'd)

Specimen	Pulse - August 6								Pulse - August 7						
	58	59	60	61	62	63	64	65	66	67	68	69	70	71	72
PZT 70															
71															
72															
74															
77															
78															
79	*+3.0	+2.9[i]	+2.9	+3.0[i]	+2.9	+3.1[i]	+3.1	+3.1[i]							
80	+1.7	+1.7[i]	+1.7	+1.6[i]	+1.6	+1.7[i]	+1.7	+1.7[i]							
D-1															
D-2															
1-A															
2-A															
3-A	-1.2	*-1.4[i]	-1.4	-1.4[i]	-1.4	-1.2[i]	-1.3	-1.2[i]							
4-A	-.6	-.5	-.6	-.6	-.6	-.5	-.6	-.6							
1-B															
2-B															
3-B	-1.2	-1.2[i]	-	-[i]	-	-[i]	-	-[i]							
4-B	-.5	*+1.2	*-.5	-.7	-.6	-.6	*+.6	*-.6							
S-1	-.9	-.8[i]	-.8	-.8[i]	-.8	-.8[i]	-.8	-.8[i]							
S-2	+1.2	+1.5	+1.5[c]	+1.5	+1.3	+1.3[c]	+1.4	+1.3							

Table VIII-b. (Cont'd)

Specimen	Pulse - August 10			Pulse - August 13							
	73	74	75	76	77	78	79	80	81	82	83
PZT 70											
71											
72											
74											
77											
78											
79				-	-	-	-	-	-	-	-
80											
D-1											
D-2											
1-A											
2-A											
3-A											
4-A											
1-B											
2-B											
3-B											
4-B											
S-1											
S-1											

Table VIII-c. REDUCED DATA

Specimen	Pulse - August 7							Pulse - August 10		
	66	67	68	69	70	71	72	73	74	75
K-1	+.4	+.6[g]	+.6	+.6	+.6	+.7	+.7	+.7	+.7	+.7
K-2	+.5	+.6[g]	+.9	+.9	1.0	+1.0	+1.0	+1.0	+1.0	+1.0
K-3	+2.3	+2.4[d, g]	-	+10[b]	-[b]	-[b]	-[b]	+10[b]	+.9[c]	+.9
K-4	+1.0	+1.1[g]	+1.1	+1.1	+1.1	+1.2	+1.2	+1.2	+1.2	+1.2
K-5	+.7	+1.1[g]	+1.1	+1.1	+1.1	+1.3	+1.3	+1.3	+1.3	+1.3
K-6	+.8	+1.3[g]	+1.3	+1.4	+1.3	+1.4	+1.4	+1.4	+1.4	+1.4[n]
K-8	+1.3	+1.5[g]	+1.6	+1.6	+1.6	+1.7	+1.7[c]	+1.6	-[b]	-[m]
K-9	+1.3	+1.5[g]	*+2.0	*+1.6	+10[b]	-[b]	-[b]	-	+16[b]	-[e, m]
K-10	+1.1	+1.1[g, n]	+1.1	+1.2	+1.2	+1.2	+1.2	+1.1	+1.1	+1.1[n]
K-11	+.7	+.7[g]	+.7[n]	+.7	+.7	+.5	+.5	+.5	+.5	+.5
K-12	+.8	+.9[g, n]	+.9	+.9	+.9	+.8	+.8	+.8	+.8	+.8
K-13	+.8	+1.1[g]	+1.3	+1.4	+1.4	+1.4	+1.2	+1.4	+1.4	-[m]
K-14	+1.0	+1.3[g]	+1.2	+1.3	+1.3	+1.2	+1.2	+1.2	+1.2	-[m]
K-16	+1.0	+1.2[g]	+1.2	+1.3	+1.3	+1.2	+1.2	+1.3	+1.2	-[m]
K-17	+1.8	+1.7[g]	+1.8	+1.8	+1.8	+1.9	+1.9	+1.9	+15[b]	+10[a]
K-18	+1.3	+1.5[g]	+1.5	+1.5	+1.5	+1.7	+1.7	+1.6	+1.6	+10[a]
K-19	+12[b]	+10[a]	-[e]	-[e]	-[e]	-[e]	+1.6[c]	+1.5	+1.5	+1.5
K-20	-[b]	+12[a]	+14[b]	+10[a]	+1.2	+1.4	1.2[c, e]	-[e]	+1.2[c]	-[m]
K-21										
K-22										
K-23										
K-24										
K-26										
K-28										
K-29										
K-31										
K-32										
K-33										
K-34										
K-36										
K-37										
K-40										

Table VIII-c. (Cont'd)

Pulse - August 13

Specimen	76	77	78	79	80	81	82	83
K-1								
K-2								
K-3								
K-4								
K-5								
K-6								
K-8								
K-9								
K-10								
K-11								
K-12								
K-13								
K-14								
K-16								
K-17								
K-18								
K-19								
K-20								
K-21	-.8	*+.4[g]	+.6	+.45	+.4	+.4	+.3	+.3
K-22	-[j]	+.9	+.9	+.9	+.9	+.9	+.8	+.7
K-23	+1.8	+8[a]	-[b]	-[b]	+20[b]	+10[a]	-[a]	+9[a]
K-24	+.7	*+8[a]	-[b]	-[b]	+20[b]	+10[a]	+10[a]	+1.3[g]
K-26	+1.6	+130[b]	-[a]	-[a]	±2[a]	+145[b]	+2.2[g]	+2.2
K-28	+1.7	+2.3[g]	-[e]	-[e]	-[e]	-[e]	+110[b]	+>30[a,f]
K-29	+1.4	+1.7[g]	-[e]	-[e]	-[e]	-[e]	+75[b]	+35[a]
K-31	-	-	-	±.1	*+.4	+.4	+.5	+.5
K-32	-	-	-	-	-	-	-	-
K-33	-[b]	-	-	*+1.5	*+2.1	+2.1	+95[b]	+30[a]
K-34	..[b]	..	-	*+1.1	*+1.6	+1.7	+1.7	+75[a]
K-36	-	-	-	*+1.1	*+1.6	+1.6	+1.6	+1.6
K-37	-	-	-	*+.9[a]	*+1.4	-[j]	+.9[h]	+.9[h]
K-40	-	-	-	+.7	+.6	+.7	+.5	+.6

Table VIII-d. REDUCED DATA

Specimen	Pulse - July 14								Pulse - July 28				
	1	2	3	4	5	6	7	8	9	10	11	12	13
Dummy 5													
10									+1.9[c]	*.3	+.3	+.3	
11		.05	.03	.05	*1.0	1.0	.9	.8	+>1.5[c,f,i]	-1.2[n]	-1.3	-1.2	
12													
13													
15													
19													
20	(780-3)	.2	.3	.2	.2	.2	.2	.2					
26													
27													
28													
29													
31													
32													
34													
35													
36													
37													
38													
39													
40													

Table VIII-d. (Cont'd)

Pulse - July 29

Specimen		14	15	16	17	18	19	20	21	22	23	24	25	26	27
Dummy	5														
	10	+.3	+.4	+.4	+.2	+.4	+.4	+.4	+.4	+.4	+.4	+.4	+.4	+.4	+.4
	11	-1.4	-1.2	-1.3	-1.3	-1.3	-1.4	-1.4	-1.4	-1.4	-1.4	-1.4	-1.4	-1.4	-1.4
	12														
	13														
	15														
	19														
	20														
	26														
	27														
	28														
	29														
	31														
	32														
	34														
	35														
	36														
	37														
	38														
	39														
	40														

Table VIII-d. (Cont'd)

Specimen	Pulse - July 30					Pulse - July 31								
	28	29	30	31	32	33	34	35	36	37	38	39	40	41
Dummy 5														
10	+.4	+.3												
11	-1.4	-1.4												
12														
13														
15														
19														
20														
26			-.6	-.5[g]	-.5	-.5	-.5	-.5	-.4	-.5	-.5	-.5	-[m]	-.5
27														
28														
29														
31		(D-2)	-1.4	-1.3	-1.3	-1.1	-1.2	-1.2	-1.3	-1.3	-1.3	-1.3	-[m]	-1.3
32														
34		(2-B)	-1.0	-.8[g]	-.8	-.7	-.7	-.7	-.7	-.7	-.7	-.7	-[m]	-.7
35		(2-A)	-.6	-.6[g]	-.5	-.5	-.5	-.5	-.5	-.5	-.5	-.5	-[m]	-.5
36														
37														
38			+.3	+.3[g]	+.3	+.3	+.4	+.5	+.5	+.5	+.5	+.5	-[m]	+.5
39														
40														

Table VIII-d. (Cont'd)

Specimen	Pulse - August 4							Pulse - August 5								
	42	43	44	45	46	47	48	49	50	51	52	53	54	55	56	57
Dummy 5				+.4[g]	+.4[g]	+.4[c]	+.4	+.4	+.5	+.4	+.4	+.4	+.4	+.5[c]	-[c, m]	+.5[c]
10																
11																
12																
13			(PZT 81)	+1.1	+1.1[g]	+1.1	+1.1	+1.1	+1.2	+1.1	+1.1	+1.1	+1.1[c]	+1.1	+1.1	+1.1
15																
19				+.3	+.2[g]	+.3	+.3	+.3	+.3	+.3[c]	+.3	+.3	+.4[g]	+.3[c, g]	+.3	+.3
20																
26	-.4	-.4	-.4													
27																
28																
29																
31	-1.4	-1.4	-1.4													
32																
34	-.7	-.7	-.8													
35	-.5	-.5	-.5													
36																
37																
38	+.4	+.4	+.4													
39																
40																

Table VIII-d. (Cont'd)

Specimen	Pulse - August 6								Pulse - August 7						
	58	59	60	61	62	63	64	65	66	67	68	69	70	71	72
Dummy 5															
10	+.6	+.6[i]	+.5	+.5[i]	+.5	+.6[i]	+.5	+.5[i]							
11															
12															
13	+1.1	+1.1	+1.1	+1.1	+1.1	+1.0	+1.2	+1.1							
15															
19	+.3	-[b]	-[b]	-[b]	-[b]	+.3[c]	+.4	+.4							
20															
26															
27															
28															
29															
31															
32															
34															
35									*-1.0	-0.8[g]	-.8	-.8	-.8	-.8	-.9
36															
37															
38															
39															
40															

Table VIII-d. (Cont'd)

Specimen	Pulse - August 10			Pulse - August 13							
	73	74	75	76	77	78	79	80	81	82	83
Dummy 5				(1060μμ) -.4	-60[b]	-[a]	-[a]	-2[a]	-50[b]	-.3	-.3
10				(79) *+1.2[g,h]	+1.0[g,h]	+.9[h]	+1.8[c]	1.8[d]	+1.8[c]	+.8[h]	-
11											
12				(cut wire) -	-	-	<-.1	<-.1	<-.1	<-.1	<-.1
13											
15							-.3	-.3	-.3	-.3	-3.[a]
19											
20				(K-40) *-[g]	-	-	+.7	+.6	+.8[c]	+.6	-
26											
27											
28											
29											
31											
32											
34											
35	-.9	-1.0	-[m]								
36											
37											
38											
39											
40											

Table VIII-d. (Cont'd)

Pulse - August 14

Specimen	84	85	86	87	88	89	90	91	92	93	94	95
Dummy 5												
10												
11												
12												
13												
15												
19												
20												
26	-.6[k]	-.6	-.6	-.6	-[b]	+7.5[b]	+1.5[a]	+.3[a,l]	-.6	-.6	-.6	-.6
27	+.03	+.07	+.06	+.06	-[b]	-.5[a]	-.5[a]	-.05[a,l]	+.05	+.05	-[b]	-[b]
28	+.4	+.4	+.4	+.4	+.4	+.4	+.4	+.4	+.3	+.3	-[b]	-4[a]
29	+.4	+.4	+.4	+.4	+.4	+.4	+.4	+.4	+.4	+.4	-[b]	-4[a]
31												
32	-1.0	-1.0	-1.0	-.9	-.9	-.9	-.9	-.9[i]	-[a]	0.4[a]	*-.1[c]	*-.9
34	*-1.2[g]	-1.1	-1.1	-1.0	-1.1	-1.1	-1.1	-1.1[i]	+2[a]	+2.5[b]	-[j]	-1.1
35												
36	+3[a]	+1[a]	-[a]	-[b]	-.7	-.7	-.7	-.7[i]	-.7	-.8[c]	-.7	*-1.4[f]
37	-.5[a]	-.5[a]	-[b]	-[b]	+.2	+.4	+.3	+.3[i]	+.3[c]	*+.06	*+.3	+.3
38												
(1050μμ) 39	+>12[a]	+22[a]	-[b]	-[b]	+.8	+.7	+.8	+.8[i]	*+1.6[c]	+1.6	+1.6[c]	+1.6
(779-1) 40	+2[b,d]	+12[b]	+6[a]	+6[a]	+1.3	+1.3	+1.3	+1.3[i]	+.5[c]	+.4[h]	*+.2[c,h]	+.2

Table IX. POWER OF TRIGA MARK F REACTOR DURING EACH PULSE

Date	No.	Time	Transient (HDL #)	Peak Power (10^6 watt)	$\int$ Power (10^6 watt-sec)
14 Jul	1	1431	2465	1000	19.2
	2	1450	2466	1020	20.1
	3	1517	2467	1000	18.9
	4	1533	2468	1040	19.2
	5	1549	2469	1040	19.2
	6	1605	2470	1020	19.2
	7	1622	2471	1020	19.2
	8	1639	2472	1060	19.8
28 Jul	9	1207	2480	1240	20.4
	10	1440	2481	1260	20.4
	11	1530	2482	1260	20.1
	12	1636	2483	1280	20.4
29 Jul	13	0947	2484	1200	19.2
	14	1003	2485	1200	19.2
	15	1025	2486	1210	19.4
	16	1107	2487	1220	19.4
	17	1132	2488	1200	19.5
	18	1150	2489	1240	19.5
	19	1327	2490	1260	19.5
	20	1359	2491	1260	19.5
	21	1421	2492	1260	19.7
	22	1439	2493	1260	19.7
	23	1504	2494	1260	19.7
	24	1538	2495	1280	19.7
	25	1605	2496	1280	19.8
	26	1627	2497	1280	19.8
	27	1645	2498	1280	19.7

Table IX. (Cont'd)

Date	No.	Time	Transient (HDL #)	Peak Power (10^6 watt)	$\int$ Power (10^6 watt-sec)
30 Jul	28	0935	2499	1240	22.5
	29	1104	2500	1240	19.8
	30	1518	2501	1240	19.8
	31	1557	2502	1240	19.8
	32	1616	2503	1260	19.5
31 Jul	33	0955	2504	1200	19.5
	34	1039	2505	1200	19.1
	35	1126	2506	1240	19.8
	36	1200	2507	1240	19.5
	37	1357	2508	1240	19.5
	38	1418	2509	1230	19.4
	39	1502	2510	1240	19.5
	40	1618	2511	1280	19.8
	41	1638	2512	1280	19.8
4 Aug	42	1008	2516	1220	19.8
	43	1045	2517	1220	19.5
	44	1148	2518	1200	19.5
	45	1402	2519	1240	20.7
	46	1522	2520	1240	20.4
	47	1622	2521	1200	19.5
	48	1646	2522	1220	20.1
5 Aug	49	0932	2523	1180	19.8
	50	1017	2524	1180	20.1
	51	1050	2525	1170	19.9
	52	1138	2526	1200	19.8
	53	1207	2527	1200	19.8
	54	1456	2528	1200	19.8
	55	1529	2529	1210	19.9
	56	1600	2530	1220	20.1
	57	1622	2531	1220	20.1

Table IX. (Cont'd)

Date	No.	Time	Transient (HDL #)	Peak Power (10^6 watt)	$\int$ Power (10^6 watt-sec)
6 Aug	58	0929	2533	1140	19.2
	59	1012	2534	1180	19.5
	60	1107	2535	1200	19.5
	61	1319	2536	1180	19.5
	62	1415	2537	1220	20.7
	63	1513	2538	1180	19.5
	64	1548	2539	1220	20.4
	65	1624	2540	1240	20.4
7 Aug	66	1153	2542	1200	20.1
	67	1355	2543	1200	20.7
	68	1431	2544	1180	19.8
	69	1519	2545	1200	19.8
	70	1541	2546	1200	19.8
	71	1625	2547	1240	21.0
	72	1647	2548	1240	19.3
10 Aug	73	1032	2549	1200	19.5
	74	1103	2550	1200	19.8
	75	1211	2551	1220	19.8
13 Aug	76	1113	2561	1120	19.2
	77	1150	2562	1140	19.2
	78	1327	2563	1140	19.2
	79	1359	2564	1140	19.2
	80	1425	2565	1160	19.1
	81	1504	2566	1140	19.2
	82	1539	2567	1160	19.7
	83	1638	2568	1140	19.4

Table IX. (Cont'd)

Date	No.	Time	Transient (HDL #)	Peak Power (10^6 watt)	$\int$ Power (10^6 watt-sec)
14 Aug	84	1045	2570	1140	19.2
	85	1110	2571	1140	19.8
	86	1127	2572	1140	19.5
	87	1145	2573	1140	19.5
	88	1344	2574	1120	19.5
	89	1402	2575	1120	19.5
	90	1423	2576	1160	19.5
	91	1448	2577	1160	19.2
	92	1519	2578	1160	19.2
	93	1541	2579	1120	19.5
	94	1606	2580	1120	19.5
	95	1624	2581	1100	19.2

Part 2: July 1965

The data accumulated during 32 pulses is presented here. There were 125 specimens and 15 dummy specimens irradiated, each from 3 to 5 times. The dummy specimens here were quartz samples of the same sizes as the ceramics and put into the same positions. Again voltage output is plotted for each pulse and each specimens. The load on each specimen was 10^6 ohms in parallel with 37 mmf for each pulse. A dash indicates that the output was not monitored although the specimen received a pulse of radiation. The first grouping of data covers the

"SANDWICHES" of 1" DISCS.

The second grouping of data covers the

SIMULATED FUSE HOUSINGS WITH CYLINDER PAIRS.

Table X. SANDWICHES OF 1" DISCS

(HDL - July 1965)

Specimen	Pulse No.	Orientation	Pulse Height (Volts) 1st	2nd	3rd	4th	5th
			GULTON - Polar				
G 1	8-11	Random	>+20	+32	-	+32	
G 2	"	"	>+20	+25	-	+26	
G 3	"	"	>+20	+33	-	+34	
G 4	"	"	>+20	+29	-	+31	
G 5	"	"	>+20	+32	-	+33	
G 6	8-11	Random	>+20	+33	-	+35	
G 7	"	"	>+20	+28	-	+29	
G 8	"	"	>+20	+35	-	+36	
G 9	"	"	>+20	+24	-	+25	
G 10	15-19	+ Forward	+18	+19	+19	-	-
G 11	15-19	+ Forward	+13	+13	+13	-	-
G 12	"	"	+10	+10	+11	-	-
G 13	"	"	+13	+14	+14	-	-
G 14	"	"	+10	-	-	+11	-
G 15	"	"	+15	-	-	+17	-
			GULTON - Nonpolar				
G 16	8-11		-4	-4	-	-4	
G 17	"		-1	-4.5	-	-4.5	
G 18	"		-2	-	-2.5	-2.5	
G 19	"		-3	-	-2	-2	
G 20	"		+5	-	+5.5	+5	
G 21	8-11		-1	-	-1	-1	
G 22	"		+3	+2.5	+2.5	+3	
G 23	"		-4	-4	-4	-4	
G 24	"		+6	+5	+5.5	+6	
G 25	15-19		+5	-	-	+5	-
G 26	15-19		-2	-2	-2	-	-
G 27	"		+5.5	+5.5	+5.5	-	-
G 28	"		+4	+4	+4	-	-
G 29	"		-3.5	-3.5	-3	-	-
G 30	"		-	-3.0	-3.0	-3.0	-3.1

Table X. (Cont'd)

Specimen	Pulse No.	Orientation	Pulse Height (Volts) 1st	2nd	3rd	4th	5th
			ERIE - Polar				
E 1	12-14		-	+6	+8		
E 2	"		-	+18	+20		
E 3	"		-	+11	+12		
E 4	"		-	+11	+13		
E 5	"		-	+7	+8		
E 6	12-14		-	+4	+5		
E 7	"		-	+8	+9		
E 8	"		-	+4	+5		
E 9	"		-	+4	-		
E 10	15-19	+ Forward	-	+4.4	+5.8	+5.8	+6.6
E 11	15-19	+ Forward	-	+1.4	+2.8	+3.2	+3.6
E 12	"	"	-	+3.2	+4.4	+4.6	+5.4
E 13	"	"	+2	+5.6	+6	-	-
E 14	"	"	ODD	+4.1	+5.2	-	-
E 15	"	"	ODD	+3.5	+5.2	-	-
			ERIE - Nonpolar				
E 16	12-14		-	+3	-		
E 17	"		-	+5	-		
E 18	"		ODD	-.25	-1		
E 19	"		-5	-5	-4		
E 20	"		-7	-7	-7		
E 21	12-14		-1	-1	-2		
E 22	"		(+3)	+2	+2		
E 23	"		(-6)	-7	-7		
E 24	"		(+2)	-.1	-.1		
E 25	"		-5	-5	-5	-5	
E 26	12-14		-2	-2	-2	-2	
E 27	"		-3.0	-3.2	-3.2	-3.2	
E 28	"		-3.0	-3	-3	-3	
E 29	"		ODD	+0.4	+0.4	+0.4	
E 30	"		-5	-5	-5	-5	

Table X. (Cont'd)

Specimen	Pulse No.	Orientation	Pulse Height (Volts) 1st	2nd	3rd	4th	5th
			CLEVITE - Polar				
C 1	20-22	- Forward	+10	+17	+20		
C 2	"	"	(+2)	+9	+13		
C 3	"	"	+10	+18	+20		
C 4	"	"	ODD	+7	+11		
C 5	"	"	-	+14	+17		
C 6	20-22	- Forward	-	+12	+14		
C 7	"	"	-	+10	+11		
C 8	"	"	-	+10	+11		
C 9	"	"	ODD	+11	+15		
C 10	26-29		ODD	+5	+8	+9	
C 11	26-29		ODD	+2	+4	+5	
C 12	"		(-2)	+4	+7	+9	
C 13	"		(-2)	+4	+6	+9	
C 14	"		+5	+8	+10	+13	
C 15	"		(-1)	+5	-	-	
			CLEVITE - Polar & Loaded				
C 16	20-22	- Forward	(+6)	+13	+16		
C 17	"	"	+12	+20	+25		
C 18	"	"	(-2)	+4	+8		
C 19	"	"	+8	+17	+21		
C 20	"	"	ODD	+5	+9		
C 21	20-22	- Forward	+5	+12	+15		
C 22	"	"	+4	+9	+13		
C 23	"	"	+6	+15	+19		
C 24	"	"	(+2)	+12	+15		
C 25	26-29		ODD	+3	+5	+6.2	
C 26	26-29		ODD	+5.7	+8.5	+10	
C 27	"		ODD	+6.4	+9	+11	
C 28	"		(-2)	+2	+4	+5	
C 29	"		(-1)	+5	+8	+10	
C 30	"		ODD	+4	+6	+7	

Table X. (Cont'd)

Specimen	Pulse No.	Orientation	Pulse Height (Volts) 1st	2nd	3rd	4th	5th
			QUARTZ - Unloaded				
Q 1	26-29		-1.2	-1.2	-1.2	-1.2	
Q 2	26-29		ODD	-.4	-.4	-.4	
Q 3	15-19		-1	-	-	-0.7	-
Q 4	20-22		-	-3	-3		
Q 5	20-22	-1.2	-1.2	-1.2			
			QUARTZ - Loaded				
Q 6	12-14		-	-2	-		
Q 7	12-14		+2 -2	-2	-4		
Q 8	15-19		-0.7	-0.8	-0.8	-	-
Q 9	8-11		+2	+2	-	+2.1	
Q 10	8-11		-3	-3	-3	-3	

Table XI. SIMULATED FUSE HOUSINGS WITH CYLINDER PAIRS

(HDL - July 1965)

Specimen	Pulse No.	Orientation Toward Reactor	Pulse Height (Volts) 1st	2nd	3rd
G 1^+	23-25	Cylinder Walls	ODD	(-.2)	ODD
G 2^+	"	"	ODD	+.6	+.7
G 3^+	"	"	ODD	-.05	ODD
G 4^+	"	"	ODD	-.05	ODD
G 5^+	"	"	ODD	+.1	+.05
G 6^+	23-25	Cylinder Walls	(-.2)	-.2	-.08
G 7^+	"	"	(-.2)	-.2	-.08
G 8^+	"	"	(-1.0)	-.6	-.5
G 9^-	"	"	-2	-2.1	-2.1
G 10^-	"	"	-2	-2.2	-2.1
G 11^-	30-32	Cylinder Bottom	-1.7	-1.8	-2.0
G 12^-	"	"	-1.8	-1.8	-2.0
G 13^-	"	"	-1.8	-1.8	-2.0
G 14^-	"	"	-1.0	-1.0	-1.2
G 15^-	"	"	-2.0	-2.0	-2.2
Q 1	30-32	Cylinder Bottom	-1.2	-1.4	-1.4
Q 2	"	"	-.8	-1.4	-1.4
Q 3	"	"	-1.4	-1.4	-1.4
Q 4	"	"	-1.6	-1.2	-1.4
Q 5	"	"	-1.8	-1.4	-1.6
C 1^+	23-25	Cylinder Walls	(-1)	-1.4	-1.2
C 2^+	"	"	(-.4)	(-.3)	-1
C 3^+	"	"	-1	-.8	-.6
C 4^+	"	"	-1	-.8	-.5
C 5^+	"	"	-1.4	-1.0	-.6
C 6^+	23-25	Cylinder Walls	-1.4	-1.0	-.7
C 7^+	"	"	-	-	-
C 8^+	"	"	-	-	-
C 9^o	"	"	-	-	-
C 10^o	"	"	-	-	-

Table XI. (Cont'd)

Specimen	Pulse No.	Orientation Toward Reactor	Pulse Height (Volts) 1st	2nd	3rd
C 11°	30-32	Cylinder Bottom	-1.4	-1.4	-1.6
C 12°	"	"	-1.2	-1.4	-1.6
C 13+	"	"	-1.0	-.6	-.4
C 14+	"	"	-1.2	-.8	-.6
C 15+	"	"	-1.5	-1.2	-.8
M 5+	30-32	Cylinder Bottom	-1.6	-1.2	-1.0
M 6+	"	"	-1.6	-1.2	-1.2
M 7+	"	"	-1.6	-1.2	-1.2
M 8+	"	"	-2.8	-2.6	-2.4
M 9+	"	"	-	-	-

n.b. Peak voltages in parenthesis in this and the previous table are estimated from outputs that are not well-formed. The entry "ODD" indicates that the pulse was so distorted that no peak height could be determined.

APPENDIX B

A COLLECTION OF PERTINENT PAPERS AND REPORTS

PART 1-A

RADIATION EFFECTS ON FERROELECTRIC MATERIALS

Summary Report

Issai Lefkowitz

Contract No. DA-30-069-507-ORD-1866

Research & Development Laboratory
GLENCO CORPORATION
A Subsidiary of
Gulton Industries, Inc.
METUCHEN, NEW JERSEY

FRANKFORD ARSENAL
Philadelphia, Pennsylvania

CONTENTS

RADIATION EFFECTS ON FERROELECTRIC MATERIALS

SUMMARY REPORT

- Issai Lefkowitz -

Introduction

Nuclear radiation effects on the properties of ferroelectric materials were investigated in this program. At the inception of this contract, there was a paucity of information in the literature on the effects of nuclear radiation on ferroelectric materials. References to these few early investigations and to published work resulting from the experimental studies carried out under this contract are contained in this report.

To evaluate the effect of radiation on characteristics of ferroelectric materials, samples of ferroelectric ceramics and single crystals were irradiated in the Brookhaven nuclear reactor.* Ferroelectric materials utilized were barium titanate-type materials. Some experiments** using a cobalt-60 gamma source and a lead titanate-lead zirconate ceramic are also included in this report as an aid in evaluating experimental results.

Studies were made to investigate the following basic questions:

(a) Would the ferroelectric ceramic materials retain their piezoelectric properties after irradiation in a nuclear reactor?

(b) Would a free surface charge result on the ferroelectric materials because of exposure to nuclear radiation?***

---

* Brookhaven National Laboratory, Upton, Long Island, New York.

** Performed under other auspices.

*** Since radiation can produce localized heating on a macroscopic scale, charge release due to this temperature increment might take place. This suggests the possibility that the induced charge may be large enough to trigger ordnance items.

Studies were also made to determine potential side effects produced in the irradiation experiments. New techniques were devised to meet experimental problems arising during the program.

Piezoelectric Properties and Nuclear Radiation

To determine whether piezoelectric characteristics of ferroelectric materials are altered by nuclear radiation, samples of polarized $BaTiO_3$ were exposed to an integrated radiation dosage of 10^{15} nvt fast neutrons and 10^{17} thermal neutrons. Measurements were made of the open circuit voltage produced by a ball drop apparatus.

The barium titanate test pieces, 3/8 in. diameter by 1/16 in. thick, were subjected to the integrated flux in the Brookhaven reactor. The facility had an ambient temperature of 60°C.

Comparison of the open circuit voltage from irradiated samples with similar measurements from unexposed titanate pieces showed no appreciable change in piezoelectric properties of the exposed ceramic materials. There was no change of the room temperature capacity, tan δ , and bulk volume resistivity.

Charge Release During Radiation Exposure

Temperature cycling in ferroelectric material produces surface charges by both primary pyroelectricity and by mechanical deformations produced by small temperature increments (secondary pyroelectricity). Since radiation effects can produce localized heating effects, an assumption was made that these small temperature increments would furnish free surface charges in a manner similar to that provided by the temperature cycling procedure.

To test this assumption, $BaTiO_3$ samples were placed in a nuclear pile environment and monitored for free surface charge. Several sample holder designs were tested. The first sample holder system consisted of a flat tray of bakelite with aluminum probe electrodes (see Figure 1).*

The design of this original holder was based on induced radio-activity considerations and the need for a sample holder system which would permit introduction of the holder into the pile while the pile was operating. Foil slots utilized in the reactor permitted the taking of measurements and changing of samples while the reactor was operating.

Measurements obtained with this first holder system were suspected of being in error because of control point anomalies. Control positions, where no samples were in place, showed a current flow well above that due to normal equipment drift, while reversal of sample polarity changed current magnitude but did not change the direction of current flow.

The inconsistent data was attributed to the intrinsic potential difference arising from the difference of work function between the aluminum and the graphite of the pile. This potential difference collected the ionized gas in the pile and resulted in a current flow measurable on the outside of the pile.

In order to test this hypothesis, measurements of current and voltage were made on coaxial wire (without a sample) and on an increased area of aluminum facing the graphite of the pile. If the validity of the work function difference assumption was correct, the coaxial system was expected to show no charge release while the increased area system furnished a larger charge release. Results of these experiments are shown in Figure 2.

* See also the Fourth Monthly Progress Report, Oct. 22 - Dec. 28, 1956

As can be seen from Figure 2, the coaxial holder system showed little above-normal drift while the enhanced-area sample holder system produced a current of almost 4 orders of magnitude larger than any that had been measured previously. A further check was made on the work function difference hypothesis by utilizing an aluminum coaxial holder system with one electrode made of tantalum.* A value of 1.4×10^{-7} amps was obtained (see Figure 2).

On the basis of the above results, the work function difference hypothesis was considered sufficiently correct to be used as a guide for designing a holder system for the pile measurements. These coaxial sample holders are shown in Figures 3 and 4. Data taken with the new coaxial holder system with and without a sample are plotted in Figure 2. The charge release obtained above that available from a standard empty coaxial holder and wire system is clearly indicated in this plot.

Surface Charge Measuring System

Charge measurements are made classically with either the ballistic galvanometer or with an electrometer. With the ballistic galvanometer, errors may be introduced if the period of charge release is comparable to the period of the galvanometer. Furthermore, the impedance level of the galvanometer must be restricted to low resistance values to obtain accurate measurements.

The impedance of the electrometer is, of course, necessarily high. It is unsatisfactory for use with barium titanate, since even with low leakage in

---

* Work function of tantalum obtained by a contact potential method was 3.96 ev. Klein and Lange[1.] indicated a value of 3.38 ev for Al using the same technique.

the measuring equipment, the conductivity of the $BaTiO_3$ may allow charge to leak off before the charge release has been completed or the voltmeter is read.

The system used for measuring surface charge in this program is shown in the diagram below. It is basically that of the Miller integrator in which the

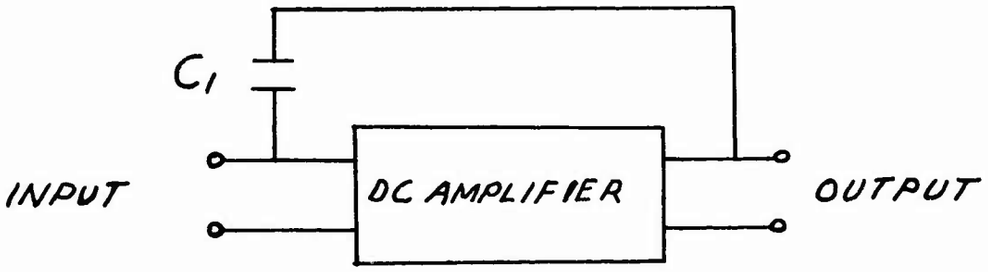

capacitor C_1 is connected between the input and output terminals of a high gain DC inverting amplifier.

If the amplifier input impedance is sufficiently high, any charge from the sample flows into the integrating capacitor C_1. The feedback of the amplifier acts to keep the potential of the amplifier input terminal as close to zero as possible. If the capacitor is charged to a potential $Q/\left[C_1 (G + 1)\right]$ where G is the amplifier gain and has a value of about 2000, the rise in input potential is for all practical purposes equal to Q/C_1G.

For a total resistance, R_L, from the amplifier terminal to ground, the decay time for the charge on C_1 is GR_LC_1 rather than R_LC_1. This increase

in decay time is due to the reduction in the leakage current by a factor of G (i.e. the voltage appearing across the leakage elements is reduced by a factor of G).

Since it tends to remain nearly at ground potential, the input to the integrator "looks" to the external circuit (i.e. the sample under test) like a very low impedance. The sample can be made to view whatever load impedance is desired, however, merely by inserting the desired resistance in series with the sample.

The present system has a response time of about one tenth of a second and a decay time of several hundred minutes when used on the 10 microcoulomb sensitive setting. Some difficulty was experienced because the feedback capacitor C_1 was connected from B+ to the grid of the input circuit.

Although a bucking potential from the plate circuit to the capacitor C_1 permits practically no DC voltage application across the integrating capacitor, when one zero sets (i.e. brings the grid down to the ground potential) a certain amount of instability causes short-term excursions. These are exhibited as a series of damped voltages on the sample face and may result in anomalous readings immediately after zero setting.

Because of these potentially erroneous readings, another circuit was developed for measurement of surface charges. In principle this circuit was similar to the one described above except for one modification - the feedback capacitor C_1 was taken from a cathode follower circuit.

The instantaneous potentials described above were eliminated with this modification, but the circuit did not possess the long-term stability (hundred minutes) of the original Miller circuit. For short-term measurements,

however, comparison of results indicated qualitative agreement in most cases. Since neither of the circuits described above represents an optimum instrumentation technique, a more passive system for future measurements is planned.

Flux Measurements

The estimate of flux at the various positions used in the Brookhaven reactor were based on symmetry considerations. Since there could be large local variations from symmetrical flux distributions, it was necessary to make flux measurements at the sample positions.

Standard foil activation methods were employed for measuring the flux distribution. During the period covered by this report, the Brookhaven reactor was being reloaded. For this reason, even stated values of the integrated dosage must actually be modified by the differences of pile spectrum due to the fuel pattern changes. At best the reported flux measurements have a high degree of uncertainty.

Electrical Probe Measuring System

Reliable charge measurements at a distance are extremely difficult to make. An added complication in this program is the maintenance of sample holder and connecting cables in a nuclear environment.

To meet the problem of measuring surface charges at a distance, a new technique was devised to establish the validity of picturing the irradiated ferroelectric material as a source of electrical energy. This method was termed a "probed measurement" system because a probing DC potential was used to test

the electrical condition of two sample positions in the previously-described flat holder assembly (Figure 1). The testing scheme is shown in the following diagrams:

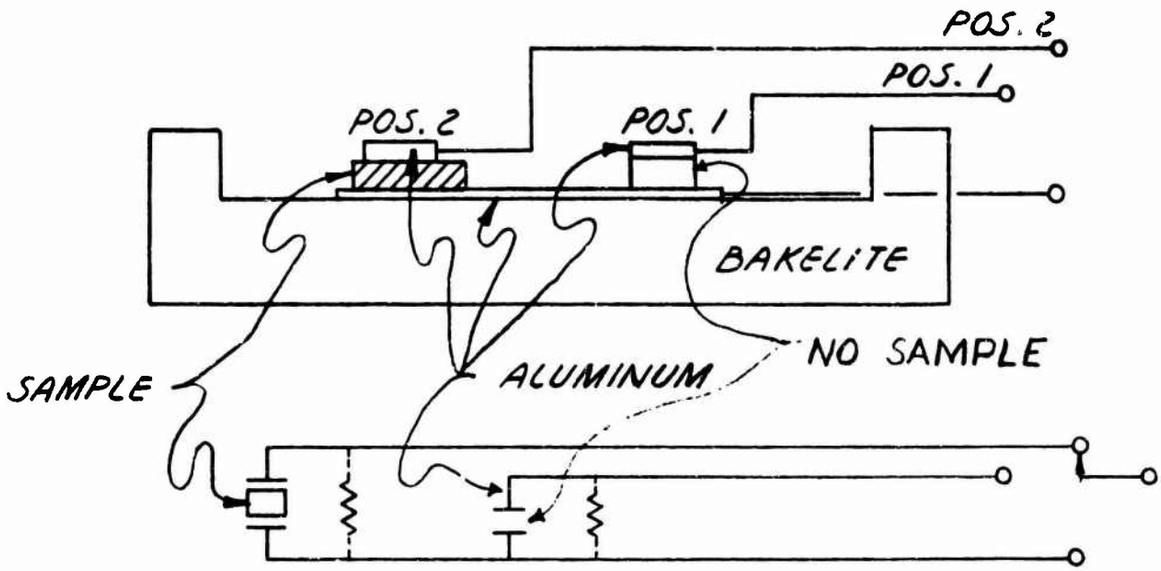

A battery was placed in series with the current integrator and measurements of current flow in both directions were made. Since the effective resistance leakage path was essentially the same, the charge slopes or currents were expected to be the same unless the following conditions prevailed:

(a) The ferroelectric material was acting as a rectifier, or

(b) The ferroelectric sample was acting as a source of emf.

Test circuits are illustrated on the following page.

The results were positive, i.e., the current was the same in Position 1 (no sample in place) and different in Position 2 (ferroelectric material in place).

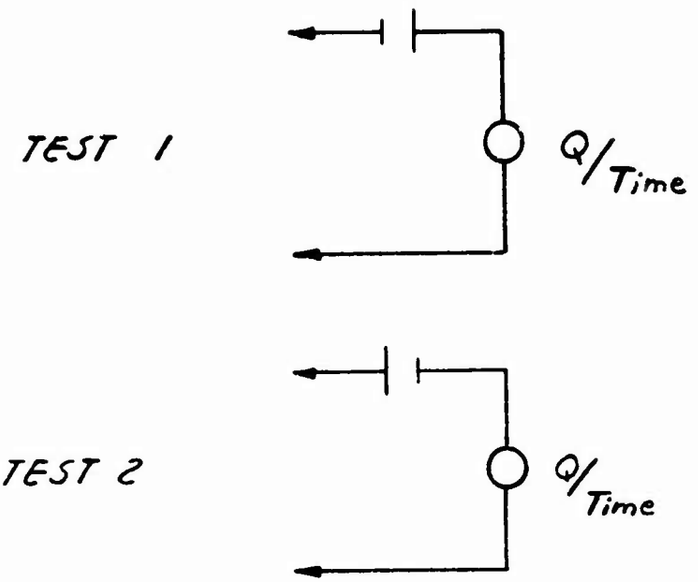
TEST 1
Q/Time
TEST 2
Q/Time

POS. 1

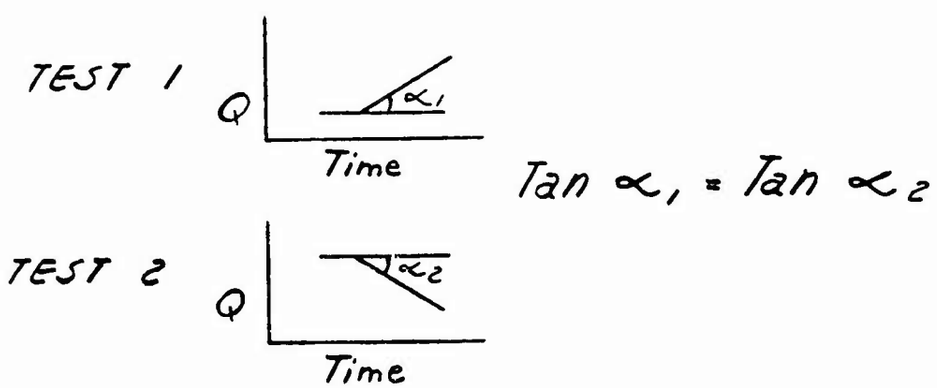
TEST 1
Q
Time
Tan ∝1 = Tan ∝2
TEST 2
Q
Time

POS. 2

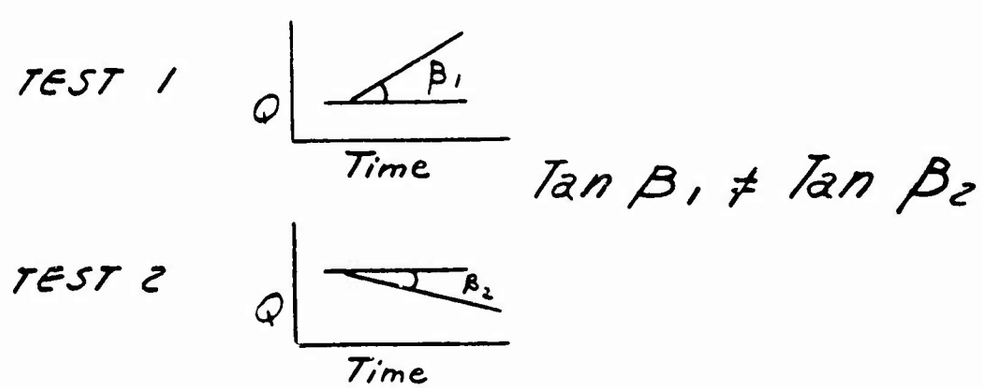
TEST 1
Q
Time
Tan β1 ≠ Tan β2
TEST 2
Q
Time

Since $BaTiO_3$ is a semi-conductor as well as a ferroelectric material, the possibility that the results obtained can be related to some kind of special rectifier phenomena cannot be wholly ruled out. The influence of rectifier phenomena that might arise from the action of the nuclear environment could not be eliminated from this experiment. The resistances, estimated from the voltage-current data of the above experimental configuration, are of an order of magnitude less than that expected from the sample. Therefore, data obtained from this experiment plus information from subsequent measurements suggests that the second possibility was the correct interpretation, namely that an irradiated ferroelectric sample was acting as a source of emf.

Materials

Ceramic barium titanate samples were composed of $BaTiO_3$ and 4 per cent $PbTiO_3$. The single crystals were grown from a fluoride flux and unless otherwise noted the surfaces were not acid-etched to eliminate flux contamination. Ceramic samples were discs of 3/8 inch diameter and 1/16 inch thick.

Silver used in ceramic measurements was a fired-on type that required subjecting the samples to temperatures up to 600°C. In the case of single crystals, measurements were made with an air-drying, water-soluble silver supplied by DuPont. This silver material was designated by DuPont as 5399-A, lot 13475.

Runs were made utilizing the aluminum coaxial holder system previously described and an effort was made to standardize the holder system geometry. Difficulty was experienced in using the soft 2S aluminum to maintain good physical contact with the sample, because the sample holder system was subjected to rather rough handling when inserted into the nuclear pile. As

experience was gained with the sample holder (Figure 3), some slight modifications were made in the mechanical geometry of the crystal holder system (Figure 4, Modified Coaxial Sample Holder).

Experimental Data

Data is presented chronologically because of the many fuel loading changes that took place during this program. Graphs are plotted with current in amperes as the ordinate and distance of sample or control point from the face of the pile as the abscissa. The 18'-9" point is the approximate geometric center of the pile.

Where specific flux information was available, it has been noted for the particular run. The sample designations describe the polarization pretreatment that the ceramics have undergone. For example, in sample number NU-25-H, the H indicates that the sample was polarized through the Curie point; while an L would indicate that polarization had been made at room temperature; and the designation N would denote that the sample had no treatment other than that provided during fabrication.

For single crystal barium titanates, area measurements were made by graphic methods. The data is presented both in terms of the absolute value of the charge collected and a corrected value for the area differences among the samples used.

Data is plotted on semi-log paper in order to cover the necessary decades observed in the measurements. For this reason, the differences between the zero runs (measurements made with no sample in place but consisting of coaxial holder, wire, and drift in the equipment) are less apparent than if they had been plotted on a linear scale.

Figure 5 shows the measurements made before the December 1956 fuel loading. The zero run coaxial holder and wire measurement is the value of the current measured with only an aluminum tube, holder sample, and polyethylene-coated inner wire. Measurements of currents from samples NU-85-H, NU-72-N, and NU-84-H are four to six times larger than the measurements with no sample in place.

After January 1957, the first fuel reloading had taken place. As can be seen from the graph in Figure 6, the output from the polyethylene drift and glass in one sample in the coaxial system was approximately the same, while the output from $BaTiO_3$ showed a decrease. The barium titanate output was only twice that of the background value.

Measurements utilizing the slightly higher flux of hole W 14 were made in the following three months and are plotted in Figure 7. Since W 14 is the facility right next to W 13, no large changes in flux at the 12 foot position were expected. As can be seen from Figure 7 at the 12 foot point, there was only a moderate increase in current. However, at the 16.5 and 16.75 foot positions measurements made with glass and $BaTiO_3$ indicate an enhancement of the outputs from the barium titanate samples.

At this time, an effort was made to increase the localized ionization by using an $n\alpha$ reaction from boron-10. A small quantity of B^{10} was placed in the holder near the sample and measurements were made with glass in place and with one of the barium titanate ceramics in place. The effect of localized ionization is shown in Figure 7 by the increased current and greater output from the $BaTiO_3$ sample compared with the glass sample.

An attempt was made at this time to investigate the effect of geometry by placing a sample in a horizontal position rather than perpendicular to the axis of the coaxial holder wire system. This test measurement is designated as NU-89-H, dated 4/23/57. The output is larger, but insufficient data prevents evaluation based on this one measurement. Evidence has been collected that the charge release phenomena observed in these ferroelectrics were not associated with their polar character. [2.]

The next measurement was made to determine whether the charge release phenomena would be observable when the materials were in the non-ferroelectrical temperature region. Measurements made by Chynoweth [3.] at Bell Laboratories have shown photovoltaic phenomena that was observable above the Curie point and, as a matter of fact, enhanced slightly as the $BaTiO_3$ reached the Curie point.

Measurements were made of the charge release phenomena up to 140°C which is about 10° above the normal transition of barium titanate. Thermocouple measurements of the sample temperature are shown in Figure 8 and charge release data are plotted in Figure 9. The sample is considered to have attained temperature equilibrium after 25 minutes in the pile.

The charge versus time plot of Figure 9 gives a value of 1.1×10^{-8} amperes. This is considerably above the previously-measured current value. Because the temperature required was so high, another facility (E 11) was used. The flux in E 11 was about the same as that of E 25 shown in Figure 11.

From this charge release experiment, it was concluded that the charge release phenomena observed is not dependent on the ferroelectric state of the

ferroelectric materials investigated. It is of interest to note that the increase of current in this temperature range agrees with the observations of Chynoweth[3.] who obtained a larger photovoltaic effect at temperatures slightly above the Curie point.

Figure 10 contains data taken to provide statistics of the observed phenomena. Of interest is the fact that the background measurements are different in sign (i.e., negative) from an arbitrarily assigned positive current flow for the ferroelectric materials.

A run made in the higher flux facility E 25 is plotted in Figure 11. As expected, both the background and the sample measurements showed an increase.

Data shown in Figures 12 and 13 were obtained under different auspices, but have been included in this report as an aid in evaluation of the experimental work. Measurements plotted in Figure 12 are for a solid solution ceramic of lead titanate-lead zirconate. This material has a high temperature Curie point (around 350°C) and was formed by a high-temperature, high-pressure technique which provides a very dense material.

The ranges of current observed are larger than those resulting from $BaTiO_3$ (ordinate scale is 10^{-9} and 10^{-8} amperes). All of the samples had been polarized to maximize their piezoelectric character. The data reflects the changes in flux (i.e., higher fast flux with higher output) with the attendant sample scatter. Figure 13 reports output from ceramic $BaTiO_3$ in a cobalt-60 gamma source. Measurements were made at room temperature.

Because of the continued large sample scatter which might be related to any one of several processes in the fabrication of the ceramics, an attempt was made to eliminate this scatter by taking measurements with barium

titanate single crystals. Figure 14 shows the first results obtained with the $BaTiO_3$ single crystals. A technique suggested in Chynoweth's[3.] work was utilized in this experiment.

Three different crystals were used to obtain the data. One crystal was polarized by application of a field while the crystal was being cooled from about 180°C through the Curie point to room temperature. The second crystal was annealed by heating to 270°C and subsequent slow cooling to room temperature. The third crystal was used as grown from the fluoride flux.

The results of this experiment indicate that the polarized single crystal showed the largest output, both in actual value for current measured and for corrected-area value. This data supports the theory that the field application had in some way enhanced the output from the $BaTiO_3$.

Single crystal measurements were made of this effect in a gamma source. Incident radiation is monochromatic and field applications to modify the effects observed are easily carried out with the cobalt-60 gamma irradiation. A simply-fabricated "in situ" oven facilitated the performance of these experiments. Results are plotted in Figures 15 through 19, "Experiments in Gamma Source."

Figure 15 is a plot of a control run made with no sample in place. It was performed at room temperature with both field and reversed field application. Also shown on this plot are runs made at 70°C utilizing the same field application procedure. The results indicate a reproducible current that reflects the drift rate of the equipment and a probable contribution by the polyethylene.

A plot of charge as a function of time (obtained with a virgin single crystal of $BaTiO_3$) is provided in Figure 16. Field pretreatment of this crystal consisted only of hysteresis loop analysis. The background for this analysis is discussed in Reference 17. The results show little above-drift-rate of the equipment. No reversal of the charge flow direction was obtained upon reversal of field application.

Similar results from an experiment on another virgin crystal at 70°C are shown in Figure 17. The data obtained in this run may not be valid since the high temperature charred the insulation sufficiently to make the parallel resistivity uncertain. In addition, when the sample holder was disassembled, the crystal was found to be in several places. This was probably due to a combination of clamping and temperature cycling.

The data plotted in Figure 18 are the results of measurements made with a polarized crystal that had one kilovolt applied while being cooled from 300°C. The results are plotted in chronological order with the first experiment "in situ" but with no attempt to reverse the charge flow. The second run was made with reverse field application to evaluate whether symmetry conditions could be reversed with a necessary reversal of the charge flow.

As can be seen, the charge flow direction was reversible. Even with a correction for the drift rate inherent in the equipment, there is still a significant amount of charge flow indicated. The information is plotted directly in microcoulombs with an area correction indicated on the drawing.

Figure 19 is a plot of data from a run made with another polarized single crystal. Results of this experiment are questionable in regard to reversal of

the internal symmetry conditions for the crystal. Although the crystal had been repolarized twice in the negative direction, it did not show immediate charge polarity reversal.

Another interesting point is the persistence in the polarity of the phenomena. This suggests that if asymmetry is produced in the barium titanate single crystals, the asymmetry is rather difficult to reverse. In a discussion with Dr. Chynoweth of Bell Telephone Laboratories, a possible explanation of this phenomena was made. This is based on observations of his "photovoltaic" effects as shown in the diagram below:

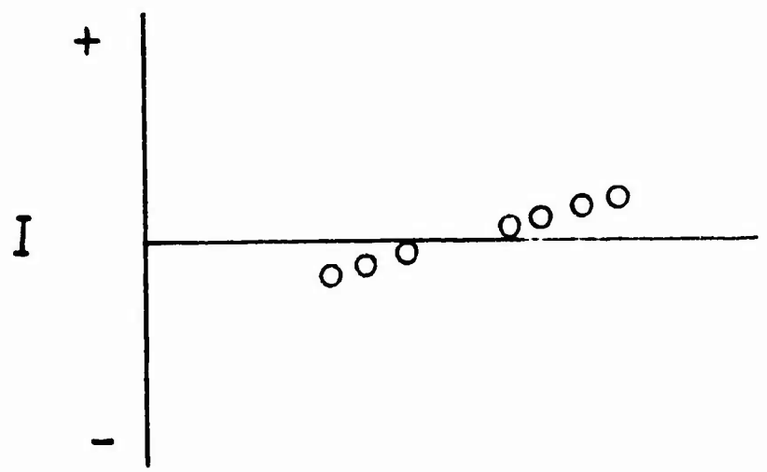

As indicated in the diagram, Dr. Chynoweth did observe a negative voltage pulse or current with a positive applied field during visible light excitation. However, this flow was reversed after a number of field applications. Chynoweth also stated that the effect between samples showed a large degree of scatter with some having a much larger effect than others.

Discussion of Results

From the results of the experimental data, it is clear that the charge release effect is fast flux dependent (see Figure 7). The effect may be directly due to the fast flux, or the charge release may be caused by secondaries from the fast flux. The results obtained from the cobalt-60 gamma source experiments suggests that the latter possibility cannot be overlooked.

The field modulation of the effect is evident in the case of single crystal $BaTiO_3$ but this is not clear for ceramic materials. How much of the field dependence is due to mechanical strain introduced into the crystal is difficult to estimate. A much larger output was observed from $BaTiO_3$ (see Figure 10) and a solid solution ceramic (see Figure 12) than from glass.

This data supports the view that the observed effects may be associated in some way with the ferroelectric or ionic character of the material rather than because the material is an insulator. The data (probe DC measurement plus the pile and gamma radiation measurements) strongly support the view that under nuclear radiation ferroelectric materials may act as a source of electrical energy.

A detailed discussion of possible mechanisms for the effects observed in the various experiments is given in the appendix. There are at least two possible mechanisms contributing to the charge release phenomena. These are flux anisotropy and the photovoltaic effect associated with the barrier layers. A third mechanism, the anomalous "dielectric polarization" observed by I. Chicurel [4.] and Berlincourt [5.], might also be involved as a contributing influence.

The currents produced by the radiation are variable. Lack of statistics, however, prevents definite predictions of current and voltage due to specific radiation sources. The data suggests that an effect exists, but the complex nature of the pile spectrum coupled with the data scatter prevents a simple analysis for determination of the relationship between the incident radiation and the release of electric charge. Several interactions are certainly taking place but isolation of the major mechanism is not evident.

Whether ordnance items can be initiated by nuclear radiation will depend on several factors, including:

(a) the total amount of available electrical energy;

(b) the rate of charge generation[4.];

(c) the time constants due to the self capacity of the ferroelectric material plus the load resistance to which it is connected.

A complete mathematical treatment was made by Frank Bennett in the "Study Program on Ceramic Transducers." [4.] Depending on circuit values, some specific predictions can be made on the basis of this mathematical study.

The hypothesis upon which Bennett based his analysis is that the observed free surface charge does have enough emf to do work. A recent radiation experiment demonstrated that this was indeed the case for the charge release phenomena observed when ferroelectrics are irradiated. A ballistic galvanometer used as a current indicator gave a continuous mechanical deflection, indicating that electrical power was being delivered while the ferroelectric material was being irradiated. The possibility therefore exists that, with utilization of very low energy initiators, ordnance items may be initiated under proper radiation pulse conditions.

Specific predictions, however, can only be made when circuit values, time constants of power generation, and geometry are all considered. This work is being continued. Future studies will include electrical measurements on samples exposed to both steady fluxes and pulsed radiation.

The following papers have resulted from the work performed on this contract:

(1) "Irradiation Changes of Acoustical and Mechanical Constants in Aluminum" - I. Lefkowitz, J. Acoust., Sec. A, 28, 152A, (1956).

(2) "Observations of Hydrogen Vibration Frequencies in Phosphates by Means of Inelastic Scattering of Cold Neutrons" - I. Pelah, I. Lefkowitz, W. Kley, and E. Tunkelo, Phys. Rev. Letters, 2, L524 (1959).

(3) "Effect of Gamma-Ray and Pile Irradiation on the Coercive Field of $BaTiO_3$" - I. Lefkowitz and T. Mitsui, J. Appl. Phys., 30, n.2, 269 (1959).

(4) "Radiation-Induced Changes in the Ferroelectric Properties of Some Barium Titanate-Type Materials" - I. Lefkowitz, J. Phys. Chem. Solids, 10, 169 (1959).

APPENDIX

Discussion of Mechanisms

In insulators irradiated by particles and by photons in the Mev region, one would expect to see the resultant Compton effect and photo-electrons have a distribution of directions weighted by the vector component of motion of the incident radiation. In the region of energy of cobalt-60 gamma rays, one can consider the Compton effect primarily and such electrons will have an energy:

$$E = \frac{2 m_o C^2 \alpha^2 \cos^2 \phi}{1 + 2\alpha + \alpha^2 \sin \phi} \qquad (1)$$

m_o = electron rest mass

C = velocity of light

ϕ = angle of deflection of electron from path of incident photon of energy $h\nu$

$$\alpha = \frac{h\nu}{m_o C^2} \qquad (2)$$

Then as ϕ goes from 0 to 90°, electron energy will go from maximum to a minimum with a zero value assigned as ϕ goes past 90°. Therefore, anisotropy of incident radiation can produce a current even in the absence of a collecting emf.

If the radiation field is truly isotropic, the net effect would be zero. This, however, is an unlikely condition. Furthermore, the currents due to this flux anisotropy will not only depend on the degree of radiation flux

anisotropy, but also on the flux magnitude. This follows from the fact that the larger the source, the larger the currents will be due to a given percentage of the oriented radiation.

Such "residual" currents have been observed in many organic insulators by several investigators. [7., 8., 9.] Even in geometries like coaxial cables, currents of 10^{-14} amps were observed when x-rays were used as the radiation source. [8.]

In the case of ferroelectric materials, the cause of current flow is severely complicated. Not only is there an observed photovoltaic effect as previously noted [3.], but one would also expect to find some contributions to charge release by the polarization state of the system, by a space charge layer (discussed later), and a possible anomalous charge release. [4., 5.]

For single crystals, the pretreatment of applied field above the Curie point has indicated modification of the charge release. Chynoweth has also reported [10.] the variability of the photovoltaic phenomena. At times he was unable to completely eliminate the photovoltaic effect by annealing, and up to about 180°C, found no threshold annealing temperature.

A layer on the surface of barium titanate single crystals has been suggested as being responsible for the photovoltaic effect. Attempts to measure these surface phenomena have been made by several investigators utilizing various methods, but with little success. X-ray diffraction methods were used by Kay and Lefkowitz and electron diffraction methods by E. Levin of Frankford Arsenal. Lardauer et al using much more elaborate x-ray methods also were unable to observe these surface strains.

The first reference in the literature postulating the existence of a surface layer on barium titanate was made by Kanzig [11]. Dealing with powdered $BaTiO_3$, Kanzig based his hypothesis on the following observations:

"1. There is a discrepancy in symmetry between a surface layer of a thickness of about 100 Å and the bulk. The misfit between the surface layer and the bulk is smaller below the Curie temperature of the bulk. Thus the structure of the surface layer is closer to the tetragonal structure of the polarized lattice than to the cubic structure of the unpolarized lattice.

2. Electron diffraction experiments indicate a tetragonal strain in the surface layer which is slightly larger than the tetragonal strain of the bulk below the Curie temperature. The tetragonal surface strain does not vanish if the crystal is heated above the Curie temperature of the bulk.

It is interesting to note that in the case of ferroelectric KH_2PO_4 no evidence for a polarized surface layer was found. As KH_2PO_4 is not a semiconductor and is generally much purer than barium titanate, this supports the view that the observed surface strain in the case of barium titanate is due to an ionic or electronic space charge layer. This layer may also account for the observation that very thin, virgin barium titanate crystals do not show normal dielectric hysteresis at low voltages V, though the apparent electric field (calculated as V/d, where d is the thickness of the crystal) is larger than the coercive field. The space charge layer has to be broken down before the normal dielectric hysteresis can be observed."

Lehovec [12] analyzes the problem in a different manner. The following is an abstract taken from his paper on "space-charge layer and distortion of lattice defects at the surface of ionic crystals."

"The paper demonstrates that an electric potential exists between the surface and the bulk of ionic crystals. The potential is expressed in terms of the energies necessary for the formation of lattice defects. The distortion of the potential and of lattice defects near the surface is calculated. The difference between the concentration of lattice defects near the surface and that in the bulk leads to a 'surface conduction.' This is calculated by Mott and Littleton [6.] for NaCl crystal using numerical values for the energies of formation of lattice defects. The effect on the surface potential of charge impurities in the crystals is discussed. The importance of the surface potential in diffusion and photoelectric phenomena is mentioned."

Lehovec treats the layer as primarily ionic in nature. The treatment is somewhat similar to the discussion by Frankel [13.] and very definitely leaves the question open as to the exact role of electronic processes in the Kanzig layer. Kanzig [14.] himself has identified this as a major difficulty in the analysis of these layers. The very fact that a photovoltaic effect exists suggests the importance played by electronic processes.

Recently S. Triebwasser [15.] reported anomalous space-charge fields using Kerr-electro-optic measurements. According to the abstract in the Physical Review Letters [15.], the measurements of capacitance above the Curie point indicate that surface layers build up in the presence of a DC field." This offers a possible explanation as to the manner in which the DC fields employed in the experiments carried out under this contract modified the layers believed to exist on the surface of the $BaTiO_3$.

Strong evidence also exists that these space charge layers are found in ceramics ("Surface and Space Charge Effects in Ceramic $BaTiO_3$" - Bussen and Subbarao [16.]).

REFERENCES CITED

1. O. Klein and E. Lange, Zeits. F. Electrochemie, 44, 542 (1938).
2. I. Lefkowitz, J. Phys. Chem. Solids, 10, 169 (1959).
3. A. G. Chynoweth, J. Appl. Phys., 27, 87 (1956);
   A. G. Chynoweth, Phys. Rev., 102, 705 (1956).
4. "Study Program on Ceramic Transducers", DAI-28-017-501-ORD(P)-1059.
5. Berlincourt, Cmolek, and Jaffee, Proc. of I.R.E., 48, N.2, 220-9, Feb. 1960.
6. N. F. Mott and M. J. Littleton, Trans. Faraday Soc., 34, 485 (1938).
7. Meyer, Bonquet, and Alger, J. Appl. Phys., 27, 1012 (1956).
8. G. D. Adams and H. E. Jones, Radiation Research, 3, 210 (1955).
9. J. W. Winston and R. S. Alger, U.S.N.R.D.L.-TR-325 (1959).
10. Private communication.
11. W. Kanzig, Phys. Rev., 93, 549 (1955).
12. K. Lehovec, J. Chem. Phys., 21, 1123 (1953).
13. Frankel, "Kinetic Theory of Liquids."
14. Private communication.
15. S. Triebwasser, Phys. Rev. Letters (Abstract), 4 n.4, 193, Feb. 15, 1960.
16. W. R. Bussen and E. C. Subbarao, Naturewissenschafte, 44, n. 19, 509 (1957).
17. I. Lefkowitz and T. Mitsui, J. Appl. Phys., 30, 269 (1959).

BIBLIOGRAPHY

1. M. Anliker, H. R. Brugger and W. Kanzig, Helv. Phys. Acta, 27, 99 (1954).

2. E. K. Weise and J. A. Lesk, J. Chem. Phys., 21, 801 (1953); A. Nishioka, K. Sckikawa, and M. Owaki, J. Phys. Soc. Japan, 11, 180 (1956).

3. J. Meisinger, Zeits.f.angew.Physik, 8, 422 (1956); P. H. Fang, Bull. Am. Phys. Soc., 2, 23 (1957).

4. W. J. Merz, J. Appl. Phys., 27, 938 (1956).

5. H. Kniepkamp and W. Heywang, Zeits.f.angew, Physik, 6, 25 (1954); L. Egerton and S. E. Koonce, J. Am. Cer. Soc., 38, 412 (1955).

6. J. R. Anderson, G. W. Brady, W. J. Merz, and J. P. Remeika, J. Appl. Phys., 26, 1387 (1955).

7. Z. Kiyasu, K. Fusimi, and K. Kataoka, J. Phys. Soc. Japan, 12, 432 (1957).

:6.

FIG. 1. SAMPLE HOLDER (FLAT)

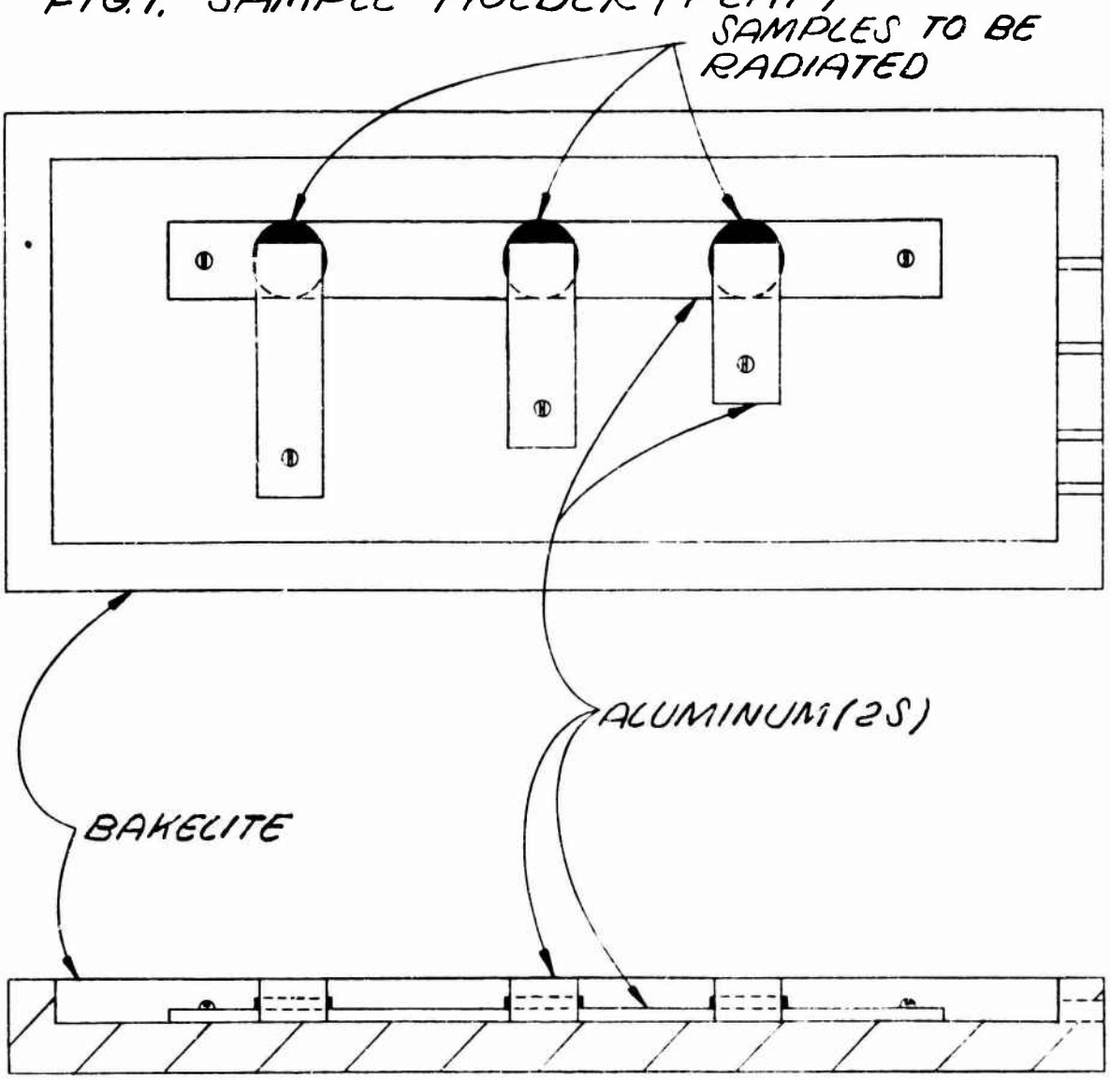

FIG. 2 WORK FUNCTION EFFECTS

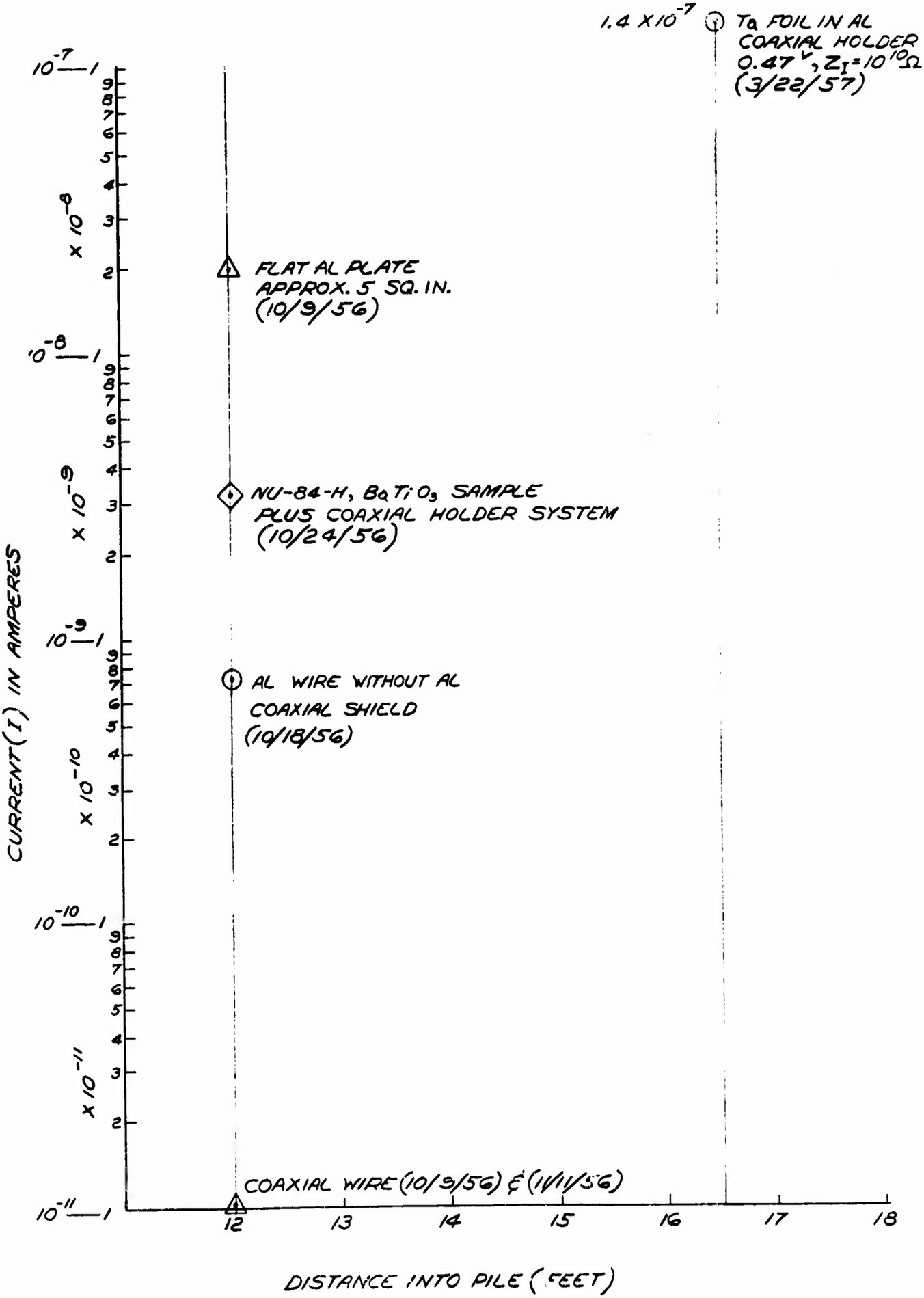

FIG. 3. COAXIAL SAMPLE HOLDER

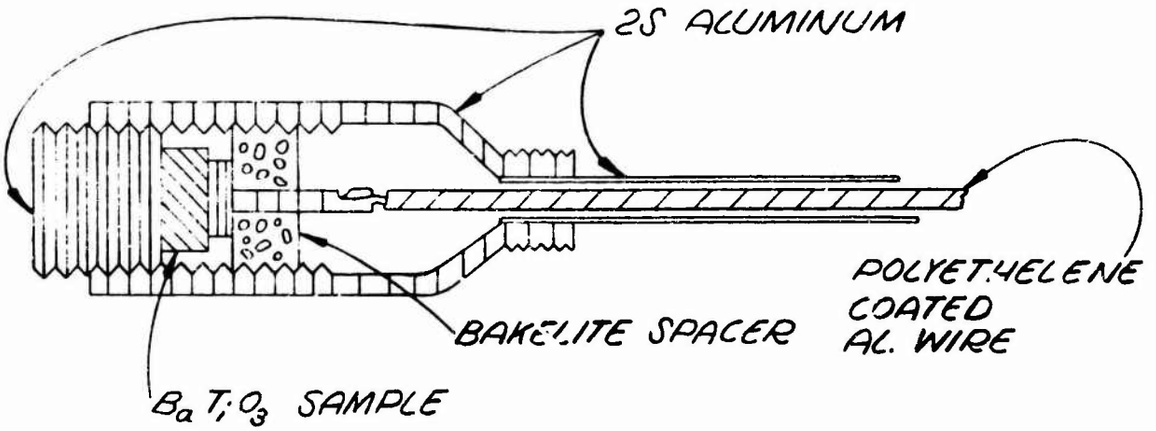

FIG. 4. MODIFIED COAXIAL SAMPLE HOLDER

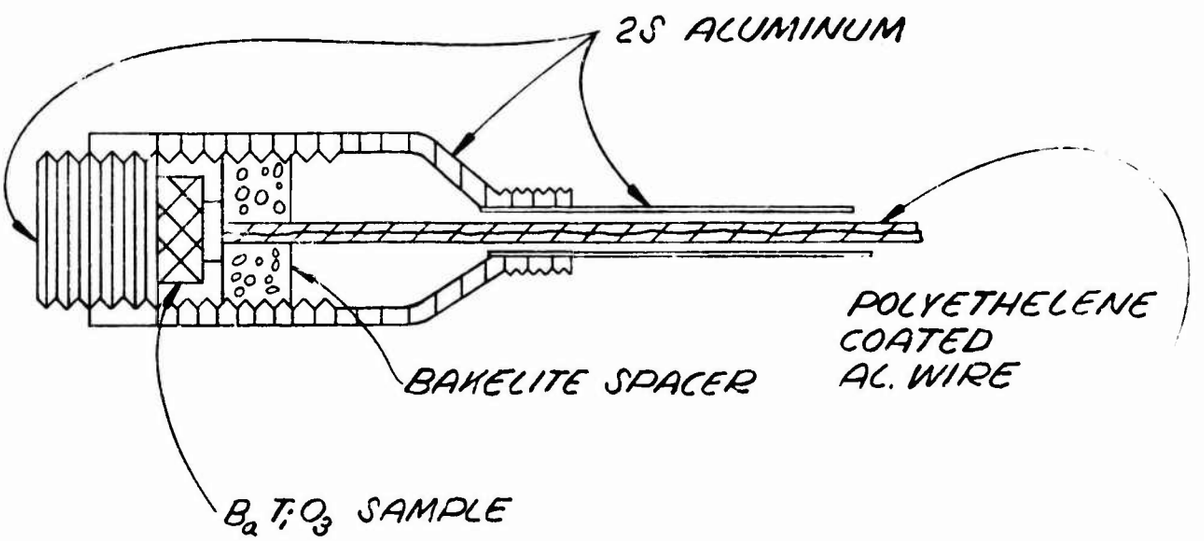

FIG 5. EXPERIMENTS IN NUCLEAR REACTOR

OLD FUEL LOADING
RUN MADE: 10/24/'56
AMBIENT TEMP: 50°C (APPROX)
FACILITY: FLUX HOLE W-13

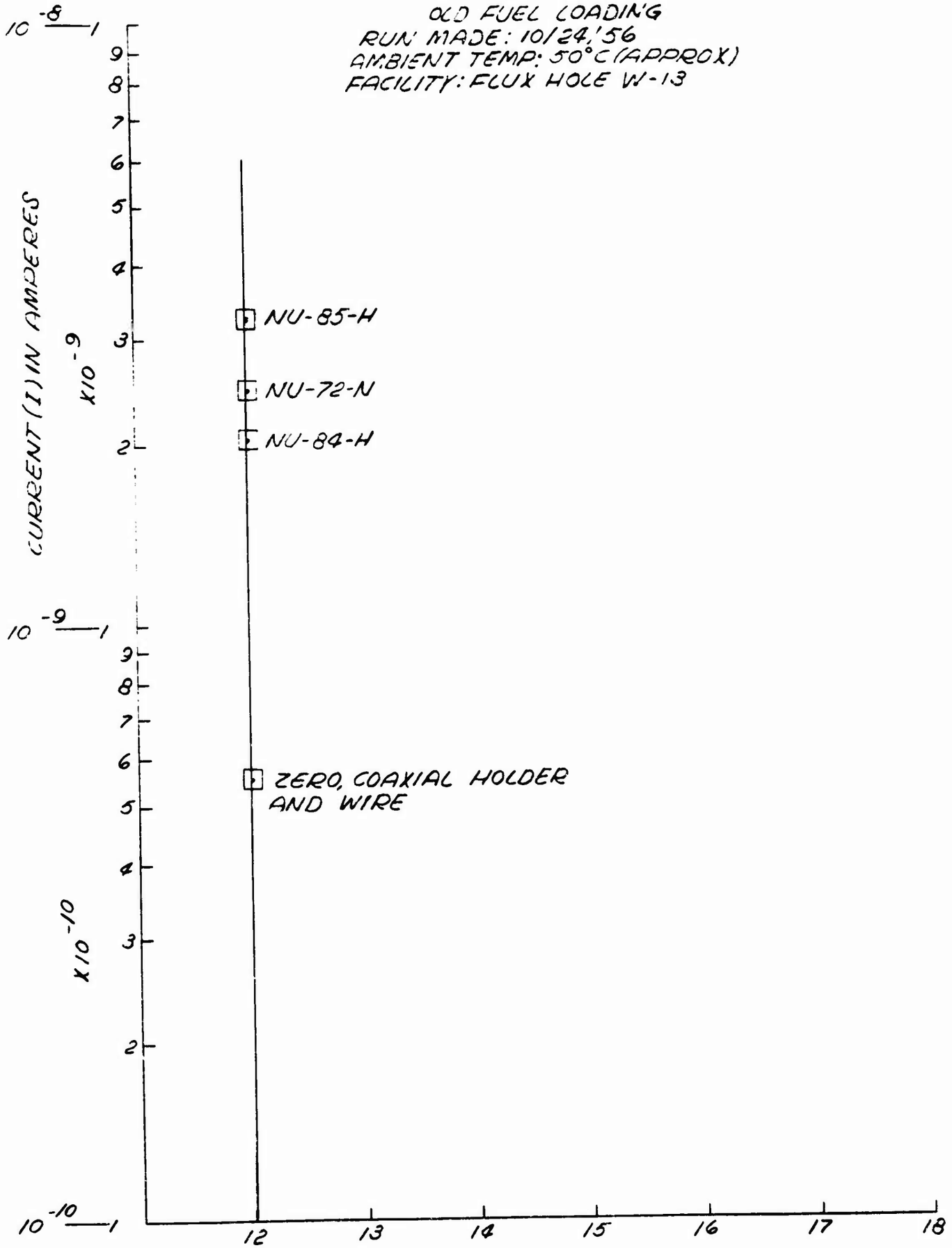

FIG 6. EXPERIMENT IN NUCLEAR REACTOR

RUN MADE : 1/57
FACILITY: FLUX HOLE W-13

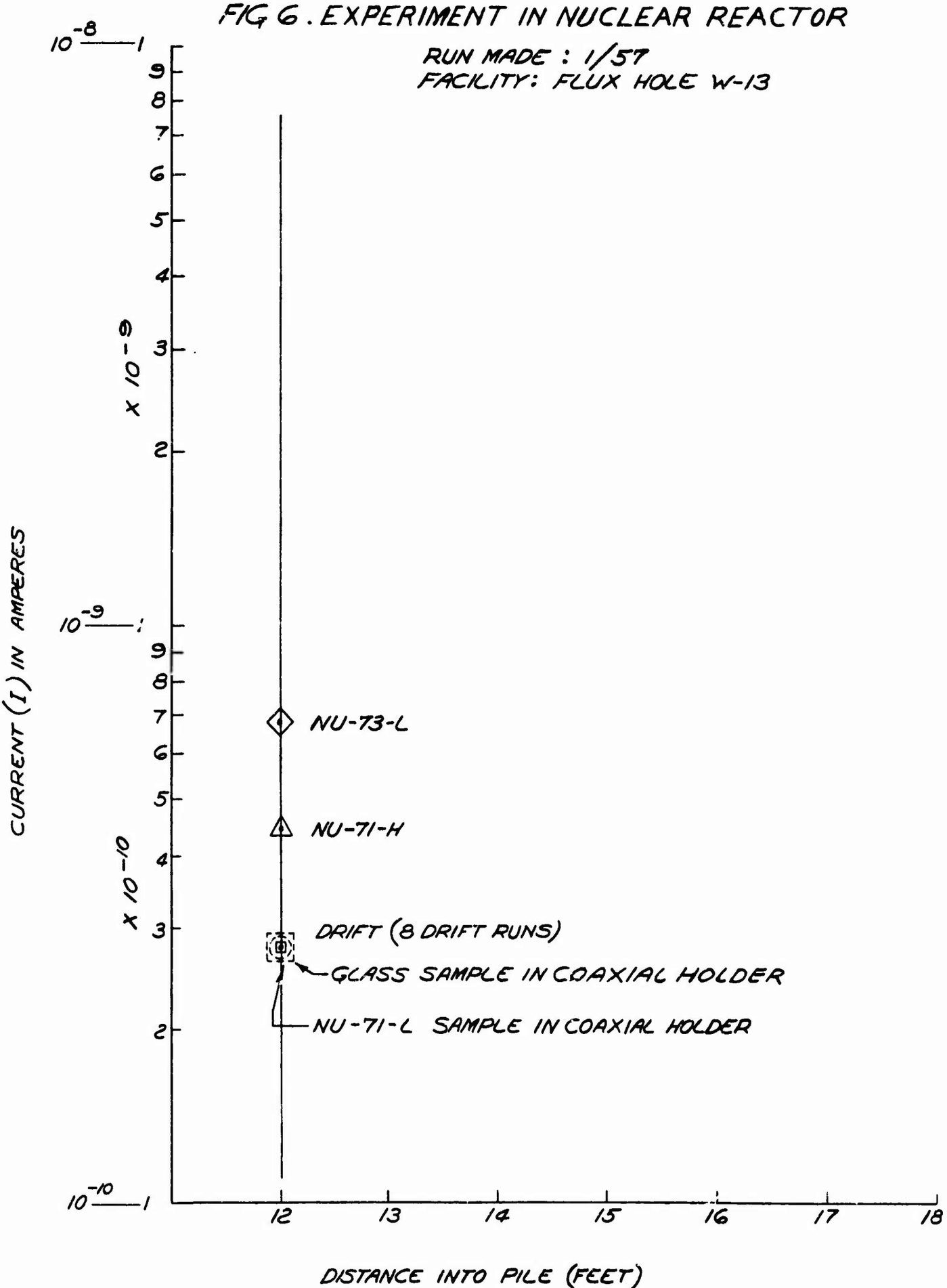

FIG. 7. EXPERIMENTS IN NUCLEAR REACTOR

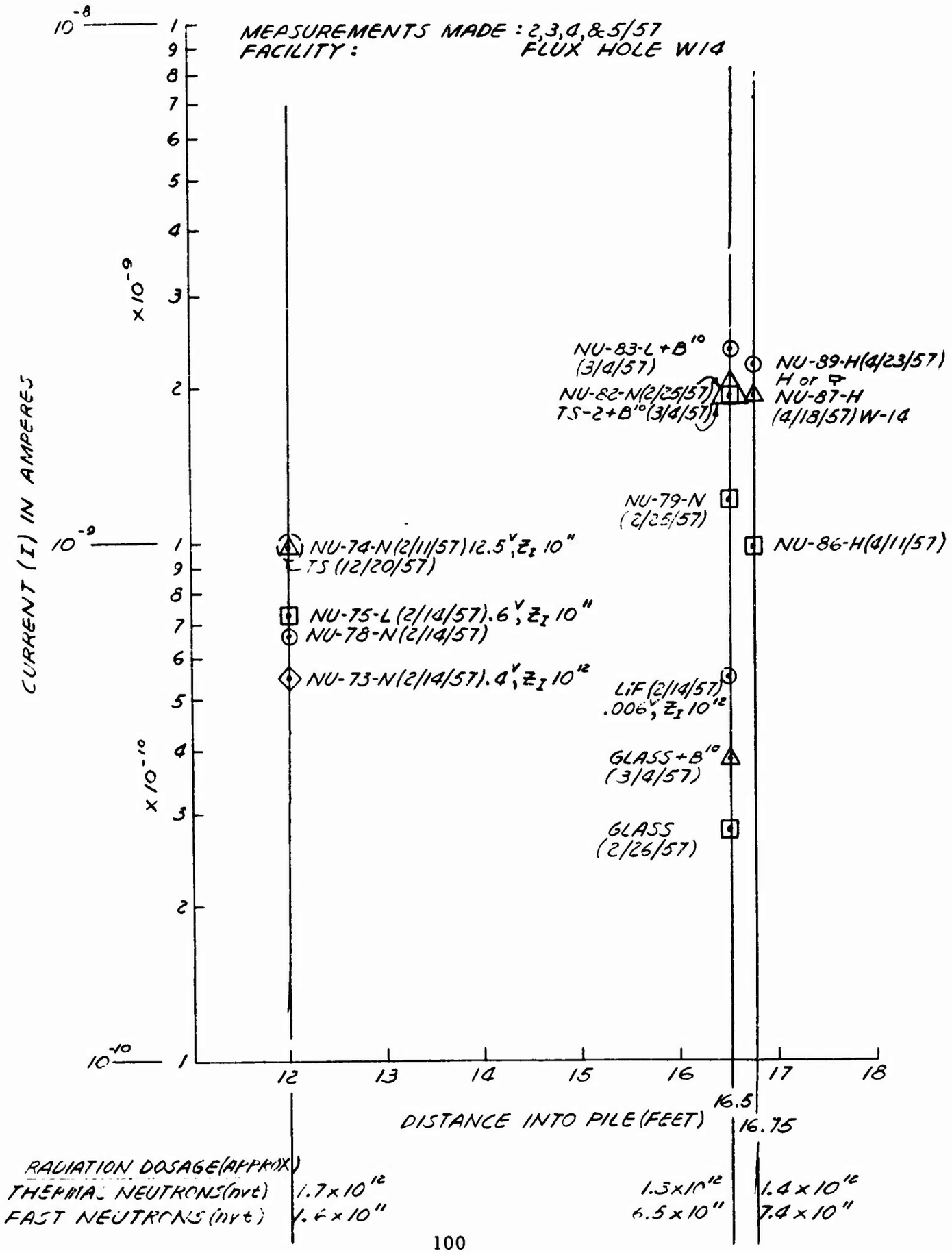

FIG. 8 TEMPERATURE MEASUREMENTS IN NON-FERROELECTRICAL REGION

DATE: 6/10/57
SAMPLE: NO. TS-6
PILE: AT 23 m.w
HOLE: E-11

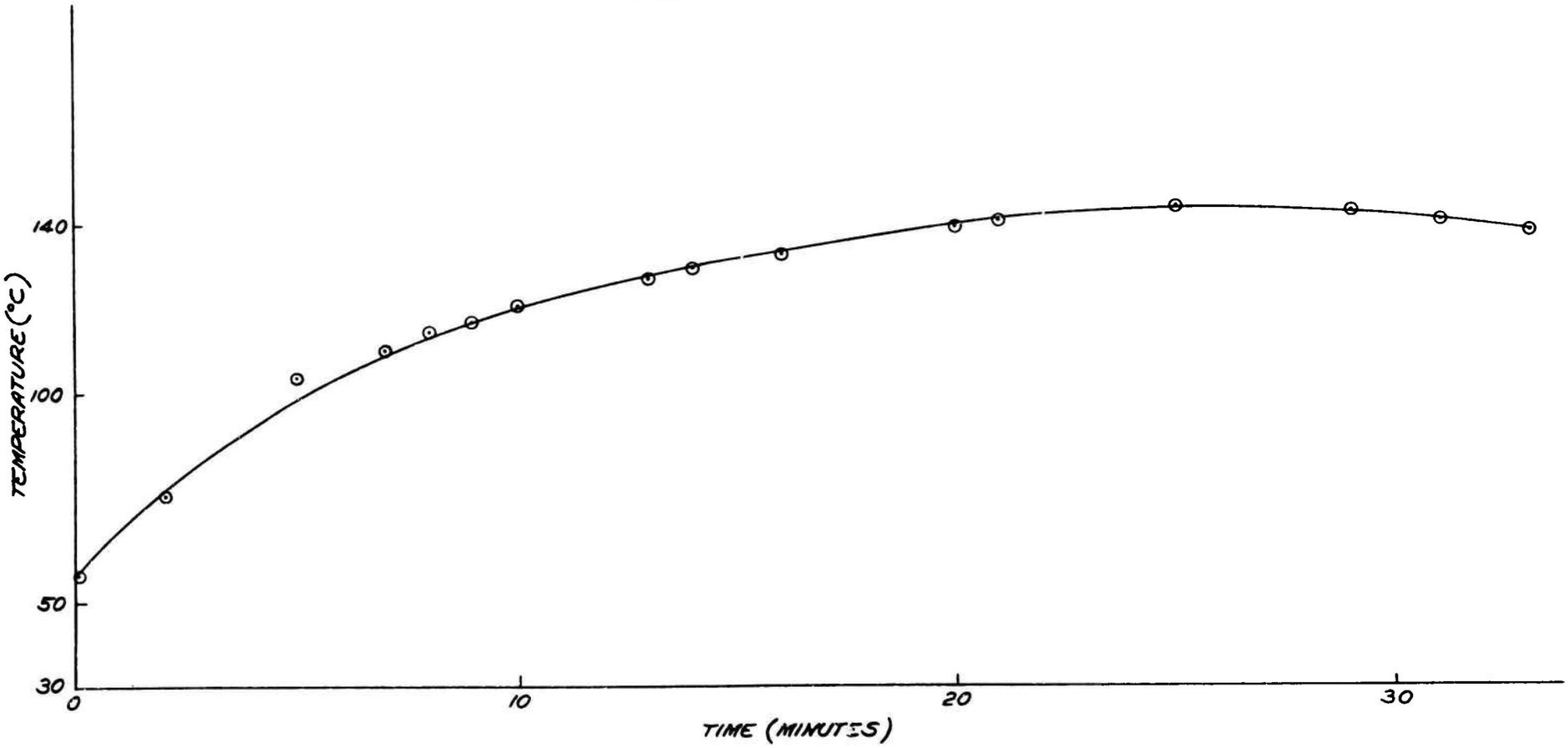

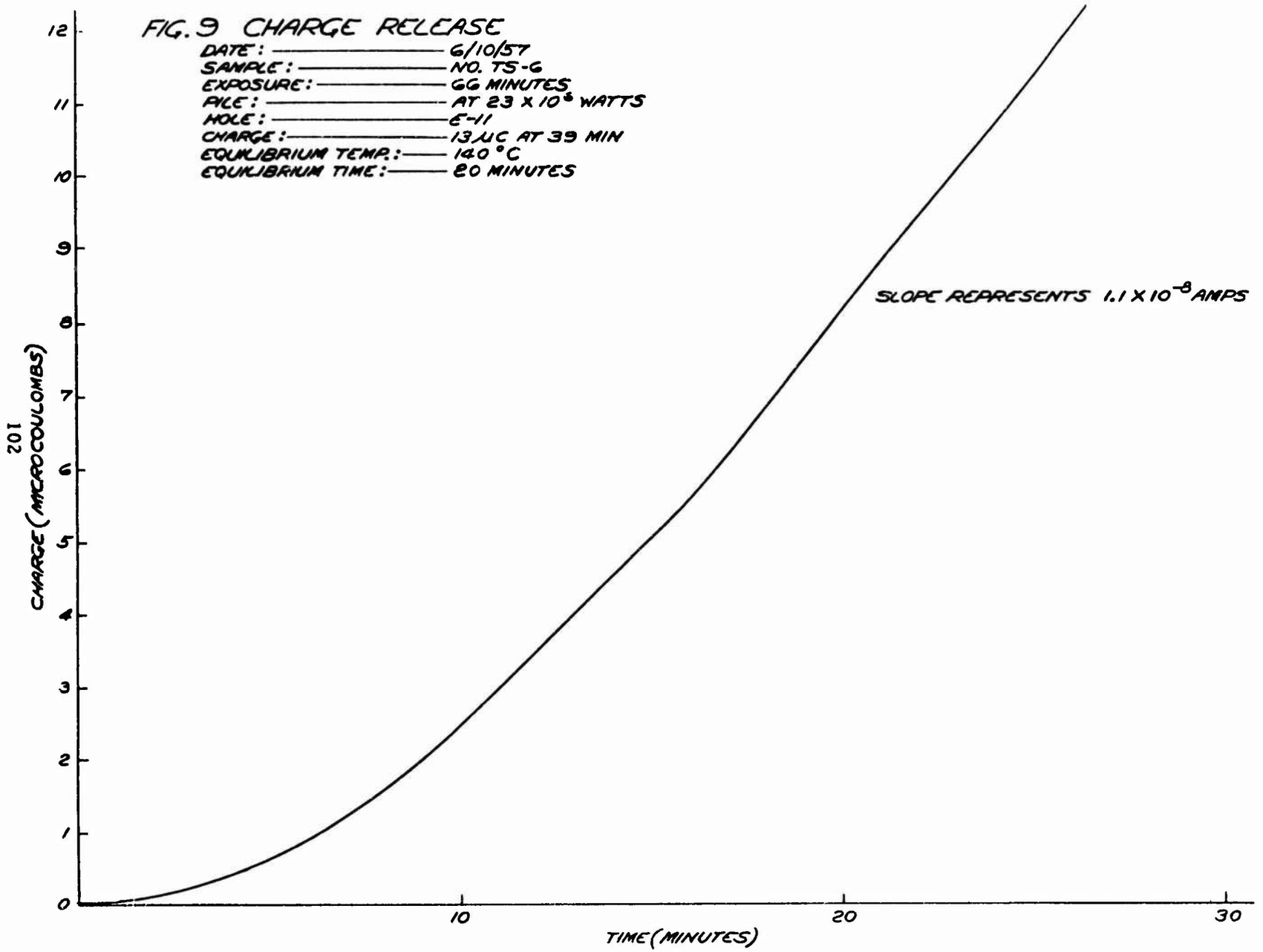
FIG. 9 CHARGE RELEASE
DATE: 6/10/57
SAMPLE: NO. TS-G
EXPOSURE: 66 MINUTES
PILE: AT 23 X 10⁶ WATTS
HOLE: E-11
CHARGE: 13 μC AT 39 MIN
EQUILIBRIUM TEMP.: 140 °C
EQUILIBRIUM TIME: 20 MINUTES
SLOPE REPRESENTS 1.1 X 10⁻⁸ AMPS
CHARGE (MICROCOULOMBS)
10²
0
1
2
3
4
5
6
7
8
9
10
11
12
10
20
30
TIME (MINUTES)

FIG. 10. EXPERIMENT IN NUCLEAR REACTOR

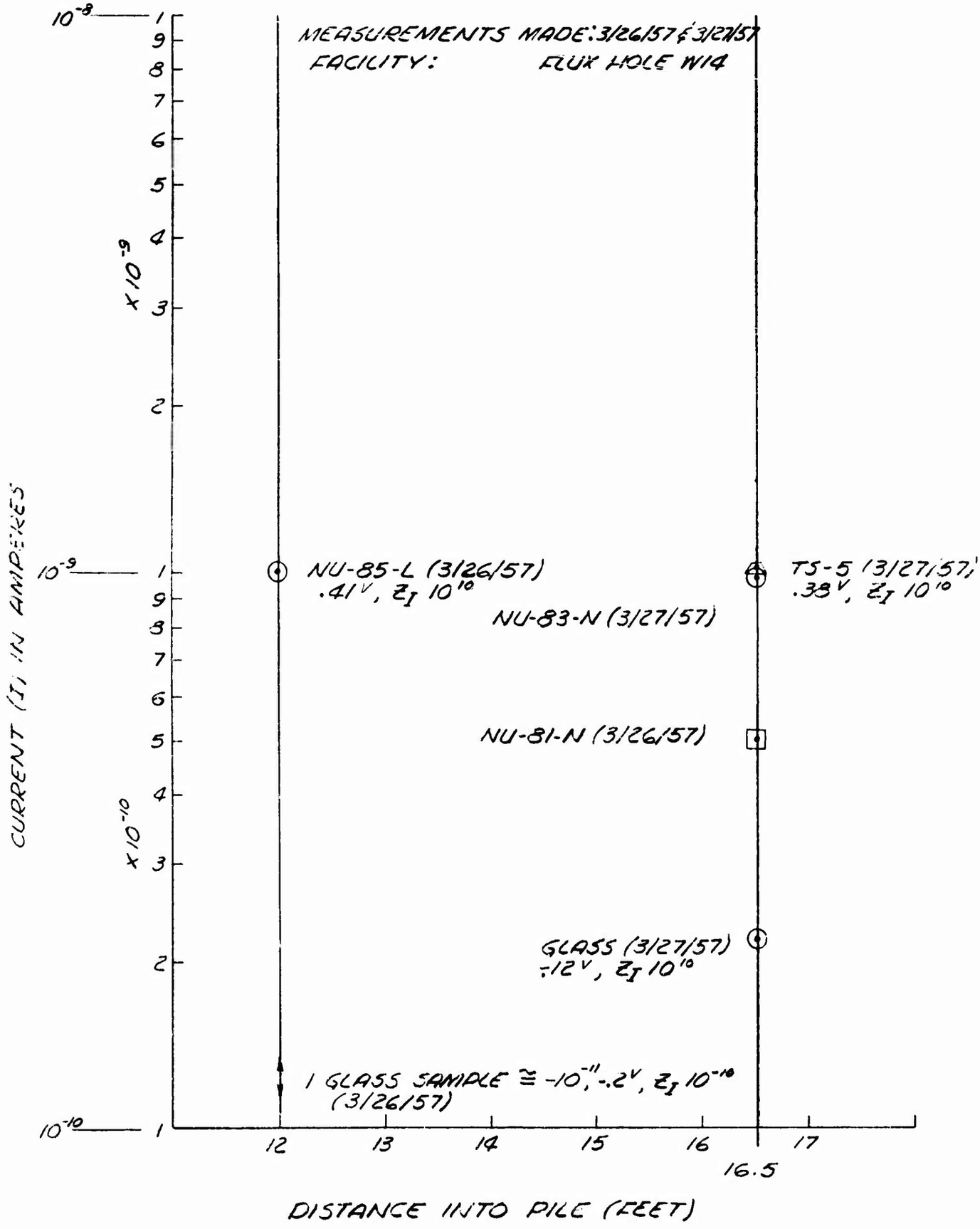

FIG. 11. EXPERIMENT IN NUCLEAR REACTOR

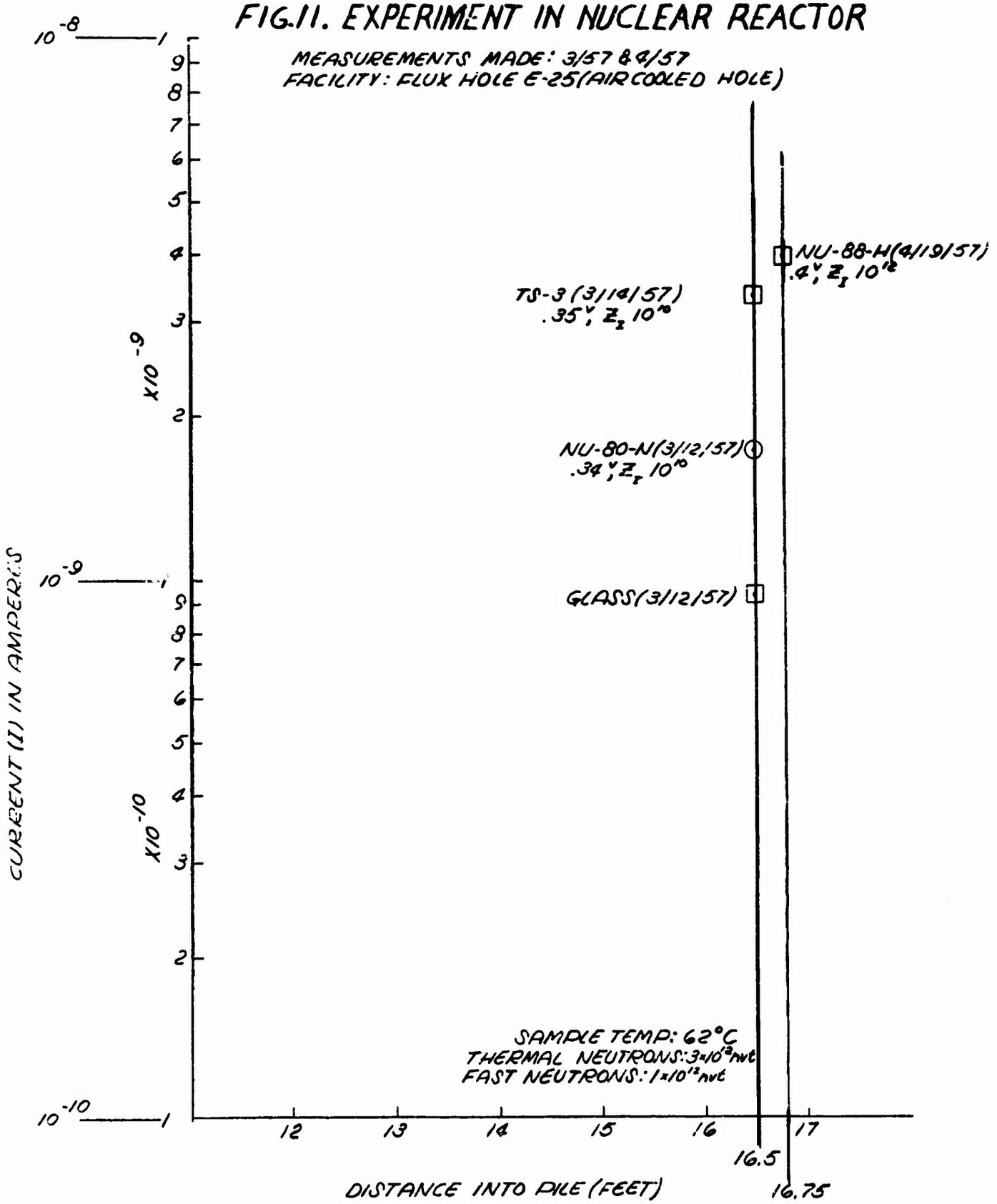

FIG. 12. EXPERIMENT IN NUCLEAR REACTOR

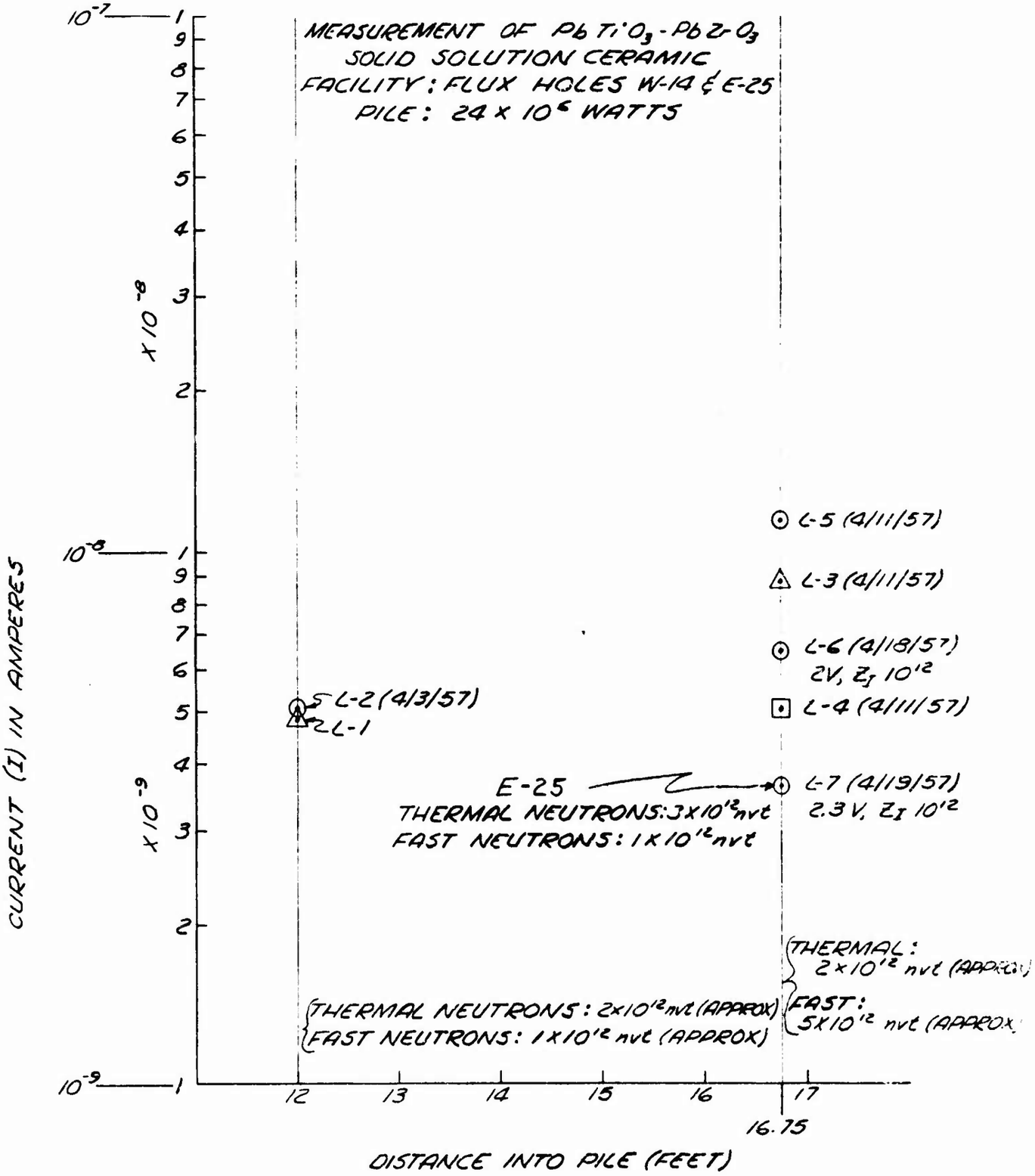

FIG. 13. EXPERIMENT IN NUCLEAR REACTOR

MEASUREMENTS IN Co^{60} GAMMA FACILITY

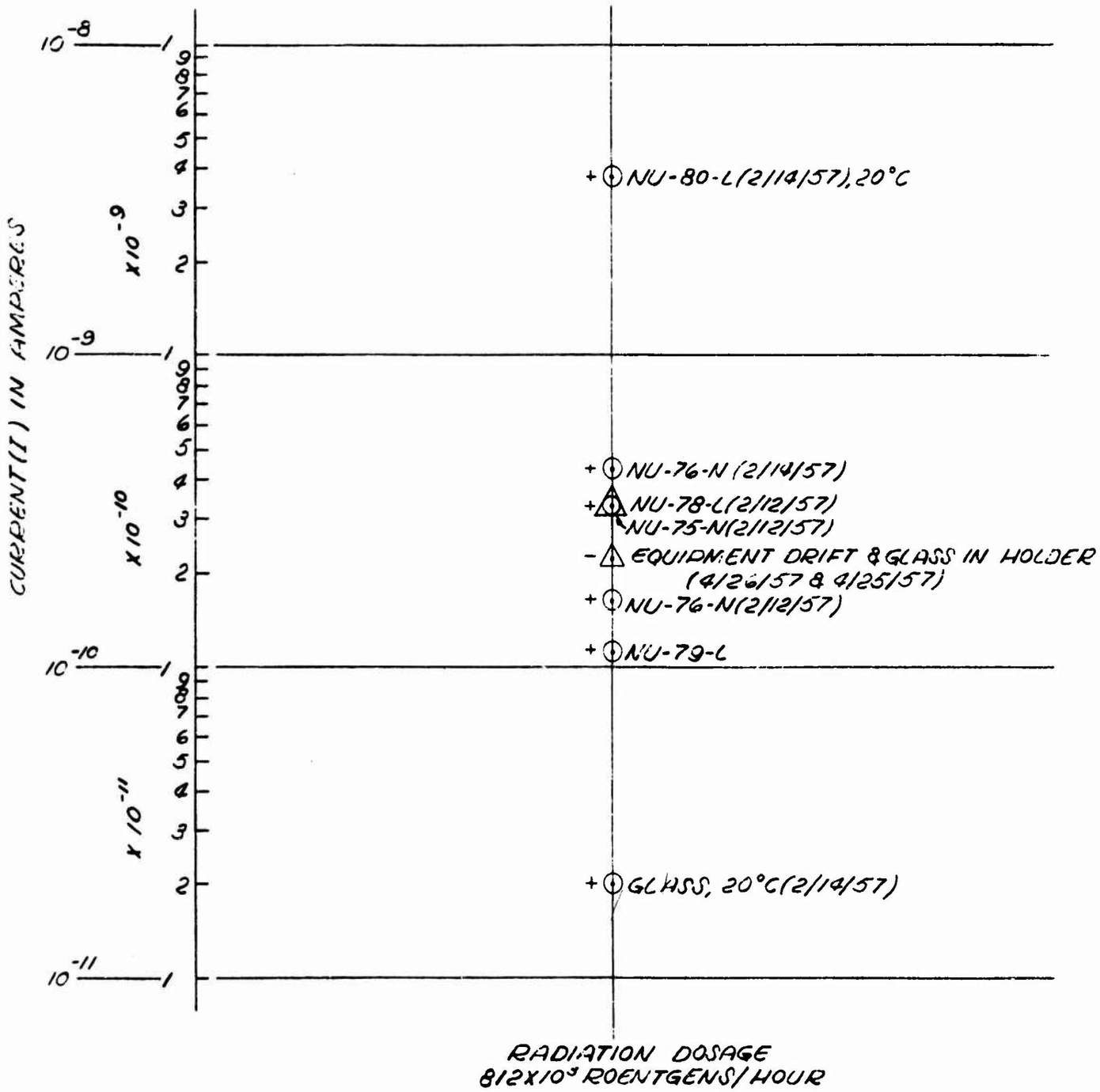

FIG. 14. EXPERIMENT IN NUCLEAR REACTOR

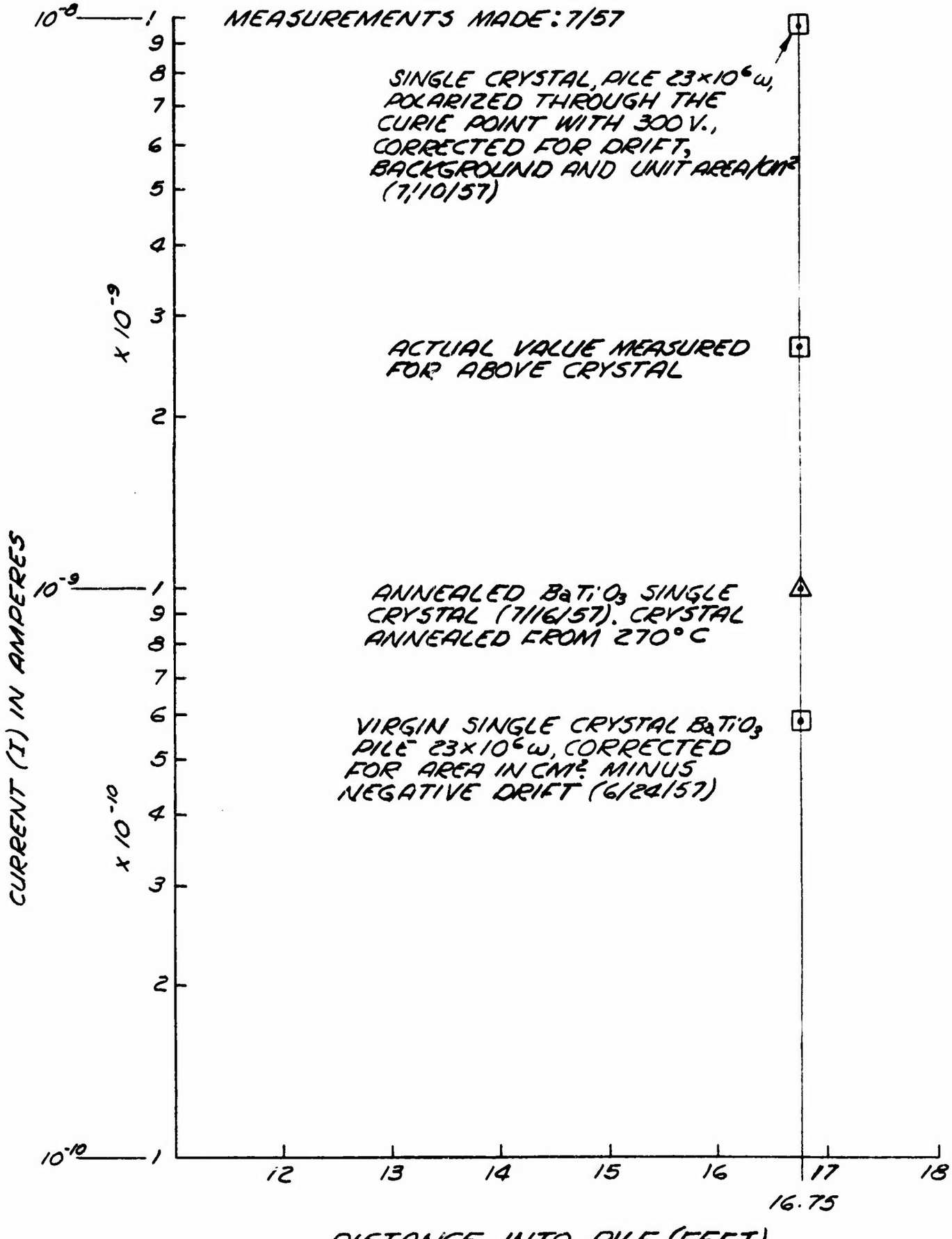

FIG. 15 EXPERIMENTS IN GAMMA SOURCE
(Co^{60} GAMMA SOURCE, 800 X 10^3 ROENTGENS/HR)

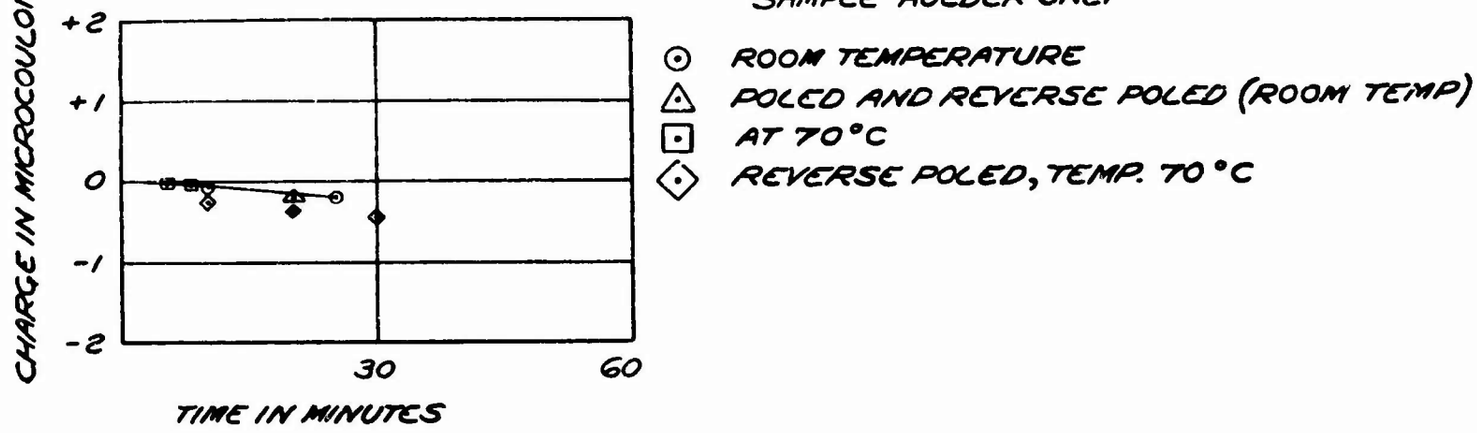

FIG. 16 EXPERIMENTS IN GAMMA SOURCE
(Co^{60} GAMMA SOURCE, 800 X 10^3 ROENTGENS/HR)
SAMPLE: VIRGIN CRYSTAL

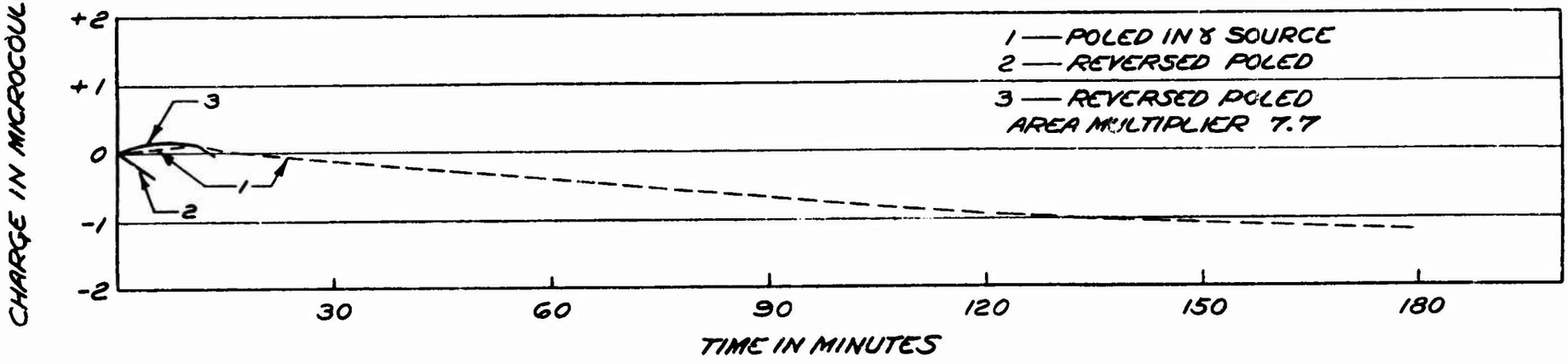

FIG. 17. EXPERIMENTS IN GAMMA SOURCE
(Co^{60} GAMMA SOURCE, 800×10^3 ROENTGENS/HOUR)
SAMPLE: VIRGIN CRYSTAL ($BaTiO_3$) AT 70°C

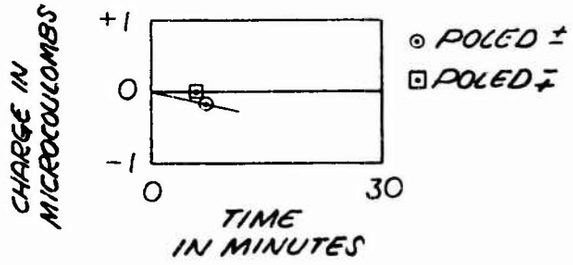

FIG. 18. EXPERIMENTS IN GAMMA SOURCE
(Co^{60} GAMMA SOURCE, 800×10^3 ROENTGENS/HOUR)
SAMPLE: POLARIZED CRYSTAL

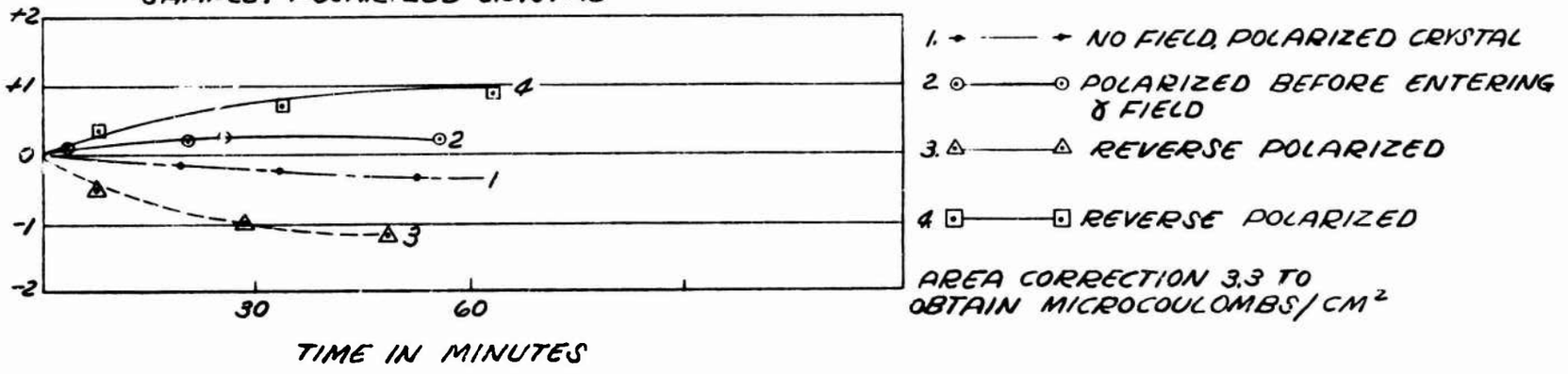

FIG. 19. EXPERIMENTS IN GAMMA SOURCE
(Co^{60} GAMMA SOURCE, 800×10^3 ROENTGENS/HOUR)

(Reprinted from Nature, Vol. 184, No. 4881, pp. 657–659. May 18, 1959)

RADIATION AND ACOUSTIC EXCITATION OF ANOMALOUS LAYERS ON PEROVSKITE FERROELECTRICS

By I. LEFKOWITZ

Crystallographic Laboratory, Cavendish Laboratory, Cambridge

THE acoustic and radiation excitation of the anomalous layers that exist on the surface of perovskite ferroelectrics have been investigated. The results support the view that a space charge layer exists on the surface of perovskite ferroelectrics and that it is randomly distributed across the sample and has different net polarities in different parts of the same sample.

W. Känzig[1] first suggested the existence of an anomalous surface layer on $BaTiO_3$ and since then a large body of experimental evidence has been built up for the existence of this surface layer[2–10] (reviewed in detail by Jona and Shirane[11]). The effects observed are: (*a*) Tetragonal surface layer above the Curie point[2]. (*b*) Thickness dependence of the switching characteristics[3]. (*c*) Modification of the dielectric constant above the Curie point by field and frequency; and the dielectric constant dependence on thickness in this temperature region[8]. (*d*) Evidence of pyroelectricity above the Curie point[4]. (*e*) Asymmetric distribution of birefringence induced by d.c. fields above the Curie point[5]. (*f*) Free surface charge observed when irradiated by γ-rays and reactor neutron flux[10].

Several models have been proposed, but the effects (*a*) (*d*) (*f*) can best be explained by the original suggestion of Känzig, namely, a layer of high potential stress (10^6 V/

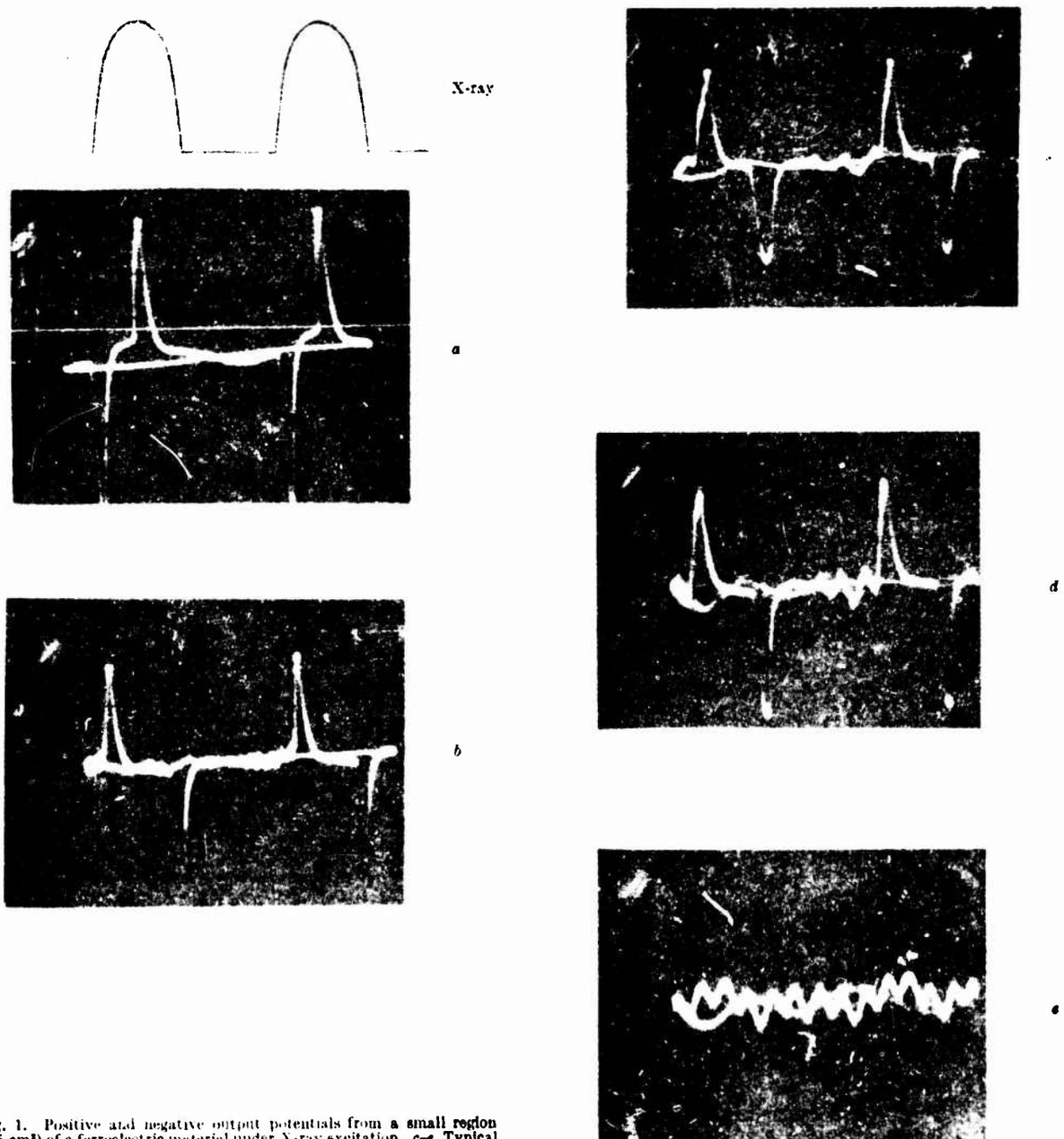

Fig. 1. Positive and negative output potentials from a small region (1·5 cm³) of a ferroelectric material under X-ray excitation. *c–e*, Typical radiation decay pattern.

c·n) at the surface. My results tend to confirm this model and, further, show that many experimental measurements and applications of ferroelectrics may be open to serious criticism if these surface layer effects are not recognized as a source of difficulty.

The samples examined were mounted in a μ metal shielded cage in which a small opening was cut permitting X-rays to enter and irradiate the sample. The fine wire mounting acted as a probe pick-up. This pick-up was connected directly to a high impedance amplifier the output of which was displayed on an oscilloscope. White radiation from iron and copper targets pulsed at 50 c.p.s. was used. No quantitative difference was found for the data obtained using different X-ray sources.

The materials examined were single crystals of $BaTiO_3$; 0·2-mm and 5–10-mm thick ceramics of $BaTiO_3$; and solid solutions $PbTiO_3$—$PbZrO_3$. Glass samples with the same electrode techniques were used as standards to check the measurements. The measurements were made in an environment of high ambient noise so that piezoelectric activity of the samples was apparent. The results for the radiation sensitivity were approximately the same when there was no acoustic excitation.

All the photographs reproduced here (Figs. 1 and 2) were made of the output from one sample of 0·2-mm thick ceramic but are representative of results obtained with the materials studied.

When the irradiation was first begun, Barkhausen pulses were sometimes observed. These were 'random' and showed no systematic time relationship to the X-ray

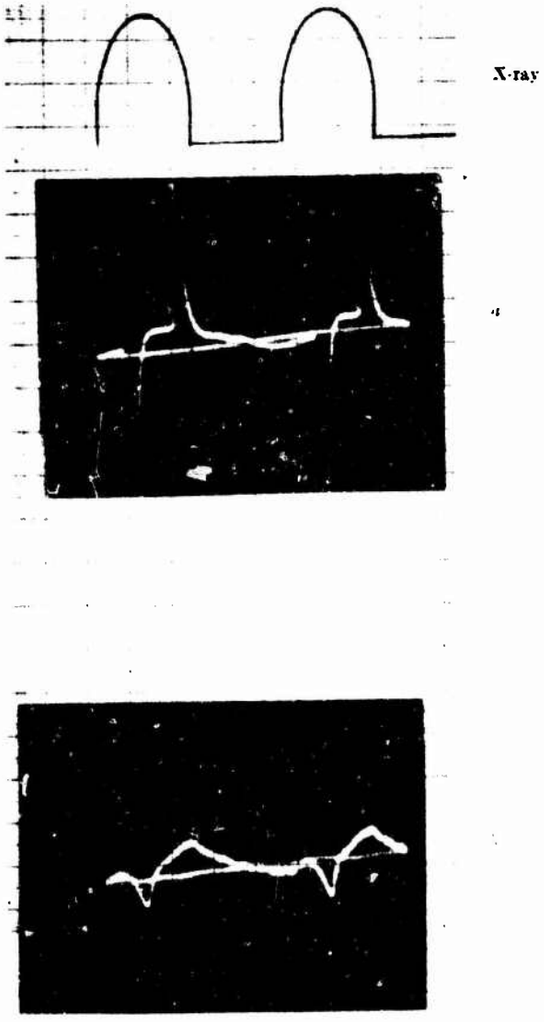

Fig. 2. Typical radiation decay pattern

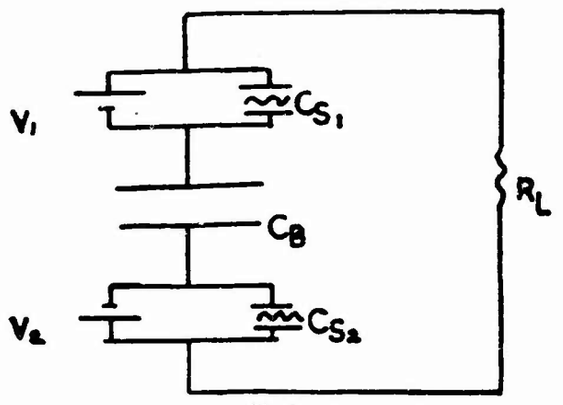

Fig. 3

repetition rate. The instantaneous 'normal' output is shown in Fig. 1*a*, sharp leading edge and exponential decay; and then the inverse. No evidence of piezoelectric output is apparent. A portion of the same sample (in fact 1·5 cm away) gave an output of opposite polarity (Fig. 1*b*). The polarity of the output changed during irradiation in some portions of the material and the final amplitudes were much reduced. After a short time (between 0·5 and 3 min) there was a decrease in pulse height and evidence of piezoelectric output during the X-ray dead-time (Fig. 1*b*). The piezoelectric sensitivity gradually returned (Fig. 1*c* and *d*), until there was small evidence of the radiation sensitivity, and piezoelectric output was observed (Fig. 1*e*). Photographs (Fig. 2*a* and *b*) were taken over a period of 5 min and show another decay pattern. No change was made in the probe position for this experiment. When the X-rays were turned off and the irradiation repeated, the pattern of output was the same (Fig. 1*b*, *c*, *d* and *e*) at the same probe position. Some sample positions showed a 'steady-state' radiation output that was stable and continued as long as the irradiation continued (several days).

The experimental evidence which supports a surface layer charge generator is: (*a*) Potential output is observed only when an intimate bond is made with the surface of the sample (foil electrodes do not work). (*b*) Radiation output is observed above the Curie point. (*c*) There is no systematic sample-thickness dependence of the potential amplitudes. (*d*) Potentials are observed only when small contact areas ($\approx 0{\cdot}2$ mm^2) are used. (*e*) Effects are observed using painted silver electrodes (Dupont silver 5399-A Lot 13475) and vapourized metal coatings of indium and gold. (*f*) Re-dipping the gold-coated sample in a mercury bath without a change in contact area increased both radiation and piezoelectric sensitivity. (*g*) Similar results are obtained from single crystal $BaTiO_3$, polarized and non-polarized ceramic. (*h*) Interdependent character of the piezoelectric and radiation sensitivity.

The experimental results demonstrate that when perovskite ferroelectrics are irradiated, they act as current generators. The polarity of the output is either negative or positive from different areas of the same sample. There is a significant contribution to the piezoelectric activity of ferroelectric materials by the surface which is nullified when the samples are first irradiated.

The models invoked by previous investigations to explain the surface effects fall into two general categories: (i) a surface layer ($\simeq 100$ Å) of high potential stress $\approx 10^5$ V cm^{-1}; (ii) a deformed surface layer (mechanical or chemical) which does not contribute to the spontaneous polarization but is a 'source' of interface charge'.

This communication shows how model (i) satisfies in a qualitative manner the observed phenomena and to emphasize the implications of the observed results.

Consider an equivalent circuit Fig. 3.

Before irradiation V_1, V_2 polarize layers Cs_1 and Cs_2, therefore the layers Cs_1, Cs_2 contribute to piezoelectric

activity. At the start of the radiation pulse photoelectrons effectively 'short' V_1 and V_2 discharging C_3 through R_L, the polarity being a function of the 'net' polarity of V_1 and V_2. As the radiation continues new 'boundary' conditions are created with a return of the equivalent circuit shown in Fig. 3. A continuous current flow under radiation conditions would depend on the final 'net' polarity.

The possible applications are many, for example, if a very thin ceramic or single crystal is excited in its 'thickness' mode of vibration, it could be used as a sensitive radiation detector. The effect described could also be used as a sensitive non-destructive test of the uniformity of transducer material. It is the primary object of this article to emphasize the sensitive condition that this effect may contribute to in complex equipment systems.

Ferroelectric ceramics are used both as transducers and capacitors. They are usually completely electroded; therefore, under normal conditions one would expect to see no contribution from these surface effects. It is just this random character that is both its source of safety and source of danger. Efforts to modify these layers by annealing has given very conflicting results. Chynoweth (private communication) reports possible evidence of their existence in some samples when annealed from 180° C. Lefkowitz[10] found similar evidence in samples that had been annealed from 300° C. Therefore, devices and systems that use these materials as capacitors and transducers which are safe and reliable, and have demonstrated themselves to be so over long periods of time under various test programmes, may still produce situations where, if surface potentials throughout the sample are 'optimized' a condition of high sensitivity may occur. The probabilities of this happening are very small if the component is well electroded and when the parallel circuit's impedance is low, but, since so little is understood about the nature of these surface effects in ferroelectric components, caution is strongly advised even in applications which have given no cause for concern in the past.

This work was supported by the U.S. Department of the Army through its European Research Office.

I thank Sir Nevill Mott and Dr. W. H. Taylor for provision of facilities and Mr. C. Chapman and Mr. D. Woollard for fabrication of the crystal holder assembly.

[1] Känzig, W., *Phys. Rev.*, **98**, 549 (1955).
[2] Merz, W. J., *J. App. Phys.*, **27**, 938 (1956).
[3] Miller, R. C. and Savage, A. J., *J. Appl. Phys.*, **31**, 662 (1960).
[4] Chynoweth, A. G., *Phys. Rev.*, **102**, 705 (1956).
[5] Wieder, H. H., and White, D. J., *NOL Corona, Tech. Mem.*, No. 42-28, May (1959). (cited in ref. 11).
[6] Triebwasser, S., *Phys. Rev.*, **118**, 100 (1960).
[7] Drougard, M. E., and Landauer, R. J., *J. App. Phys.*, **30**, 1663 (1959).
[8] Harman, G. G., *Phys. Rev.*, **111**, 27 (1958).
[9] Drougard, M. E., and Schlosser, H. J., *J. Appl. Phys.*, **32**, 1227 (1961).
[10] Lefkowitz, I., *J. Phys. Chem. Solids*, **18**, 169 (1959); *Summary Rep.* Contract No. DA-36-039-sc-507-0 *RD*-1966, *Gulton Industries Inc. for Frankford Arsenal* (Philadelphia, Penn.)
[11] Jona, F., and Shirane, G., *Ferroelectric Crystals* (Pergamon Press, 1962).

Printed in Great Britain by Fisher, Knight & Co., Ltd., St. Albans.

APPENDIX B

PART 2

PICATINNY ARSENAL TECHNCAL REPORT 3045

PRELIMINARY REPORT ON NUCLEAR RADIATION EFFECTS ON PIEZOELECTRICS

ROBERT KESSELMAN

JANUARY 1963

PICATINNY ARSENAL
DOVER, NEW JERSEY

Technical Report 3045

PRELIMINARY REPORT ON NUCLEAR RADIATION EFFECTS ON PIEZOELECTRICS

by

Robert Kesselman

January 1963

Reviewed By: JW Gregorits
JOHN W. GREGORITS
Chief, Advanced Concepts Section

Approved By: WR Benson
W. R. BENSON
Chief, Engineering Sciences Laboratory

Engineering Sciences Laboratory
Feltman Research Laboratories
Picatinny Arsenal
Dover, N. J.

TABLE OF CONTENTS

ACKNOWLEDGEMENT

Mrs. Luella Ellington of the Engineering Sciences Laboratory, Feltman Research Laboratories, is acknowledged for her contribution to the work performed at the Triga Reactor.

ABSTRACT

Nuclear radiation has become another environment which the engineer must consider when designing circuitry. Piezoelectrics have important military applications and it is, therefore, necessary to know how they function during and after nuclear radiation. This report summarizes the preliminary data that this Arsenal has obtained on nuclear effects on lead zirconium titanate and barium titanate crystals. These results represent preliminary information on a statistically small number of samples, but certain trends seem evident (e.g., capacitance and charge release decrease under radiation). Further work is planned in order to determine accurately the different effects produced by varying levels of neutron and gamma radiation on PZT as well as the damage mechanisms involved.

CONCLUSIONS AND RECOMMENDATIONS

It is concluded that piezoelectrics seem relatively radiation resistant, but a great deal of additional work is needed to determine accurately the levels at which the crystals are affected and damage mechanisms involved.

INTRODUCTION

In recent years, great interest has been shown in the manner in which components and systems will function in nuclear environments. This has become an important consideration in the design of military systems. A cursory check through the literature will reveal an abundance of data on nuclear effects on transistors, diodes, resistors, and many other passive and active elements. However, this is not the case for piezoelectrics for which a very scanty amount of information exists.

Since piezoelectrics have important military applications, Picatinny Arsenal began a program of reactor and gamma source irradiation on these components. This report summarizes the preliminary data obtained on nuclear effects on lead zirconium titanate and barium titanate. Further work is planned, in order to determine accurately the different effects produced by varying levels of neutron and gamma radiation on PZT as well as the damage mechanisms involved. Present work on this project is being sponsored by Army's Diamond Fuze Laboratories.

DISCUSSION

Barium Titanate

In 1956, Rogers irradiated barium titanate, $BaTiO_3$, to a dose of 10^{21} nvt at the Hanford facility. After such a dose, the typical dielectric constant peak disappeared and the dielectric constant was reduced to a nearly constant value over the temperature range 30°C to 140°C. This irradiated value was about half of the pre-irradiated room temperature dielectric constant [1]. In 1957, Wittels and Sherill reported that a phase transformation is produced in a single barium titanate crystal after a dose of 1.8×10^{20} n/cm^2. Here a change from the tetragonal to the cubic was noted [2]. In 1958, Lefkowitz reported that $BaTiO_3$ with additives shows a reduction of the dielectric-constant peak at the Curie point and also a reduction in the Curie temperature with reactor irradiation. On the other hand, pure $BaTiO_3$ showed no shift in the Curie point while demonstrating a decrease in the dielectric-constant peak. There is an increase in tan δ with irradiation and after 1×10^{18} n/cm^2 no hysteresis loops could be obtained [3]. This represented all the information that could be culled

from the open literature.

In order to determine the permanent damage produced by reactor irradiation on $BaTiO_3$, five of these piezoids were irradiated to $1 \times 10^{18} n/cm^2$ at the Brookhaven National Laboratories, Upton, New York. The results of these tests are summarized below.

Voltage (Volts)*

Unit No.	Before Irradiation	After Irradiation	% Δ
124	5.7	2.9	-49.0
46	5.0	3.9	-22.0
35	5.3	4.1	-22.6
22	4.4	3.4	-22.7
16	5.0	3.9	-22.0

Resonant Frequency (Kc)

124	275.5	310.0	+12.5
46	277.0	283.8	+ 2.4
35	277.5	323.0	+16.4
22	276.0	285.5	+ 3.4
16	278.2	286.5	+ 3.0

Samples of $BaTiO_3$ were irradiated at Picatinny Arsenal with a pure Cobalt-60 source to a total dose of $1.7 \times 10^8 R$ at a rate of $3.74 \times 10^5 R/hr$. The effect of this irradiation on the dielectric properties of the material is summarized below.

Capacitance (μμf)

34	530	520	-1.9
108	520	508	-1.9
105	535	525	-1.9
84	515	505	-2.3

The post irradiation measurements on d_{33} were too erratic to be meaningful.

* Force = 150 lbs.

Lead Zirconium Titanate

Clevite Corporation obtained the following data on the permanent damage produced on a PZT-5 type composition by pure Cobalt-60 irradiation.

Dose 10^7R

	Kp	Frequency Constant	Dielectric Constant	% Change in d_{33}
Pre-Irradiation Data	.453	1536 Kc mm	1046	
Post Irradiation Data	.456	1546 Kc mm	975	-3.4

Dose 10^8R

Pre-Irradiation Data	.474	1536 Kc mm	1075	
Post Irradiation Data	.476	1551 Kc mm	975	-5.2

In addition, Clevite reported that irradiation has the further effect of arresting aging, or even starting a slow deaging cycle.[4]

PZT crystals were tested for permanent damage at Picatinny Arsenal's Cesium-137 facility. The latter has a dose rate of 1.9×10^5R/hr. These crystals were tested for permanent effects on their capacitance, D, d_{33}, and hysteresis curves at doses of 1.09×10^6R and 1.35×10^7R.

Dose 1.09×10^6R

Capacitance ($\mu\mu$f)

Crystal No.	Before Irradiation	After Irradiation	% Δ
3	355	297	-16.3
6	450	420	- 6.7
7	405	325	-19.8

Dose 1.09×10^6R

D

Crystal No.	Before Irradiation	After Irradiation	% Δ
3	.0210	.0250	+19.1
6	.0168	.0145	-13.7
7	.0243	.0175	-27.4
	Voltage (volts)*		
3	7.3	6.4	-12.3
6	6.9	8.1	+17.4
7	7.0	5.9	-15.7

There seems to be no major change in the hysteresis curves due to this irradiation.

Dose 1.35×10^7R

Capacitance (μμf)

10	500	355	-29.0
11	675	418	-26.2
13	480	457	- 4.8
	D		
10	.0158	.009	-43.0
11	.0155	.0092	-40.6
13	.0055	.011	+100.0
	Voltage (volts) *		
10	10.5	6.6	-37.1
11	15.7	9.3	-40.8
13	8.9	9.0	+ 1.1

There seemed to be no major change in the hysteresis curves due to this irradiation.

* Force = 150 lbs.

Picatinny Arsenal has also conducted permanent damage studies on PZT-5 ceramics at the Brookhaven National Laboratories' reactor. The temperature of the samples during irradiation was 40°C. The results are summarized below for the permanent change of resonance frequency and output voltage after a total neutron dose of 10^{18} nvt.

Unit No.	Resonance Frequency (Kc) Before Irradiation	After Irradiation	% Δ
X-1	200.0	207.8	+3.9
X-2	196.5	208.5	+6.1
X-3	200.0	211.0	+5.5
X-4	196.0	200.5	+2.3
X-5	199.6	206.0	+3.2
	Voltage (volts)*		
X-1	14.1	9.4	-32.0
X-2	13.8	12.9	- 6.5
X-3	13.7	11.1	-19.0
X-4	13.8	9.4	-31.8
X-5	14.0	13.1	- 6.4

Picatinny Arsenal tested units composed of 2 PZT crystals in a steel housing at the Triga reactor. The purpose of these tests was to determine the magnitude, if any, of any voltage spike induced by a pulse of 10^{16} n/cm^2/sec. (total neutron dose of $2 \times 10^{13} - 10^{14}$ n/cm^2/pulse) in these units. The greatest voltage spike produced during irradiation was 0.2 volts. The transient irradiation results on the units are given below. It will be noted that these units were subjected to varying numbers of shots. The flux given is total integrated flux. An average flux per shot may be obtained by dividing the integrated flux by the number of shots.

Unit No.	Peak Transient Voltage Detected (volts)	Flux (nvt)	
1	0.2	4×10^{14}	(4 shots)
2	0.1	2.4×10^{13}	(2 shots)
3	0.0	6.6×10^{13}	(1 shot)
4	0.0	4×10^{14}	(1 shot)
5	0.0	2.2×10^{14}	(2 shots)

*Force Applied = 150 lbs.

These results are, in general, in agreement with work done by the Sandia Corporation at the Godiva pulsed reactor where the output from piezoelectrics subjected to pulsed neutron radiation was reported to be less than 1 volt[5].

The following two scope traces show the transient voltage output pulses as a function of time for Units No. 1 and 2.

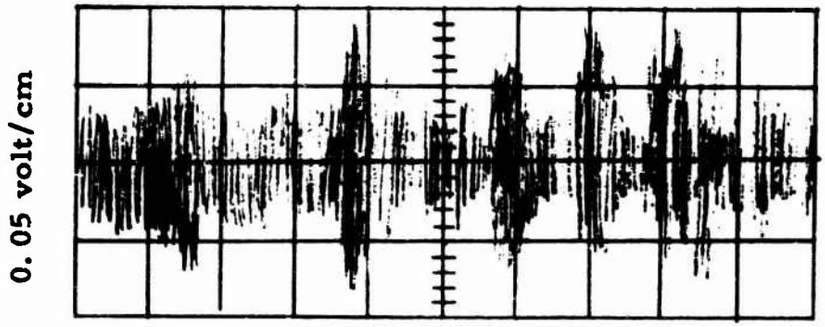

#2 10 millisecond/cm

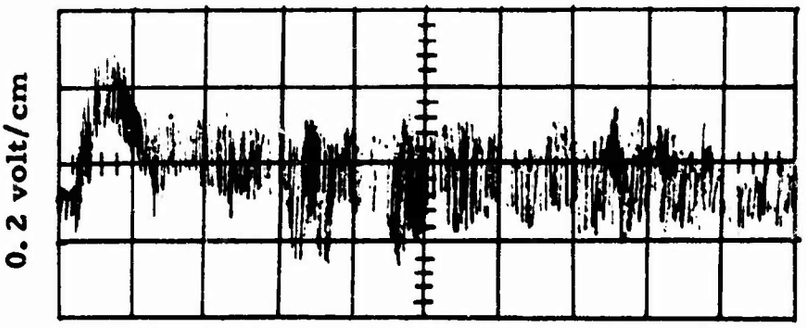

#1 10 millisecond/cm

Permanent damage measurements were made on these units when they were brought back to Picatinny Arsenal. The results are summarized below.

Capacitance (μμf)

Unit No.	Before Irradiation	After Irradiation	% Δ
1	100	110	+10.0
2	100	104	+ 4.0
3	100	112	+12.0
4	97	106	+ 9.3
5	101	113	+11.9

Voltage (volts)

1	510	480	- 5.87
2	625	510	-18.40
3	600	480	-20.00
4	600	520	-13.25
5	615	480	-22.00

These results agreed with the work done by AVCO on PZT-5 at the Godiva II facility. Measurements made 15 seconds after irradiation at 20°C showed no significan affect in d_{33}. After 40 minutes, resistivity, dielectric constant, and d_{33} were measured and found not to have been significantly affected.[6]

Picatinny Arsenal conducted tests at the Watertown Arsenal reactor where the neutron flux is roughly 2×10^{12} n/cm^2-sec-Megawatt and the gamma dose is 50R/hr-watt. The following data was obtained.

Dose of 10^{13}nvt and 6.1×10^4R

Capacitance (μμf)

Crystal No.	Before Irradiation	After Irradiation	% Δ
6	602	355	-41.0
7	630	415	-28.6
8	627	440	-29.8
9	635	315	-50.4
10	645	360	-44.2

Dose of 6.8×10^{14} and 4.7×10^{6}R

Crystal No.	Capacitance (μμf) Before Irradiation	After Irradiation	% Δ
11	630	420	-33.3
12	630	510	-19.0
13	610	440	-27.4
14	615	490	-20.5
15	620	435	-29.8

Dose of 5.8×10^{16} nvt and 4×10^{8}R

	Capacitance (μμf)		
1	645	350	-45.7
2	610	370	-39.3
3	650	365	-42.4
4	635	415	-34.6
5	640	410	-36.0

An examination of the hysteresis curves of these 15 crystals showed no major effect as a result of irradiation. A set of typical photographs for the hysteresis curves of a pre and post irradiated sample is presented below.

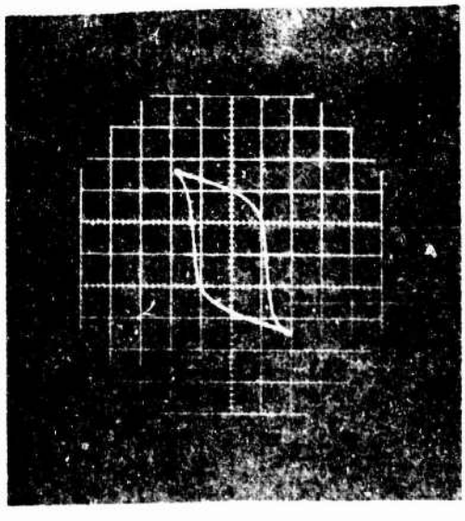

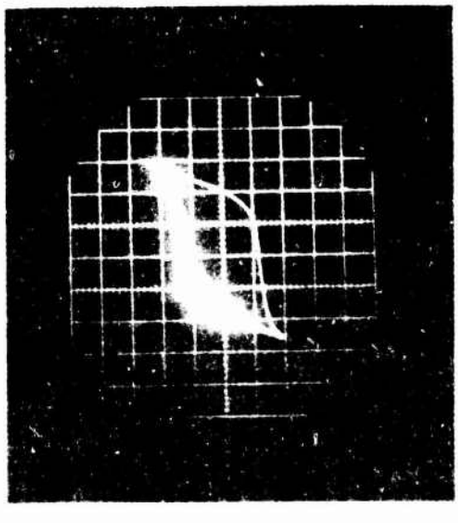

REFERENCES

1. Rogers, Jr., F. T., "Effect of Pile Irradiation on the Dielectric Constant of Ceramic $BaTiO_3$", Journal of Applied Physics, Vol. 27 No. 9, Sep 1956, pp 1066-7.

2. Wittels, M., and Sherrill, F., "Fast Neutron Effects in Tetragonal Barium Titanate", Journal of Applied Physics, Vol. 28, No. 5, May 1957, pp 606-9.

3. Informal communication with I. Lefkowitz of Gulton Industries.

4. Informal communication with H. Krueger of Clevite Corporation.

5. Trip Report of Mr. R. D. Wehrte of Sandia Corporation to Los Alamos Scientific Lab., R & D File 7-3, Nov 1957.

6. Trip Report of Mr. J. J. Siegel of AVCO Corporation to Los Alamos Scientific Lab., EEDM-5-2085, Mar 1959.

APPENDIX B

PART 3

USE OF FERROELECTRICS FOR GAMMA-RAY DOSIMETRY

D. L. Hester, D. D. Glower, and L. J. Overton
Sandia Corporation, Albuquerque, New Mexico

ABSTRACT

A gamma-ray dosimeter employing a poled ferroelectric as the transducer element has been studied. Irradiation with gamma rays causes a release of charge by the ferroelectric element. The magnitude of the charge released has been determined experimentally to vary linearly with gamma-ray dose. The current in a shunting resistor with no external voltage applied varies linearly with gamma-ray dose rate. A constant of proportionality of 10^{-12} coul per rad (H_2O) per cm^2 of electroded ferroelectric surface has been measured for polycrystalline $Pb(Zr_{.65}Ti_{.35})O_3$ + 1 w% Nb_2O_5 irradiated in the Sandia Pulsed Reactor. The contribution to the charge release from the neutron irradiation has been determined experimentally to be negligible. Irradiation in the 0.6 Mvp flash X-ray also produces a linear relationship between current and gamma-ray dose rate. A similar release of charge has been observed in poled ceramic barium titanate.

INTRODUCTION

Thin disks of ferroelectric ceramic electroded on the flat surfaces and polarized in the axial direction have been used sucessfully as dosimeters on the Sandia Pulsed Reactor (SPR) and on a 0.6 Mvp flash X-ray generator. Although both barium titanate and lead zirconate titanate ceramics have been used, the data reported herein are for $Pb(Zr_{.65}Ti_{.35})O_3$ + 1 w% Nb_2O_5.

The transducer portion of the dosimeter consists of a ferroelectric ceramic disk and a shunting resistance; no voltage source is required. When the ferroelectric element is subjected to gamma irradiation, a charge is released which flows through a shunting resistance. For small values of resistance, the instantaneous current produced varies linearly with the instantaneous gamma-ray dose rate. Large values of resistance produce an integrator, and the maximum current measured is then proportional to gamma-ray dose. The value of resistance determines the mode of operation; the quantity of charge released is independent of the magnitude of the resistance. By selecting the desired value of resistance and providing the necessary voltage monitoring equipment, either gamma-ray dose rate, gamma-ray dose, or both, can be measured.

The linear relationship between charge released and gamma-ray dose (H_2O) was observed for irradiations in the SPR and in the flash X-ray sources. The constant of proportionality between the charge released and the dose (H_2O) was not the same, since the energy spectra of the two sources are quite different; the comparatively low-energy X-ray spectra produces a dose to PZT that exceeds the dose to H_2O, because an appreciable absorption in PZT occurs by the photoelectric effect.

*This work was supported by the United States Atomic Energy Commission. Reproduction in whole or in part is permitted for any purpose of the U. S. Government.

EXPERIMENTAL TECHNIQUE

Ferroelectric elements used in this experiment were disks ranging in thickness from 0.035 to 0.39 cm with diameters of 1 to 9 cm. All elements were electroded with air-drying silver, fired-on silver, or fired-on platinum. No differences in response resulting from the method of electroding were observed.

Although data reported herein pertains to $Pb(Zr_{.65}Ti_{.35})O_3$ + 1 w% Nb_2O_5, similar results have been obtained with various other PZT compositions and with barium-calcium titanate. The 65/35 PZT was purchased from several different suppliers, with all of the elements giving essentially the same results.

Radiation damage to the material, as determined from hysteresis loops, capacitance, dissipation factor, and resonant frequency measurements, was negligible. One sample was exposed to 25 bursts in the SPR, and a like number in the flash X-ray, with no measurable changes in properties observed. This is in agreement with the radiation damage data of Glower and Warnke.[1]

The charge release was measured with the circuit depicted in Figure 1 and an oscilloscope. The shunting resistance was not exposed to the radiation, and the coaxial cable was shielded with lead. Total charge released was obtained by integrating the current-time waveforms, or by replacing the 50 ohm resistor of Figure 1 with a 1M resistor and reading the peak voltage.

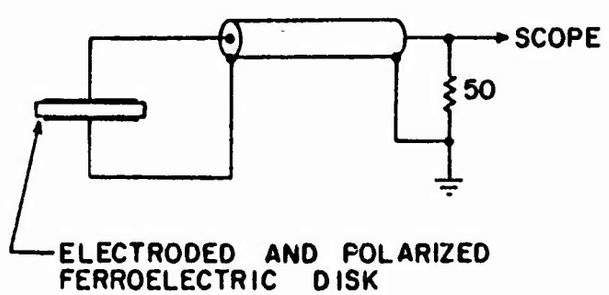

Fig. 1—Diagram of Circuit Used to Evaluate Charge Release.

A typical measurement of the gamma-ray dose rate for the SPR is shown in Figure 2. The peak dose rate measured varied from about 10^6 to 10^8 rad(H_2O)/sec, depending on the distance from the source. The resulting gamma-ray doses ranged from approximately 10^2 to 10^4 rad(H_2O), with an accompanying exposure of 10^{11} to 10^{13} nvt (E > 0.01 Mev). Flash X-ray irradiations gave gamma-ray doses from 0.1 to 4.0 rad(H_2O), peak dose rates being similar to those obtained in the SPR.

In the SPR, the reference gamma-ray dose was measured with silver-activated phosphate glass rods[2,3], and gamma-ray dose rate versus time was determined with a U^{235} fission chamber. (The U^{235} chamber measures [nv(t)], but $\frac{\dot{\gamma}(t)}{[nv(t)]}$ is constant and the shape of the current pulse from the U^{235} chamber is characteristic of $\dot{\gamma}(t)$.) Gamma-ray dose for the flash X-ray source was read from exposed photographic film. No gamma-ray dose rate dosimetry was available for the X-rays, but the shape of the dose rate versus time was obtained by measuring the current of a reverse biased semiconductor diode.

EXPERIMENTAL RESULTS

A. Sandia Pulsed Reactor Results

The monotonically increasing portion of the curve of gamma-ray dose rate versus time, as shown in Figure 2, is characterized by

$$\dot{\gamma}(t) = Be^{\alpha t} \qquad (1)$$

where $1/\alpha$ is the reactor period. For this experi-

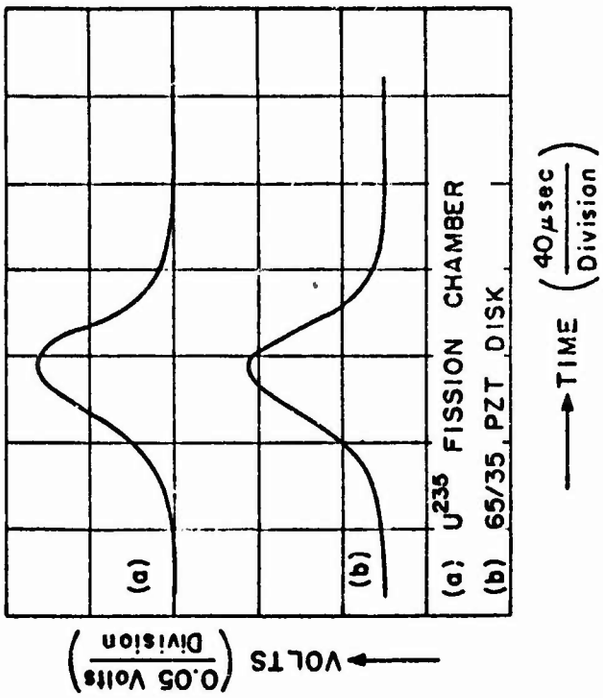

Fig. 2—Typical Gamma-Ray Dose Rate Versus Time Curve for the SPR.

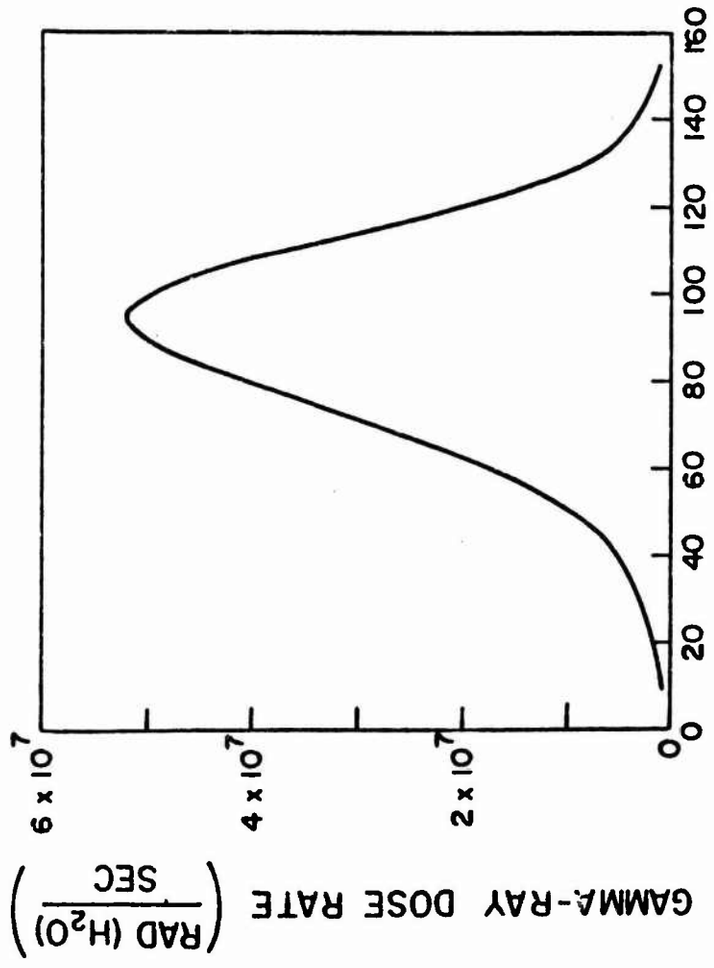

Fig. 3—Typical Waveforms for 65/35 Disk and U235 Fission Chamber Irradiated in the SPR.

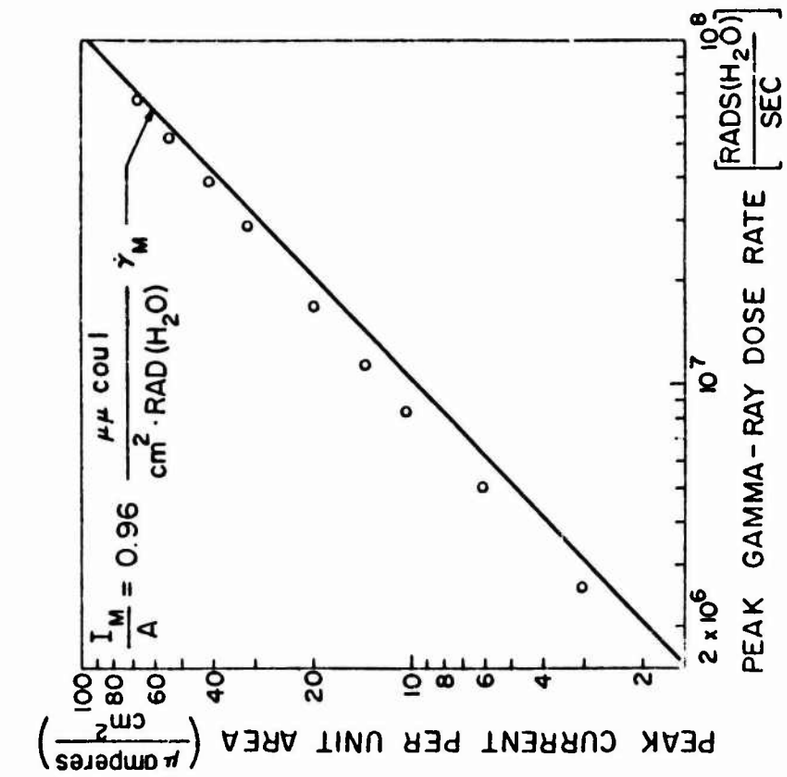

Fig. 5—Peak Current as a Function of Peak Gamma-Ray Dose Rate for 65/35 PZT Irradiated in the SPR.

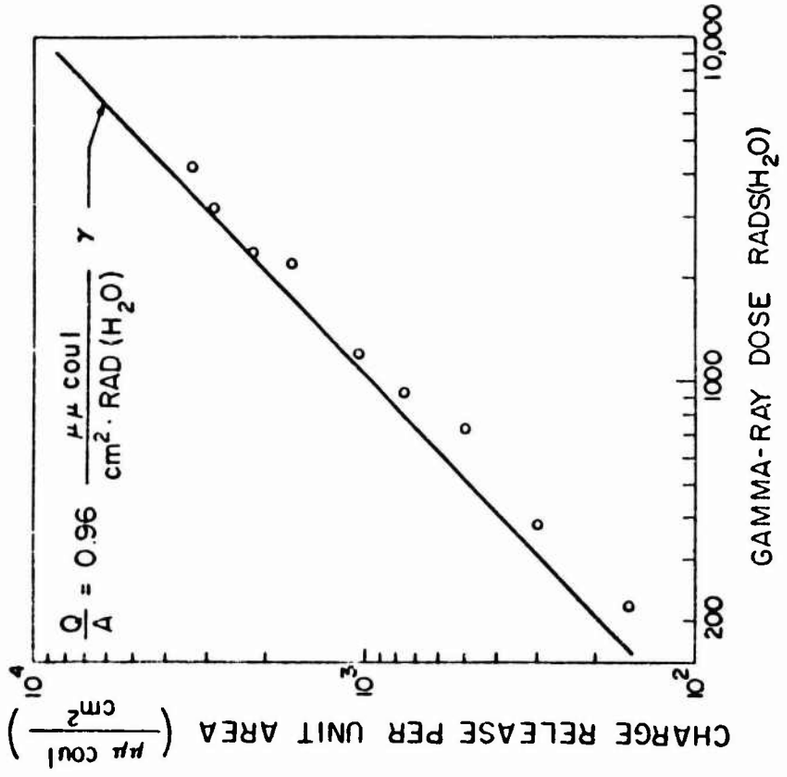

Fig. 4—Charge Release as a Function of Gamma-Ray Dose for 65/35 PZT Irradiated in the SPR.

ment $1/\alpha$ was approximately 17 μsec. Therefore, a dosimeter capable of response times of 17 μsec or less is required to insure adequate dose rate versus time data. The response time of the ferroelectric dosimeter is given by

$$T = RC \qquad (2)$$

where R is the shunting resistance and C the capacitance of the sample. For the samples used in this portion of the experiment, C was approximately 6×10^{-9} fd and R was 200 ohms. The resulting time constant of 1.2 μsec was short enough to fulfill the aforementioned requirement.

A typical voltage versus time waveform for a 65/35 disk irradiated in SPR is given in Figure 3. Total charge released was obtained by integrating the current. Figure 4 is a plot of the total charge released versus gamma-ray dose. The experimental data points fit a linear relationship of the form

$$Q/A = K\gamma \qquad (3)$$

where Q/A is the total charge released per unit area, γ is the gamma-ray dose, and K is a constant. The derivative of Equation (3) with respect to time gives

$$i/A = K\dot{\gamma} \qquad (4)$$

where i/A is the current per unit area and $\dot{\gamma}$ the gamma-ray dose rate. Thus the instantaneous current should vary linearly with the gamma-ray dose rate. A plot of peak current versus peak gamma-ray dose rate (Figure 5) shows this to be true. Although two different methods of measuring gamma-ray dose and dose rate were used, a value of K = 0.96 gives an acceptable fit for both sets of data points. A slightly larger value of K would give a better fit for Figure 5, and a smaller value is indicated for Figure 4. This difference is probably due to the lack of consistency between the two dosimetry methods used. The scatter of the data points is, to a large

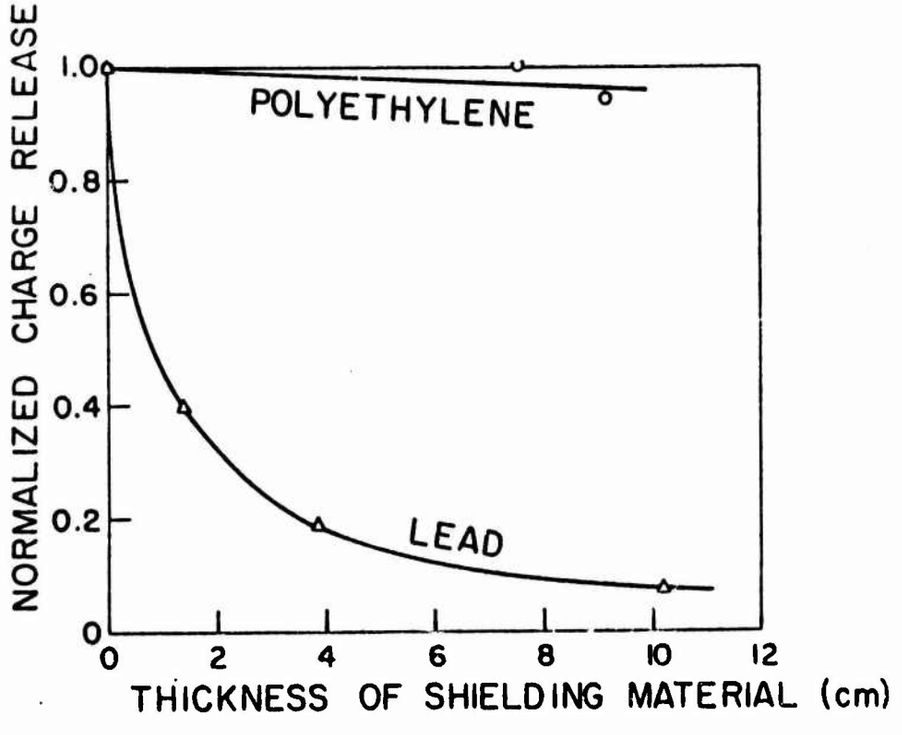

Fig. 6—Peak Current as a Function of Thickness of Polyethylene and Lead Shielding for the SPR.

extent, a result of the uncertainty in the reference dosimetry. For example, two glass rod dosimeters exposed simultaneously at the same location may give readings which differ as much as 15 to 20 percent.

Since neutrons accompany the gamma-rays from SPR, their contribution to the release of charge was evaluated. Polyethylene shielding placed between the ferroelectric disk and the source reduced the integrated neutron flux (E > .01 Mev) by a factor of three, but did not significantly reduce the amount of charge released. In comparison, lead gamma-ray shielding greatly decreased the output, as shown in Figure 6. From these data it was concluded that the neutron component of charge release was negligible.

Effects of sample thickness on the output have also been evaluated, and the results are given in Figure 7. From this figure it is evident that the thickness of the sample does not affect the output. Therefore, the thickness of the element may be increased to lower the capacitance and, hence, the time constant, without reducing the output. This is an important consideration in designing fast response dosimeters.

In addition to being unaffected by sample thickness, the magnitude of the charge release is also independent of the value of the shunting resistance. Instantaneous current is no longer proportional to gamma-ray dose rate if the resistance is too large, but the quantity of charge released is not affected. Figure 8 is a plot of the charge released versus the magnitude of the shunting resistance for a constant gamma-ray dose. The magnitude of the charge released was the same for 20 ohms as for 10^4 ohms. Data (not shown in Figure 8) from recent experiments with resistance values as large as 10^6 ohms gave the same results. In this case the current was observed to be proportional to the integral of the dose rate and the total dose was measured directly.

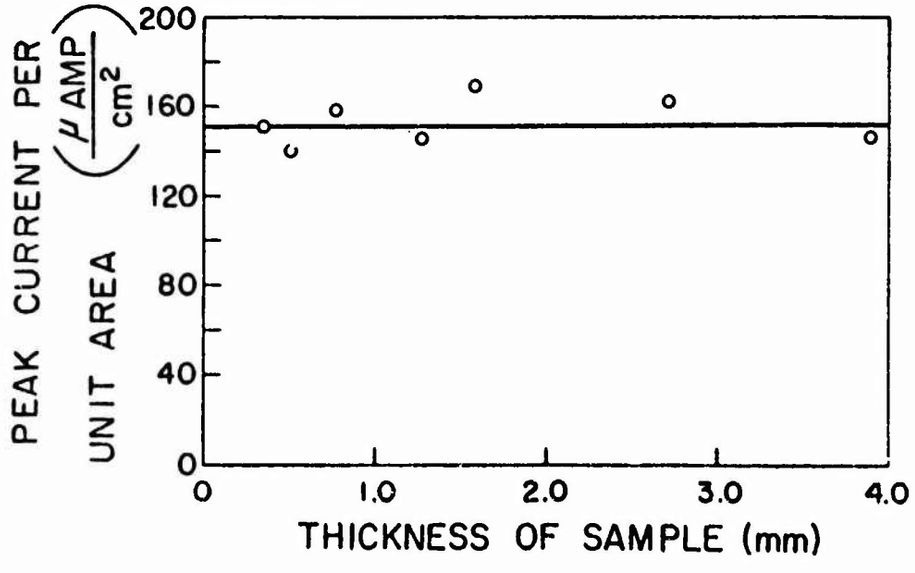

Fig. 7—The Effect of Sample Thickness on the Magnitude of Charge Release for 65/35 PZT Irradiated in the SPR.

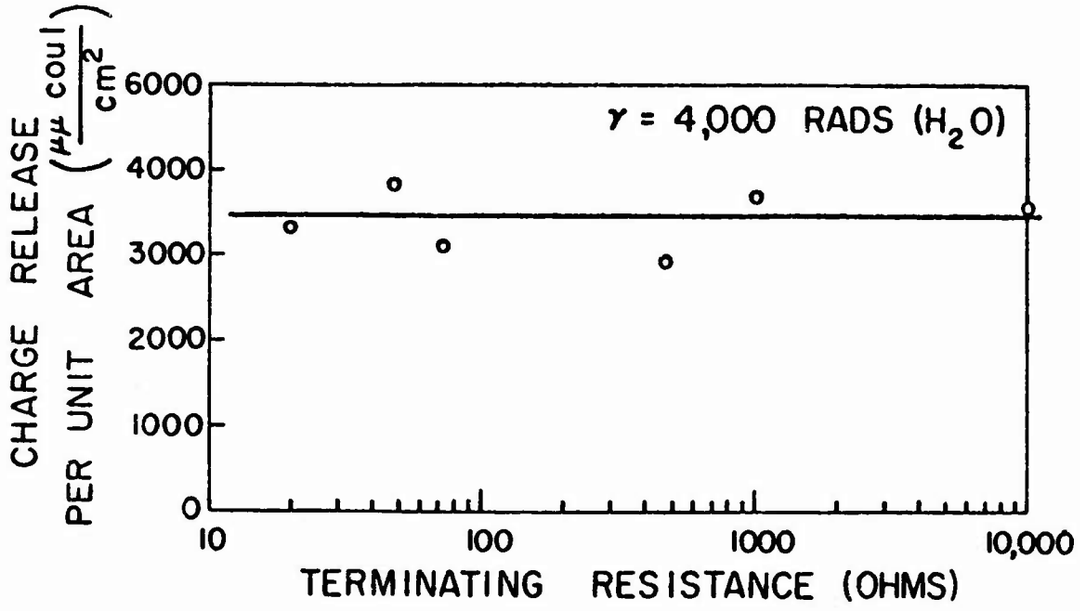

Fig. 8—Charge Release as a Function of the Magnitude of Shunting Resistance for 65/35 PZT Irradiated in the SPR.

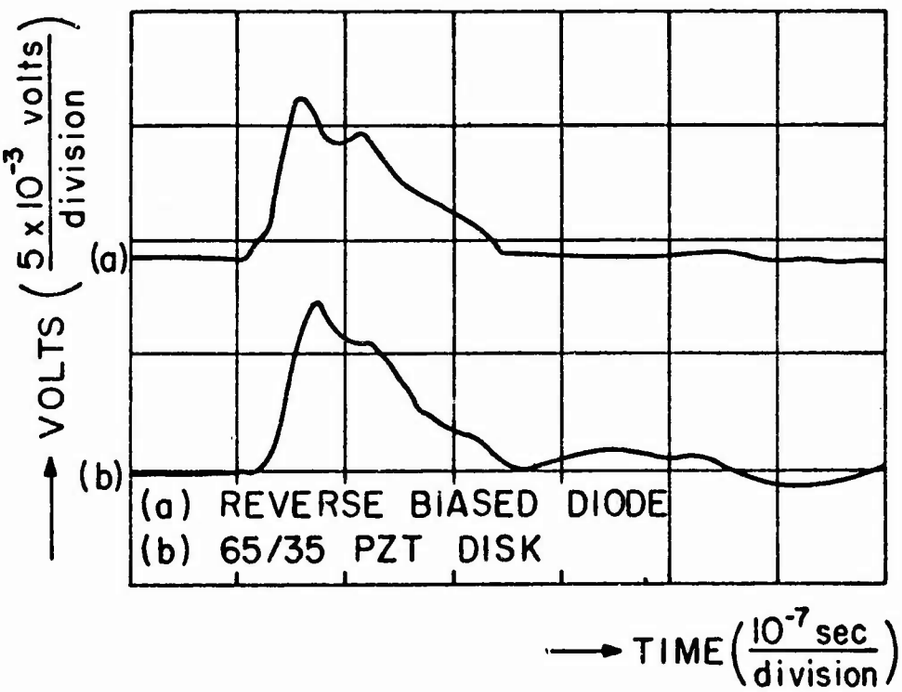

Fig. 9—Typical Waveforms for 65/35 PZT Disk and Reverse Biased Diode Irradiated in the 0.6 Mvp Flash X-ray.

B. Flash X-Ray Results

In comparison to the SPR, the flash X-ray source gives a very short duration pulse of radiation. The Flexitron Model 20100 0.6 Mvp X-ray source used in this experiment gave a pulse width of only 0.2 μsec, with a rise time of approximately 25 nanosec. The ferroelectric disks employed as dosimeter elements were 1 cm in diameter and 0.08 cm thick with a capacitance of $\sim 5 \times 10^{-10}$ fd. A 50 ohm shunting resistance was used, so the resulting time constant was 25 nanosec. As was the case in the SPR, the circuit of Figure 1 was employed. A typical voltage waveform is given in Figure 9. The two traces, one for the PZT disk and the other for a reverse-biased semiconductor diode, were recorded on a dual beam oscilloscope. The waveform for the PZT disk is in good agreement with the reverse-biased diode waveform. Waveforms taken with a scintillometer were substantially the same as those for the diode. Figure 9 reveals two differences between the response of the diode and the PZT: (1) the PZT waveform has an oscillatory tail, and (2) the second peak of the PZT waveform is not as sharp as the one for the diode. Oscillatory tails are frequently observed with ferroelectric disks and it is believed they are the result of resonance phenomena since piezoelectric crystals vibrate with characteristic frequencies when shocked. The smoothing out of the second peak is probably due to the 25 nanosec time constant of the dosimeter-resistance combination.

Total charge released is plotted against gamma-ray dose in Figure 10, and a curve of the form of Equation (3) is included for reference. A linear relationship between charge released and gamma-ray dose is observed, but the value of K is 10.5 compared to 0.96 for the SPR. This is probably due to the difference in energy spectra, as will be discussed later.

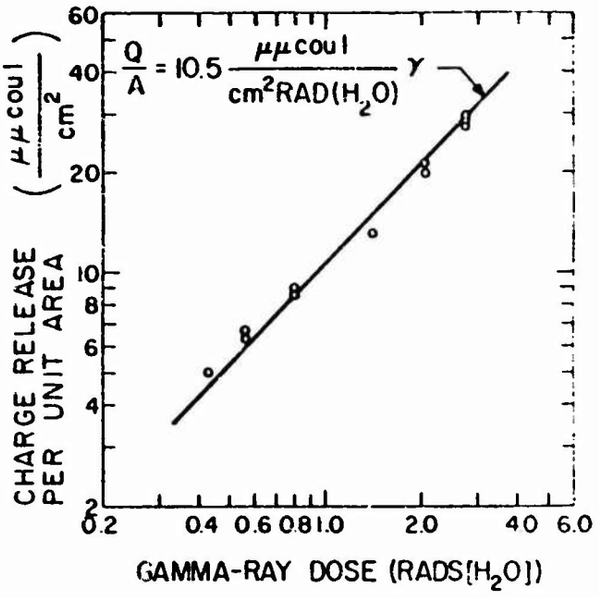

Fig. 10—Charge Release as a Function of Gamma-Ray Dose for 65/35 PZT Irradiated in the 0.6 Mvp Flash X-ray.

DISCUSSION AND CONCLUSIONS

The feasibility of using ferroelectrics as pulsed gamma-ray dosimeters has been established. Their desirability for a particular application can be evaluated by considering the sensitivity and response times required.

If the dosimeter is to be used to measure gamma-ray dose rate, then the maximum voltage output will be

$$v_m = ARK \dot{\gamma}_m \quad (5)$$

where the symbols are defined as in Equation (4). For a disk, the time constant is

$$T = \frac{\epsilon RA}{d} \quad (6)$$

where ϵ is the dielectric constant and d the thickness. Dividing Equation (5) by Equation (6) gives

$$d = \frac{\epsilon V_m}{K \dot{\gamma}_m^{\circ} T} . \quad (7)$$

Thus, for an application where $\dot{\gamma}_m^{\circ}$ is known, the selection of a desired voltage maximum and response time fixes the minimum thickness of the ferroelectric disk to be used. The value of the desired voltage maximum also determines the required resistance-area product. From Equation (5)

$$RA = \frac{V_m}{K \dot{\gamma}_m^{\circ}} . \quad (8)$$

Equations (7) and (8) can be used to determine the dimensions needed for a particular dose rate dosimetry application.

If gamma-ray dose rather than dose rate is required, the time constant must be long to provide the required integration. In this case the voltage produced, V, will be

$$V = \frac{Q}{C} = \frac{K\gamma d}{\epsilon} \quad (9)$$

assuming the sample is a disk. Solving for thickness gives

$$d = \frac{\epsilon V}{K\gamma} . \quad (10)$$

Again the sample thickness is fixed when a desired response is chosen. Multiplying Equation (6) by Equation (9) and solving for RA gives

$$RA = \frac{VT}{K\gamma} . \quad (11)$$

Equations (10) and (11) give the required thickness and resistance-area product for a particular application where gamma-ray dose is to be measured.

Design of a ferroelectric dosimeter can be accomplished by using Equations (7) and (8) for a dose rate dosimeter, or with Equations (10) and (11) for a dosimeter to read total dose. If PZT is to be used as the ferroelectric element, a value of K of 1 $\mu\mu$ coul per cm^2 per rad(PZT) and a relative dielectric constant of 500 should be used in the calculation. Although the design techniques discussed above are for dosimeters to read either dose or dose rate, both can be read simultaneously if additional electronic circuitry is added to a dose rate dosimeter.

In addition to the restrictions imposed by the physical size of the ferroelectric element (as determined by the above calculations), some consideration should be given to the effect of radiation damage in the material. For 65/35 PZT total doses of 10^{16} nvt (E > 0.1 Mev) and 10^{8} rad(H_2O) have been received without serious degradation of material properties.[1] If total doses higher than these are expected as the result of many exposures, replaceable transducer elements could be used.

As mentioned earlier, irradiations in the flash X-ray gave a different value of K than irradiation in the SPR. If, however, the constants are related to rad(PZT) rather than rad(H_2O), the two values of K would be about the same. An exact calculation of this nature is difficult; approximate calculations using gamma absorption coefficients for PZT and the energy spectrum for the X-rays indicate that K for the X-rays should be between 10 and 25 times greater than K for the SPR.

The causes of the radiation-induced charge release are currently being investigated. One of the possible causes, a loss of polarization during irradiation, seems reasonable since a positive charge is always released by the positive polar plate* regardless of beam direction. Permanent

*The positive polar plate is the plate to which a positive voltage was applied during poling.

depolarizing of the ferroelectric by radiation damage does not seem to be the answer, however, since a depolarizing rate of 1 $\mu\mu$ coul per cm^2 per rad(H_2O) would indicate a complete loss of polarization after exposure to 3×10^7 rad(H_2O), a fact not borne out by experimental observations.[1] Thermal depolarization by the gamma-ray energy absorbed seems to be a more reasonable answer. Assuming the disk to be adiabatic during the radiation pulse, the resulting temperature rise, although very small, would be sufficient to produce a charge release of the same order of magnitude as the observed charge release. An analysis similar to the one given by Chynoweth[4] for barium titanate crystals irradiated with light pulses gives a linear relationship of the form of Equation (4) with

$$K = \frac{1}{c}\frac{dP}{dT} \qquad (12)$$

where c is the specific heat of the material and $\frac{dP}{dT}$ the rate of change of polarization (P) with temperature (T). For 65/35 PZT the value of K calculated by Equation (12) is 0.55 compared to an experimental value of 0.96. The difference in the two values is probably due to a photovoltaic or photoconductivity component of current that must be added to the thermal component to give total current. A photovoltaic current was reported by Chynoweth[4] and irradiation of PZT with Co^{60} gamma-rays has been observed to produce a steady-state component of current. A thermal depolarization current would decrease to zero under steady irradiation, since an equilibrium temperature would be reached. Therefore, a nonzero equilibrium value of current under steady irradiation indicates the presence of a current component that cannot be attributed to thermal depoling. Experiments are underway which will give a better understanding of the mechanisms involved in the charge release, and the results will be reported at a later date.

REFERENCES

1. Glower, D. D. and Warnke, D. F., Nuclear Rad. Eff. Conf., IEEE Summer General Meeting, CP-63-1137, June (1963).

2. Schulman, J. H., Shurcliff, W., Ginther, R.J., and Attix, F. H., Nucleonics, 11, 52, October, (1953).

3. Schulman J. H. and Etzel, H. W., Science 118, 184 (1953).

4. Chynoweth, A. G., Phys. Rev., 102, 705 (1956).

UNCLASSIFIED
Security Classification

DOCUMENT CONTROL DATA - R&D

(Security classification of title, body of abstract and indexing annotation must be entered when the overall report is classified)

1 ORIGINATING ACTIVITY (Corporate author) FRANKFORD ARSENAL Philadelphia, Pa. 19137	2a REPORT SECURITY CLASSIFICATION Unclassified 2b GROUP

3 REPORT TITLE
FERROELECTRICS: THEIR ELECTRICAL BEHAVIOR DURING, AND SUBSEQUENT TO, IONIZING RADIATIONS

4 DESCRIPTIVE NOTES (Type of report and inclusive dates)
Final technical report

5 AUTHOR(S) (Last name, first name, initial)
LEFKOWITZ, I.
KRAMER, K.
KROEGER, P.

6 REPORT DATE November 1965	7a TOTAL NO. OF PAGES 143	7b NO. OF REFS
8a CONTRACT OR GRANT NO. AMCMS 5023.11.14200.01 b PROJECT NO. IN22601A085 c. d.	9a ORIGINATOR'S REPORT NUMBER(S) R-1779 9b OTHER REPORT NO(S) (Any other numbers that may be assigned this report)	

10 AVAILABILITY/LIMITATION NOTICES
Distribution of this report is unlimited. Release to CFSTI is authorized.

11 SUPPLEMENTARY NOTES	12 SPONSORING MILITARY ACTIVITY Picatinny Arsenal Dover, N. J.

13 ABSTRACT

A study has been made on certain ferroelectric materials which are among those used extensively in military applications, both in a polarized condition in such items as impact fuzes and in an unpolarized condition as capacitors. The transient voltages across a load produced by charge generated on the surface of various types of ferroelectric specimens during irradiation have been measured. These outputs were found to vary widely in amplitude and polarity even from specimens ostensibly alike (i.e., from the same lot of a given manufacturer), and even from a single specimen pulsed repeatedly with gamma and neutron radiation. Pulses were found to vary from background levels to a high of 300 volts on a large specimen with a load of 10^7 ohms and radiation of 5.4×10^{14} fast (Pu) neutrons and associated gammas. The maximum voltage possible is unknown, as are the factors causing the variation. Both polarized and unpolarized specimens showed outputs well above background transients. Some specimens were identical to those used in impact fuze applications and were in simulated housings which reproduce the mechanical environment of the device. Some fuze circuits in present use are discussed with reference to their use of ferroelectric materials and a calculation of the energy transferred by a voltage pulse to a load is presented. An investigation of various specifications for Army devices shows that

(Cont'd)

DD FORM 1 JAN 64 1473

UNCLASSIFIED
Security Classification

14. KEY WORDS	LINK A		LINK B		LINK C	
	ROLE	WT	ROLE	WT	ROLE	WT
Piezoelectrics						
Ferroelectrics						
Dielectrics						
Capacitors						
Fuzes						
Radiation effects						
Reliability						
Lead titanate-lead zirconate						
Perovskites						

INSTRUCTIONS

1. ORIGINATING ACTIVITY: Enter the name and address of the contractor, subcontractor, grantee, Department of Defense activity or other organization *(corporate author)* issuing the report.

2*a*. REPORT SECURITY CLASSIFICATION: Enter the overall security classification of the report. Indicate whether "Restricted Data" is included. Marking is to be in accordance with appropriate security regulations.

2*b*. GROUP: Automatic downgrading is specified in DoD Directive 5200.10 and Armed Forces Industrial Manual. Enter the group number. Also, when applicable, show that optional markings have been used for Group 3 and Group 4 as authorized.

3. REPORT TITLE: Enter the complete report title in all capital letters. Titles in all cases should be unclassified. If a meaningful title cannot be selected without classification, show title classification in all capitals in parenthesis immediately following the title.

4. DESCRIPTIVE NOTES: If appropriate, enter the type of report, e.g., interim, progress, summary, annual, or final. Give the inclusive dates when a specific reporting period is covered.

5. AUTHOR(S): Enter the name(s) of author(s) as shown on or in the report. Enter last name, first name, middle initial. If military, show rank and branch of service. The name of the principal author is an absolute minimum requirement.

6. REPORT DATE: Enter the date of the report as day, month, year; or month, year. If more than one date appears on the report, use date of publication.

7*a*. TOTAL NUMBER OF PAGES: The total page count should follow normal pagination procedures, i.e., enter the number of pages containing information.

7*b*. NUMBER OF REFERENCES: Enter the total number of references cited in the report.

8*a*. CONTRACT OR GRANT NUMBER: If appropriate, enter the applicable number of the contract or grant under which the report was written.

8*b*, 8*c*, & 8*d*. PROJECT NUMBER: Enter the appropriate military department identification, such as project number, subproject number, system numbers, task number, etc.

9*a*. ORIGINATOR'S REPORT NUMBER(S): Enter the official report number by which the document will be identified and controlled by the originating activity. This number must be unique to this report.

9*b*. OTHER REPORT NUMBER(S): If the report has been assigned any other report numbers *(either by the originator or by the sponsor)*, also enter this number(s).

10. AVAILABILITY/LIMITATION NOTICES: Enter any limitations on further dissemination of the report, other than those imposed by security classification, using standard statements such as:

(1) "Qualified requesters may obtain copies of this report from DDC."

(2) "Foreign announcement and dissemination of this report by DDC is not authorized."

(3) "U. S. Government agencies may obtain copies of this report directly from DDC. Other qualified DDC users shall request through _____."

(4) "U. S. military agencies may obtain copies of this report directly from DDC. Other qualified users shall request through _____."

(5) "All distribution of this report is controlled. Qualified DDC users shall request through _____."

If the report has been furnished to the Office of Technical Services, Department of Commerce, for sale to the public, indicate this fact and enter the price, if known.

11. SUPPLEMENTARY NOTES: Use for additional explanatory notes.

12. SPONSORING MILITARY ACTIVITY: Enter the name of the departmental project office or laboratory sponsoring *(paying for)* the research and development. Include address.

13. ABSTRACT: Enter an abstract giving a brief and factual summary of the document indicative of the report, even though it may also appear elsewhere in the body of the technical report. If additional space is required, a continuation sheet shall be attached.

It is highly desirable that the abstract of classified reports be unclassified. Each paragraph of the abstract shall end with an indication of the military security classification of the information in the paragraph, represented as *(TS)*, *(S)*, *(C)*, or *(U)*.

There is no limitation on the length of the abstract. However, the suggested length is from 150 to 225 words.

14. KEY WORDS: Key words are technically meaningful terms or short phrases that characterize a report and may be used as index entries for cataloging the report. Key words must be selected so that no security classification is required. Identifiers, such as equipment model designation, trade name, military project code name, geographic location, may be used as key words but will be followed by an indication of technical context. The assignment of links, rules, and weights is optional.